UNIVERSITAT POLITÈCNICA DE CATALUNYA BARCELONATECH

Multiphysics simulation in buildings

Oussama Souaihi

UPC **CTTC**

Multiphysics simulation in buildings

Centre Tecnològic de Transferència de Calor
Departament de Màquines i Motors Tèrmics
Universitat Politècnica de Catalunya

Oussama Souaihi
Doctoral Thesis

Multiphysics simulation in buildings

Oussama Souaihi

TESI DOCTORAL

presentada al

Departament de Màquines i Motors Tèrmics
E.S.E.I.A.A.T.
Universitat Politècnica de Catalunya

per a l'obtenció del grau de

Doctor per la Universitat Politècnica de Catalunya

Terrassa, November 2017

Multiphysics simulation in buildings

Oussama Souaihi

Directors de la Tesi

Dr. Roser Capdevila Paramio

Dr. Joaquim Rigola Serrano

Dr. Assensi Oliva Llena

Tribunal Qualificador

Dr. Jose Manuel Pinazo Ojer
Universidad de Valencia

Dr. Antonio María Pascau Benito
Universidad de Zaragoza

Dr. Carles Oliet Casasayas
Universitat Politècnica de Catalunya

Acknowledgements

The accomplishment of this work has taken me more than five years, a time period in which i have learned a lot of thing in both professional and personal aspects. Many people have influenced and inspired me during this period. In particular, I want to show my gratitude to:

Prof. Assensi Oliva, for giving me the opportunity to do my doctorate and to form a part of the *Heat and Mass Transfer Technological Center* (CTTC).

Roser Capdevila for supervising my work during this thesis and for her patient guidance and advices.

Joaquim Rigola for his motivation and encouragement to develop the thesis and to meet the deadlines of the different projects.

Joan López for helping me on the code design and programming issues.

Prof. Chiheb bouden and Hamdi Kessentini for their support and encouragement from the *National Engineering school of Tunis* (ENIT).

I would also like to thank:

All my laboratory colleagues with whom i had nice time and shared a lot of coffees, barbecues, football matches and many other good moments.

My fiancée Eva for giving sense to my life and supporting me every day.

Finally, to my family for pushing me till the end and giving me all the support from Tunisia to achieve the highest education level and to succeed in life. Without them I wouldn't have done what I did.

Dedicated to my mother Amel, my father Mohsen and my two little sisters Asma and Ichrak.

Abstract

Numerical simulation play an important role in the design, engineering, operation and management of buildings. It can help reducing energy consumption, improving indoor air quality and thermal comfort and provide quantitative data supporting decision making, e.g. choosing the best solution for designing, retrofitting or choosing the optimal HVAC system. Besides, buildings are composed more and more of different complex elements and systems which make the simulation of only thermal physics in buildings not enough to evaluate their whole performance. All the involved physical phenomena like moisture, airflow and pollutants should be considered and coupled in order to reproduce the reality with the highest possible level of details.
In this context, this PhD thesis presents the models and the simulations of multi-physics inside buildings using an in-house developed modular and object oriented tool called NEST. All the physics of the coupled heat, moisture, airflow and pollutants transfer that take place inside buildings are considered and solved. In addition, the software allows the simulation of a building system as a collection of different numerical elements, like walls, rooms, HVAC systems, outdoor, etc., connected with each other and able to exchange boundary conditions. In this manner any building configuration can be set and simulated.
The physical and mathematical formulations of the implemented elements are presented. Then, in order to assure the credibility of the developed software, the implemented models are validated and verified with different test cases from the literature. The list of test cases cover all the aspects of heat, moisture, airflow and pollutants transfer in the whole building and it can be used as a reference list for the validation of other buildings simulation tools. Special emphasis is placed on the simulation of buildings performance in real applications. First, the hygrothermal behaviour in different public buildings with different climates conditions are analysed before retrofitting them. Several weak points in the thermal and moisture resistance of the façades layers are identified and thermal and moisture loads before and after the expected retrofitting solutions are evaluated. Second, a residential building (semi-detached house) in Netherlands is simulated and the airflow, heat and CO_2 transfer inside it is studied in order to optimize the energy consumption while maintaining acceptable levels of thermal comfort and indoor air quality.

Contents

1

Introduction

1.1 Current context and motivations

This thesis has been developed within the framework of the collaboration between the Heat and Mass Transfer Technological Center (CTTC) [1] of the Technical University of Catalonia (UPC) and Termo Fluids S.L [2]. The CTTC is dedicated to the research and innovation in the heat and mass transfer and fluid dynamics (CFD). Termo Fluids S.L. is a spin-off founded by members of the CTTC that own TermoFluids and NEST software. This company is devoted to the development of new numerical methods and software tools for High Performance Computing (HPC) applied to thermal systems and equipments.
The collaborative work of both entities has led to a big experience and a large set of numerical tools for the resolution of different physical phenomena such as heat transfer, turbulence, multi-phase flow, HVAC, aerodynamics, etc. Among them, it can be highlighted: CFD&HT-DNS/LES [3–6] and a set of models for simulating fluid dynamics and heat transfer [7–9]. In order to go further and analyze the real-world problems with a high level of details, the need to combine and exploit these computational tools has raised in order to simulate the problems involving multiple physical phenomena simultaneously.
In this context, a parallel object-oriented software platform, called NEST, for the simulation of multiphysics systems has been developed. By means of this new software platform, different physical phenomena of specific applications can be integrated into a single simulation tool. The philosophy of NEST consists on representing the different phenomena involved in a multiphysic problem into elements (source code object). These elements interact with each other and with the surroundings in different ways. Then they can be coupled with each other in order to form a system for a specific application. In this way the same elements can be reused to form a part of a system or another, e.g. The element representing a chamber can be used and coupled with

other elements in order to simulate a system of a building, a compressor or a solar collector and reusing the same code without re-implementing the model each time. This concept allows the NEST source code to be abstract, flexible and can be adapted to any application.
The NEST platform is designed on the basis of the Object Oriented Programming (OOP) and written using the C++ programming language. This is also a key point in the feasibility, usability and sustainability of the code developed in this software. The OOP programming language provides a high level of abstraction and makes the code more readable and easy to maintain and debug [10].
Developing such a platform is a hard task that requires a lot of programming effort. The CTTC and the Termo Fluids researchers have been working on the development of this software during the last decade. Actually, the software platform consists of thousands of code lines that are distributed in several libraries depending on the application and managed by different work teams. In the current context, this PhD thesis presents the development and the application of NEST software for the simulation of multiphysics systems in general and buildings systems in particular.

Towards buildings
Buildings are responsible for more than 40% of global energy use and one third of global greenhouse gas emissions, both in developed and developing countries where the HVAC&R (Heating Ventilating and Air-Conditioning & Refrigeration) systems account for almost half of the energy consumed [11]. As a consequence, many countries have followed energy reduction strategies and have increased the number of building standards that apply more restrictions and requirements to achieve low (or net zero) energy buildings. In EU the requirements include the incorporation of renewable energy, the use of energy efficient appliances and HVAC systems and the certification of all the new buildings as nearly zero energy buildings [12]. In order to fulfill the requirements, computer simulation tools and computational techniques have been used to simulate and study building performance, energy optimization, different construction materials and operation behavior. They can help reducing energy consumption, improving indoor air quality and thermal comfort and provide quantitative data supporting decision making, e.g. choosing the best solution for designing or retrofitting or choosing the optimal HVAC system. That makes building simulation to be involved increasingly in the design, engineering, operation and management of buildings and becoming an indispensable part of building industry.

The development of building simulation tools is traced back to the 1960's and 1970's focusing on building thermal performance, load calculation and energy analysis [13], DOE-2 and BLAST are some of the earliest initiatives codes sponsored by U.S Department of Energy (DOE) and U.S Department of Defense (DOD), respectively

[14]. It is only till the beginning of the 1990s that the focus was changed from the energy consumption to many other building performance characteristics like airflow, ventilation, heating, cooling, etc. [15] and by the end of the 90s, a range of simulation applications were extended from the research community to the professional practice, allowing the appearance of different simulation tools for a variety of users [13]. Currently there are several powerful buildings simulation tools with different levels of complexity and details such as Energy Plus [16], ESP-r [17] and TRNSYS [18]. All of them are able to solve one or different phenomena of heat, airflow, moisture and pollutants transfer within buildings nevertheless they do not involve and combine together all these physics inside one simulation tool [19].
In this context, a library for buildings simulation inside NEST is developed to handle all the possible physics that take place inside buildings in order to be a complete tool that cover and couple together all the features of heat, moisture, airflow, CO_2, VOC, solar radiation, thermal radiation, wind effect, stack effect, HVAC, control system, occupants, etc.

1.2 Objectives

The aim of this thesis is to develop a software in which different elements can be combined in order to produce a computer program for a complete simulation of buildings systems.
The elements have to be implemented in a general way so they can be adapted to any other applications. To do so, the code should be structured in different levels of abstraction, ranging from high level code which are the elements implemented in very abstract concepts (e.g. geometric, mathematical or algorithmic entities) to the low level code which represent the most specific elements (e.g. rooms, walls, openings..).
Furthermore, the sub-library containing the low level code must be intuitive and transparent to the users. It should hide all the complexities of the numerical resolution and coupling details.
Moreover, the software should give the ability to add and test new codes and models and behave as a virtual laboratory and test environment. For that reason, all the implemented models must be assessed and validated with benchmark or reference cases in buildings simulations to ensure always the accuracy and the credibility of the code,. In that manner, a test suite including a collection of different validation cases is created and it should be executed by the developer every time after editing or adding new code in order to detect any functionality problem and ensure the good quality of the simulated results by the software.
Finally, the potential of the developed simulation tool has to be shown and applied in real cases. It is aimed to simulate, in a fast and reliable way, the airflow, heat, moisture

and pollutants transfer in any type of building and lead to several applications like: predict thermal and moisture transfer in buildings materials in order to avoid deterioration and increase thermal and moisture resistances. Simulate and analyse the use of different materials, HVAC systems and control strategies in buildings in order to help in the decision making of the optimum ones and reduce energy consumption. Study the pollutants transfer inside buildings in order to maintain a good indoor air quality while reducing the energy consumption.

1.3 Structure of this thesis

The thesis is structured in four chapters, this introduction and three more chapters as follows.
In chapter 2, the development approach of NEST for buildings simulations is described. Special emphasis is placed on the modelling of buildings physics and their implementation as elements, which is important to create a good buildings simulation tool. The second part of the chapter addresses the validation and the verification of the implemented models with experimental and numerical cases, respectively.
In the remaining two chapters, the potential of the software is illustrated through its application to simulate real existing buildings.
In chapter 3, the NEST is used to simulate and analyse the hygrothermal behaviour of different public buildings (two hospitals in Spain, a school in Sweden and a university in UK) before their retrofitting. The heat, moisture and HVAC simulation of different representative rooms in the buildings has led to identify different problems and weak points in the buildings materials which help to adopt the best retrofitting solution for each building. A parametric study is conducted to place a special emphasis on the importance of moisture simulation in buildings.
Finally, in chapter 4, the airflow, thermal and pollutants transfer in a real residential house located in Lemmer (Netherlands) is simulated and analysed. Different performance simulations have been realized in order to optimize the indoor air quality, energy consumption and control system. An external interactive controller software (based in Python) has been embedded into NEST program in order to test the impact of different control routines on the air quality and the energy performance of the house.

References

[1] Centre tecnològic de transferència de calor. `http://www.cttc.upc.edu/`.

[2] Termo Fluids S.L. `www.termofluids.com`.

[3] F.X. Trias, O. Lehmkuhl, A. Oliva, C.D. Pérez-Segarra, and R.W.C.P. Verstappen. Symmetry-preserving discretization of navier-stokes equations on collocated unstructured grids. *Journal of Computational Physics*, 258:246–267, 2014.

[4] I. Rodríguez, O. Lehmkuhl, R. Borrell, and A. Oliva. Direct numerical simulation of a naca0012 in full stall. *International Journal of Heat and Fluid Flow*, 43:194–203, 2013.

[5] O. Lehmkuhl, I. Rodríguez, R. Borrell, and A. Oliva. Low-frequency unsteadiness in the vortex formation region of a circular cylinder. *Physics of Fluids*, 25(8), 2013.

[6] O. Lehmkuhl, I. Rodríguez, R. Borrell, J. Chiva, and A. Oliva. Unsteady forces on a circular cylinder at critical reynolds numbers. *Physics of Fluids*, 26(12), 2014.

[7] R. Damle. *Modular simulation of thermal systems*. PhD thesis, Universitat Politècnica de Catalunya, 2009.

[8] J. López, O. Lehmkuhl, J. Rigola, C.D. Pérez-Segarra, and A. Oliva. Numerical study of suction gas flow in the shell of hermetic refrigeration compressors. pages 395–404, 2009.

[9] J. Rigola, N. Ablanque, C.D. Pérez-Segarra, and A. Oliva. Numerical simulation and experimental validation of internal heat exchanger influence on co2 transcritical cycle performance. *International Journal of Refrigeration*, 33(4):664–674, 2010.

[10] J. López. *Parallel object-oriented algorithms for simulation of multiphysics. Application to thermal systems*. PhD thesis, Universitat Politècnica de Catalunya, 2016.

[11] L. Pérez-Lombard, J. Ortiz, and C. Pout. A review on buildings energy consumption information. *Energy and Buildings*, 40:394–398, 2008.

[12] European Commission. `https://ec.europa.eu/energy/en/topics/energy-efficiency/buildings`. Last update: 26-04-2017.

[13] A. Baba, L. Mahdjoubi, P. Olomolaiye, and C. Booth. State-of-the-art on buildings performance energy simulations tools for architects to deliver low impact building (LIB) in the UK. *International Journal of Development and Sustainability*, 2(3):1867–1884, 2013.

[14] D.B. Crawley, Lawrie L.K., F.C. Winkelmann, W.F. Buhl, Y.J. Huang, C.O. Pedersen, R.K. Strand, and R.J. Liesen. EnergyPlus: creating a new-generation building energy simulation program. *Energy and Buildings*, 33:319–331, 2001.

[15] G. Augenbroe. Integrated building performance evaluation in the early design stages. *Building and Environment*, 27(2):149–161, 1992.

[16] D.B. Crawley, L.K. Lawrie, C.O. Pedersen, and F.C. Winkelmann. *EnergyPlus: an update*. 2004.

[17] ESP-r. `www.esru.strath.ac.uk`.

[18] Solar Energy Laboratory. *TRNSYS A Transient System Simulation Program*, volume 1. 1994. University of Wisconsin-Madison.

[19] D.B. Crawley, J.W. Hand, M. Kummert, and B.T. Griffith. *Contrasting the capabilities of building energy performance simulation programs*. 2005.

2

Buildings simulation in NEST

2.1 Introduction

The core of all buildings simulation tools is composed of building envelope and indoor space models. The building envelope can be modelled in one, two or three dimensions and one or different phenomena of heat, air and moisture and volatile organic compounds (VOC) transfer through it can be solved. DELPHIN [1], WUFI-Plus [2] and HAM-tools [3] are some of the software focusing in the simulation of combined heat, air and moisture (HAM) transfer in building envelope, while VOC-tools [4] is a tool just focused on the simulation of VOC transfer in the envelope. The indoor space model can include one or different phenomena of airflow, heat, moisture and pollutants transfer and it can be modelled with a granularity going from a very fine-grained method using computational fluid dynamics (CFD) to a fine-grained method using zonal method or to an intermediate-grained method using multi-zone [5]. First, the CFD method, adopted in software like FLUENT [6] and COMSOL [7], is applied to provide a detailed visual and quantitative results of the air movement and distribution inside a space, although it requires high computational resources and it is not practical for simulating complex building during a long period of time. Second, the zonal method in building simulation is based on subdividing a single room into a number of sub-zones in which air parameters are assumed to be homogeneous. It is reviewed by Megri and Haghighat [8] and integrated in software such as SimSPARK [9]. Finally, the multi-zone method assumes a uniform air temperature, pressure, humidity and contaminants concentration (VOC and CO_2) in a room, the air movement inside the same room is neglected, which makes it much faster than CFD and zonal methods and the most used approach for modeling heat and mass

transfer in indoor spaces. It is adopted in software like COMIS [10], CONTAM [11], AIRNET [12], ASCOS [13] and BREEZE [14].

All the buildings simulation tools need to be validated and verified in order to assure a certain level of a credibility and simulation quality. The validation of a building simulation tool is a long and continuous process. There have been many international efforts to develop test cases for building simulation, such as those developed within the International Energy Agency Annexes (IEA), within different research and experimental projects or within software development [15]. Most of the references in the literature are classifying test cases by the phenomena that they are solving. Each set of test cases is focusing on the validation of a specific phenomena inside the building (e.g, HAM, energy, VOC, airflow, etc.). Such as for the validation of the combined HAM transfer in building envelope, different benchmark and experimental test cases are presented by Hagentoft [16] and by authors like Van Belleghem [17], Maalouf [18] and Talukdar [19].
For the validation of thermal model in the whole building (both envelope and indoor space), ASHRAE standard 140-2001 [20] based on BESTEST presented different cases for the validation of energy in buildings and HVAC equipments, while IEA Annex 41 [21] included test cases for the validation of coupled HAM transfer model in the whole building.
For the airflow model, the evaluation of COMIS presented in IEA Annex 23 [22] shows different validation cases for the multi-zone indoor ventilation.
For the pollutant VOC transfer model, authors like Yang [23], Huang [24], Cheng [25] and Xiong [26] have studied and presented experimental validation cases for different building materials and different VOC species.
As shown above and explained by Strachan [27], references and studies are focusing on the validation of specific models inside buildings however there is a lack of references presenting validation cases including together all the physical phenomena inside buildings.

The NEST building simulation tool is developed to perform dynamic simulations of all the phenomena that take place inside buildings, such as HAM and VOC transfer in building envelope, multi-zone airflow, heat, moisture and pollutants transfer in rooms, solar radiation gains through windows and walls, thermal radiation exchange between walls, wind and stack effects, HVAC systems and their control, and occupants presence and activities.
In this chapter, all the implemented models for buildings simulation are presented and then the numerical resolution within NEST is described. The simulation tool is verified and validated with a test suite of significant and simple to implement reference cases for building assessment. As mentioned above, there is a lack of references presenting

the validation cases of all the building physics altogether. Therefore the test cases in this thesis have been selected from different references in a manner that they cover all the physical phenomena of airflow, heat, moisture and pollutants transfer in the whole building. Hence the test list can be used as a reference test suite for the validation of any other building simulation tools.

2.2 Modelling of a building system

A library for buildings simulation inside NEST has been developed within this thesis, it contains a set of elements able to solve the models of airflow, heat, moisture and pollutant transfer in the whole building. The Figure 2.1 shows the two basic models inside buildings, which are the building envelope and the indoor sapace. They are the core of buildings simulation software since they allow the resolution of heat, moisture, airflow and pollutants transfer.

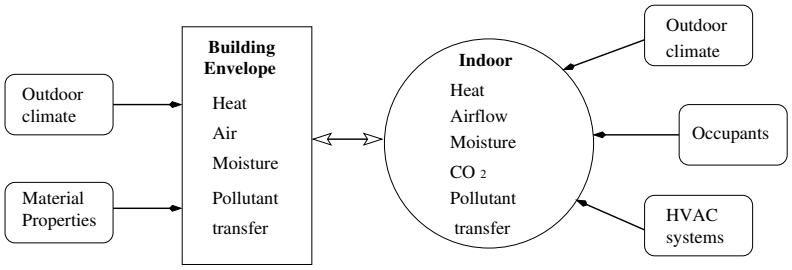

Figure 2.1: Overall model of a building in NEST software.

The implemented elements provide an abstraction of these basic models, equipments (e.g., HVAC systems), boundary conditions (e.g., outdoor), events (e.g., occupants activities). The elements are implemented in a low level code, as described in the first chapter, in order to be transparent to the users. Table 2.1 shows the implemented elements in the library, their application inside the building, a description of the modelled phenomena and the other elements that can be connected with.
Therefore, the whole building in NEST is reduced into a set of elements connected with each other and able to exchange boundary conditions. In this way, a network of elements can be arranged in order to create an overall model of the building. This is illustrated in Figure 2.6, where a room and its conceptual graph using NEST are shown.

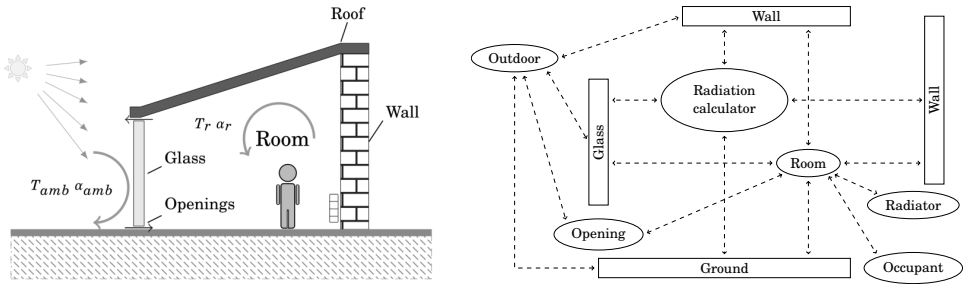

Figure 2.2: Modelling a room in NEST software.

Table 2.1: Elements implemented inside the building library of NEST.

Element	Application	Model description	Connections
Room	Rooms, air cavity into composite wall or window	Resolution of airflow and heat, moisture, CO_2 and VOC transfer using multi-zone method.	Wall, Duct, Opening Radiator, Occupants
Opening	Doors, windows, gaps and orifices	Evaluation of the mass flow rates through small or large openings.	Room, Outdoor
Duct	Ventilation tubes	Evaluation of the mass flow rate inside ducts.	Room, Outdoor, Duct Ventilation box
Ventilation box	Mechanical ventilation systems	Creation of pressure drop using one or several fans to extract or inject air in a building.	Duct
Wall	Walls, composite walls, glasses, multi-glasses	Resolution of transient one-dimensional heat, air, moisture and VOC transfer.	Room, Outdoor, FSolD Wall, RadBox
FSolD	Transmitted solar radiation	Distribution of the transmitted solar radiation among the room internal surfaces.	Wall
RadBox	Thermal radiation	Evaluation of the thermal radiation transfer between the room internal surfaces.	Wall
Outdoor	Weather conditions	Provide weather data conditions.	Wall, Opening, Duct
Radiator	Heating elements	Introduction of heat source gain.	Room
Boiler	Central heating system	Supply of heated water flow inside radiators.	Radiator, Room
Controller	HVAC control	Control of the heating set point temperature and the mechanical ventilation speed.	Boiler, Ventilation box
Occupants	Occupants behaviour	Creation of events and generation of heat, moisture and CO_2 gains.	Room

2.3 Building elements

2.3.1 Wall

The wall element is used to simulate the building envelope, it is the physical separator between the interior and the exterior of a building. Most building materials are porous, so the air and moisture transfer through the wall pores can cause significant effects in thermal performance, indoor air quality and material durability. The wall is modelled in general way, the heat, air, moisture and VOC transfer models are presented in this section. Specific types of walls like glass, composite wall and composite glass are described as well.

Heat, air and moisture transfer in a wall

The wall model solves the coupled HAM transfer through the wall layer. The moisture is transported inside the porous wall under vapour and liquid phases where the total moisture flow rate is:

$$g_m = g_{m,v} + g_{m,l} \tag{2.1}$$

The water vapour is diffused due to partial vapour pressure gradient while the liquid is sucked due to suction pressure gradient. The water vapour flow consists of a diffusive part (first term) and a convective part due to the airflow inside the wall (second term) [28]:

$$g_{m,v} = -\delta_p \frac{\partial p_v}{\partial x} + g_{air} C_{cst} p_v \tag{2.2}$$

where C_{cst} is a constant for approximating the water vapour content function of vapour pressure $C_{cst} = 6.21 \cdot 10^{-6}$ [29]. The liquid flow through the wall is proportional to the gradient of suction pressure and it is expressed as [30]:

$$g_{m,l} = k_l \frac{\partial p_s}{\partial x} \tag{2.3}$$

The transient moisture balance through the wall is then written as:

$$\frac{\partial w}{\partial t} = -\frac{\partial g_m}{\partial x} = -\frac{\partial}{\partial x}\left(k_l \frac{\partial p_s}{\partial x} - \delta_p \frac{\partial p_v}{\partial x} + g_{air} C_{cst} p_v\right) \tag{2.4}$$

This equation can be expressed using different driving forces: moisture content w, suction pressure p_s, vapour partial pressure p_v or relative humidity ϕ. The relative humidity ϕ is chosen for this model since it is continuous at the interface between multi-layered walls [31]. The moisture transport equation through the wall can be then rewritten as a function of the relative humidity:

$$\xi \frac{\partial \phi}{\partial t} = D_\phi \frac{\partial^2 \phi}{\partial x^2} + D_T \frac{\partial^2 T}{\partial x^2} - C_\phi \frac{\partial \phi}{\partial x} - C_T \frac{\partial T}{\partial x} \tag{2.5}$$

where

$$D_\phi = \delta_p p_{sat} + \frac{k_l \rho_l R}{M_w} \frac{T}{\phi}; \qquad D_T = \delta_p \phi \frac{\partial p_{sat}}{\partial T} + \frac{k_l \rho_l R}{M_w} \ln \phi \tag{2.6}$$

$$C_\phi = g_{air} C_{cst} p_{sat}; \qquad C_T = g_{air} \phi \frac{\partial p_{sat}}{\partial T} \tag{2.7}$$

The liquid water density ρ_l is assumed to be 1000 kg/m^3. D_ϕ represents the moisture diffusion coefficient, D_T the moisture diffusion due to the temperature gradient, C_ϕ the moisture convection coefficient and C_T the moisture convection due the temperature gradient.
The heat flux through the wall combines conductive and convective parts:

$$q = q_{cond} + q_{conv} \tag{2.8}$$

The conductive part is proportional to the gradient of the temperature:

$$q_{cond} = -\lambda \frac{\partial T}{\partial x} \tag{2.9}$$

while the convective part is the sum of latent specific enthalpy flow of the vapour and the sensitive specific enthalpy flow of the air inside the material:

$$q_{conv} = -L_v \delta_p \frac{\partial p_v}{\partial x} + g_{air} c_{p,a} T \tag{2.10}$$

where the mass specific phase transition enthalpy water liquid-vapor L_v is assumed to be $2.5 \cdot 10^6 J/kg$.
The heat balance through the wall is then given by the relation:

$$\rho_0 c_{p0} \frac{\partial T}{\partial t} = -\frac{\partial q}{\partial x} = (\lambda + L_v D_{T,v}) \frac{\partial^2 T}{\partial x^2} + L_v D_{\phi,v} \frac{\partial^2 \phi}{\partial x^2} - C_T \frac{\partial T}{\partial x} \tag{2.11}$$

where

$$D_{T,v} = \delta_p \phi \frac{\partial p_{sat}}{\partial T}; \qquad D_{\phi,v} = \delta_p p_{sat}; \qquad C_T = g_{air} c_{p,a} \tag{2.12}$$

By observing equations (2.5) and (2.11) it can be seen that in a porous wall the moisture transport equation depends on the heat transfer equation and vice versa. So, both equations are coupled and they need to be solved simultaneously at each node of the discretized wall, as shown in Figure 2.3, using an iterative process to completely solve heat, air and moisture transfer in the building envelope with single or multiple material layers.

The coefficients λ, c_{p0}, ξ, δ_p and k_l depend on the temperature and moisture distribution in the material [29]. If only the heat transfer is taken into account, the coefficients g_{air}, δ_p and k_l are set to zero in order to neglect air and moisture transfer through the wall and the equation reduces to the transient conduction equation.

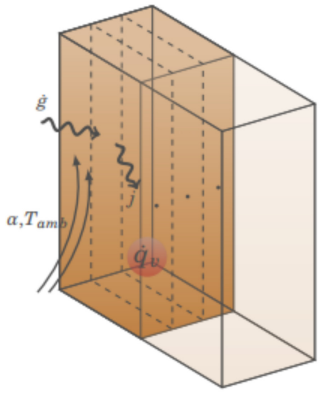

Figure 2.3: Wall element.

VOC pollutant transfer in wall

The VOC pollutant transfer in a wall is modelled as the diffusion of the concerned species which may be emitted by the building material. Concentration gradient is the driving force for VOC transport in the material with no chemical reaction inside. The transient VOC diffusion equation is given by:

$$\frac{\partial C_{voc}}{\partial t} = D_{voc} \frac{\partial^2 C_{voc}}{\partial x^2} \tag{2.13}$$

where D_{voc} is the VOC diffusivity and depends on the pore structure, the material, species properties, temperature and the VOC concentration in the material [23]. The governing equation is descritized and solved at each node of the wall of Figure 2.3.

Glass

By default the wall material is assumed to be opaque having an absorptivity, a reflectivity but a nil transmissivity. However, semi-transparent materials, like glasses, can be also considered by setting these optical properties (absorptivity, reflectivity

and transmissivity). In this case, the solar energy absorbed is introduced as uniform heat generated over the volume of the glass layer instead of being absorbed by the surface. The values of absorptivity, reflectivity and transmissivity are inputs that depend on glass material properties. With reference to Figure 2.4, the solar radiation is divided into two components: positive component IP entring the building and negative component IN leaving the building. The net transmitted solar radiation is calculated using an iterative process [32] taking into account the room, outdoor solar radiation and reflectivity at each side.

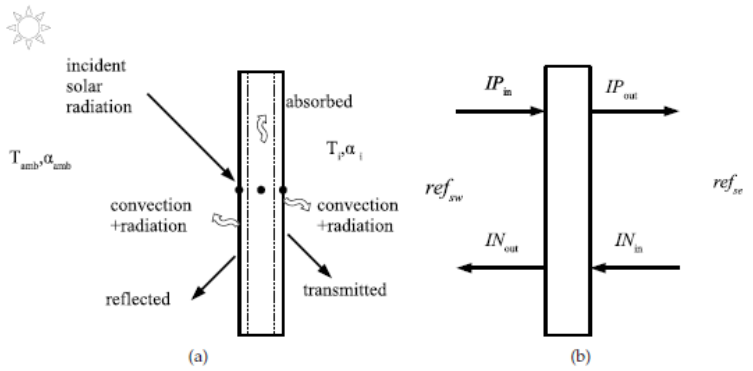

Figure 2.4: Glass element (a) transparent glass with heat transfer; (b) positive IP and negative IN components for solar radiation calculation.

Composite wall

NEST enables to arrange several elements and compact them as they were a single element. These types of elements are called sub-systems. Hence, several walls of different materials can be packed into a unique composite wall element. This is an appealing property of NEST, since it enables to deal with different walls layers in a building as a simple composite wall element.
When a wall is composed of two or more layers, the heat and moisture transfer through each one is described with the transport equations of the section 2.3.1. In the interface the contact is assumed to be perfect by neglecting the moisture and thermal contact resistances between the porous materials. In this way the temperature and the suction pressure are assumed to be continuous at the surface between two different materials.

Composite glass

The same concept of the composite wall is exploited for simulating multilayer glasses with inner air chambers (e.g. double/triple pane) as shown in the Figure 2.5. Composite glass is a sub-system of N Glasses and N-1 rooms.

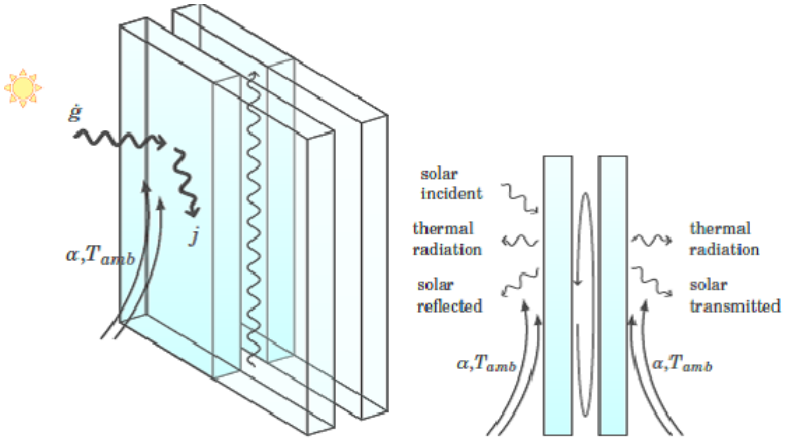

Figure 2.5: Multi-glass element.

The thermal radiation between the glass layers is approximated as the heat transfer between two infinite opaque parallel plates [33]. Heat transfer by natural convection between the glass layers is calculated as it will be shown in the room model (section 2.3.2) using the energy equation 2.15.

2.3.2 Room

The room element is used to simulate the indoor spaces, it is based on the multi-zone method where the building is divided into different zones, where each zone represents a room or a set of rooms. A room (or zone) is modelled using one control volume (CV), as shown in Figure 2.6, having a node P in the centre that contains air at uniform conditions of pressure, temperature, humidity, VOC and CO_2. The room can exchange boundary conditions with walls, openings (doors, windows, orifices, ducts,...) and have internal generation gains of heat, moisture, CO_2 and VOC from different sources like radiators, occupants, appliances, etc. The openings are responsible for evaluating the airflow rates incoming/leaving the room from/to its neighbours rooms and they are represented by nodes k at the sides of the room CV.

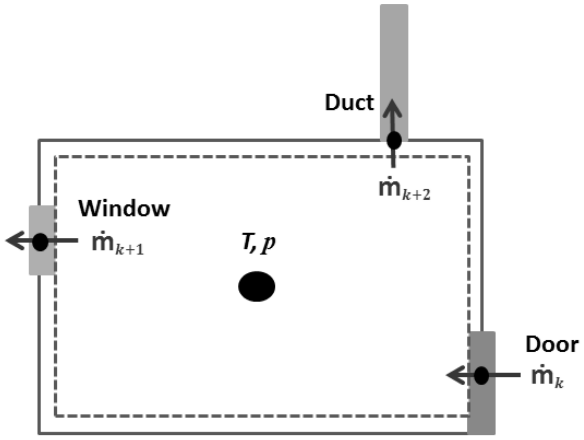

Figure 2.6: Room control volume surrounded by walls and openings.

The continuity, energy, humidity, CO_2 and VOC pollutant equations over the CV are written, respectively, in general terms as:

$$\frac{\partial m_P}{\partial t} = \sum_{k\in\text{in}} \dot{m}_k - \sum_{k\in\text{out}} \dot{m}_k \tag{2.14}$$

$$m_P c_{p,a} \frac{\partial T_P}{\partial t} = \sum_{k\in\text{in}} \dot{m}_k c_{p,a}(T_k - T_P) + \sum_{i\in\text{walls}} \alpha_i A_i (T_{wall,i} - T_P) + Q_{src} \tag{2.15}$$

$$\rho V \frac{\partial x_P}{\partial t} = \sum_{k\in\text{in}} \dot{m}_k (x_k - x_P) + \sum_{i\in\text{walls}} \beta_i A_i (P_{v,wall,i} - P_{v,P}) + M_{src} \tag{2.16}$$

$$\frac{\partial m_P C_{co_2,P}}{\partial t} = \sum_{k\in\text{in}} \dot{m}_k (C_{co_2,k} - C_{co_2,P}) + C_{co_2,src} \tag{2.17}$$

$$\frac{\partial m_P C_{voc,P}}{\partial t} = \sum_{k\in\text{in}} \dot{m}_k (C_{voc,k} - C_{voc,P}) + \sum_{i\in\text{walls}} \beta_{voc,i} A_i (C_{voc,wall,i} - C_{voc,P}) + C_{voc,src} \tag{2.18}$$

The equations account for the ventilation inside the room, the heat, moisture and VOC fluxes from the walls and the internal heat, moisture, CO_2 and VOC generation from occupants and appliances sources.
The airflow and the heat transfer are dependent: Airflow has a direct impact on the heat transfer by convection between rooms and heat transfer has an impact on the

gradient of air density between rooms which affects the airflow rates due to natural convection. Moreover the airflow in the building affects directly humidity, CO_2 and VOC transfer, since a high ventilation rate in a room leads to a high transport of mass and thus it decreases or increases the humidity and CO_2 and VOC concentrations. Hence a coupled resolution between heat, air and mass transfer in building is necessary [34].

2.3.3 FSolD

The FSolD object, which stands for Fictitious Solar radiation Distributor, takes the net transmitted solar radiation from the glazed windows of a room to set the total radiation per unit area. The aim of this object is to distribute this heat input between the floor and the internal walls of the room.

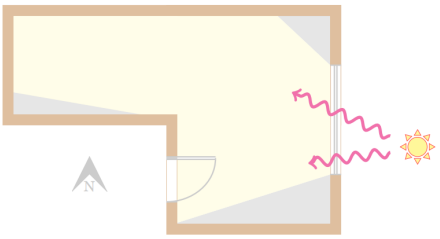

Figure 2.7: Conceptual graph of FSolD element.

2.3.4 RadBox

The RadBox object (radiative box) is used for evaluating the thermal radiation fluxes between the wall surfaces of a room. Every surface of the room gives its temperature and its emissivity to the RadBox. Then, the element calculates the view factors in order to evaluate the thermal radiation corresponding to each surface by means of the Net Radiation Method [35]. The element is able to calculate the view factors of non-cubic geometries, considering shadows and the windows in the walls.

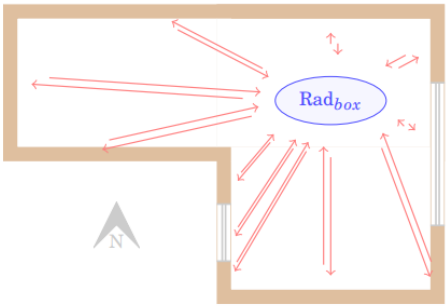

Figure 2.8: Conceptual graph of RadBox element

2.3.5 Opening

The opening is an element that connects two rooms or a room with outdoor where the air circulates through it from one space to another. It can be either one-way opening where the air circulates only in one direction or double-way opening where the air circulates in one or both directions at a time. The two types of openings models are presented below.

One-way opening

The one-way opening (also called orifice, small opening or unidirectional opening) model is used to simulate orifices, cracks and gaps through closed windows and doors. It is considered to be a restriction for the air flow between two rooms since the cross-section area of the opening is usually smaller than the cross-section area of the room (Ar) (see Figure 2.9).

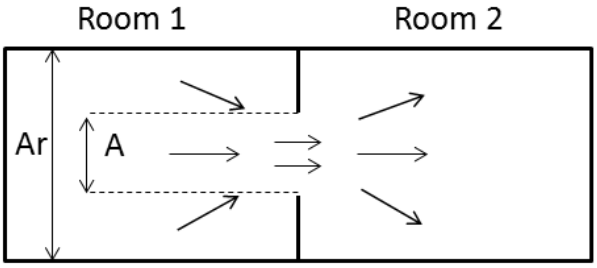

Figure 2.9: Airflow through one-directional opening.

As long as the air speed is sufficiently subsonic in buildings (Mach < 0.3), the incompressible Bernoulli equation for orifices [36] is used for the description of the pressure drop through the one-way opening as a function of the air velocity. By considering the relation between mass flow rate and velocity, the mass flow rate expression through one-way opening function of the pressure difference between two linked rooms i and j can be written as:

$$\dot{m} = C_d A_s \sqrt{2\rho|p_i - p_j|} \tag{2.19}$$

The density ρ is taken from the upstream room, C_d is the discharge coefficient that accounts for the viscosity, turbulence and the opening geometry. Different approximations and correlations exist in the literature for the discharge coefficient in buildings. All of them indicate that the coefficient value range goes from 0.25 up to 0.7 [37]. The default value of C_d coefficient in NEST is fixed to 0.6. The equation 2.19 is used by default in NEST to model small openings, however the empirical power law equation can be also used if desired [38]:

$$\dot{m} = \rho C|p_i - p_j|^n \tag{2.20}$$

where the flow coefficient C depends on the size of the opening while the flow exponent n characterises the flow regime and lies between 0.5 (fully turbulent) and 1.0 (fully laminar).

Double-way opening

The double-way opening (also called large opening) can have simultaneous flows circulation in both directions. This can be due to temperature stratification, density gradients, effects of ventilation or heating systems and turbulence effects in the rooms. Due to the high number of parameters involved and the complexity of the physical phenomena, the following assumptions were made in order to simplify and describe the phenomena as an application of the continuity equation and Bernoulli's theorem on both sides of the large opening [39]: Each room is considered as a semi-infinite volume, streamlines of the flow in the opening are assumed to be parallel and horizontal and a steady flow of an incompressible and inviscid fluid is driven only by density gradients on both sides of the opening.

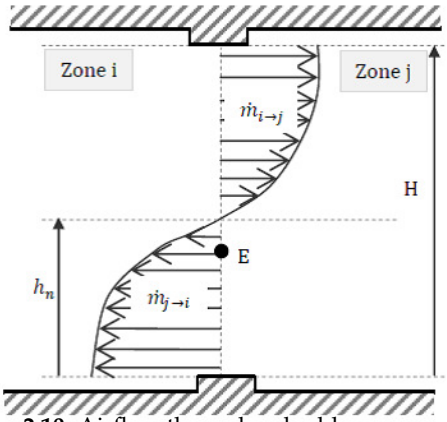

Figure 2.10: Airflow through a double-way opening.

The neutral plan h_n as seen in Figure 2.10 is defined as the height inside the opening where the pressure difference between both sides is zero, so it is the level where the flow change its direction and is calculated as:

$$h_n = \frac{p_j - p_i}{g(\rho_j - \rho_i)} \tag{2.21}$$

where the subscripts i and j refer to the rooms at both sides of the opening.

In the case where the densities of air on either sides of the opening are equal, equation (2.21) tends to infinity and there is no air circulation driven by density gradient. In this case the opening is assumed to have the same behaviour as a one-way opening and it is modelled using equation (2.19) as described in the subsection 2.3.5.

In the case where the densities on either sides of the opening are different, the possible situations that can occur are:

- If $0 < h_n < H$ the neutral plan is located inside the opening and air flow circulation is bi-directional, as shown in Figure 2.10. The absolute value of mass flow rates at the top and the bottom of the opening can be written as [40]:

$$\dot{m}_{top} = \frac{2}{3} C_d W \sqrt{2g\rho|\Delta\rho||H - h_n|^3} \tag{2.22}$$

$$\dot{m}_{bottom} = \frac{2}{3} C_d W \sqrt{2g\rho|\Delta\rho||h_n|^3} \tag{2.23}$$

- If $h_n \leq 0$ or $h_n \geq H$, the neutral plan is located outside the opening, so the airflow circulation is one-directional. The absolute value of mass flow rate is then evaluated as [41]:

$$\dot{m} = \frac{2}{3} C_d W \sqrt{2g\rho|\Delta\rho|} \quad \left| |H - h_n|^{\frac{3}{2}} - |h_n|^{\frac{3}{2}} \right| \tag{2.24}$$

The air density in the mass flow equations (2.22), (2.23) and (2.24) depends on the direction of the flow. A sign is attributed to the mass flow rates depending on the sign of $\Delta\rho$ to indicate the direction of the flow (positive if entering and negative if leaving a room).

Connection of the opening with a room

As described in subsection 2.3.2, using the multi-zone method the pressure is assumed to be uniform in all the room. However, the pressures used to evaluate the mass flow rates through the openings should take into account the static and the dynamic effects of the air due to thermal buoyancy and wind action, respectively.
When an opening is linking two rooms, the wind effect is neglected and only the thermal buoyancy is taken into account. This is illustrated in the example presented in Figure 2.11, where an opening is located at a height H_{1-2} for the room 1 and room 2. The ground of the room is assumed to be the reference level of the hydrostatic pressure. For each room the pressures p_1 and p_2 at the height of the opening are different than the pressures at the node of each room, p_{P1} and p_{P2}, and they depend on the elevation and the air density.

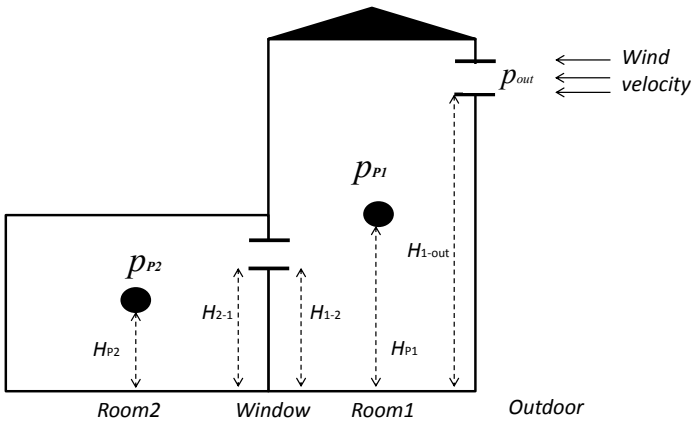

Figure 2.11: Static and dynamic effects through openings in a building (front view).

The pressure at the opening side of the room i linking with the room j, can be

expressed in general form as:

$$p_i = p_{Pi} - \rho_i g(H_{i-j} - H_{Pi}) \tag{2.25}$$

If the opening is linking a room with the outdoor as shown in Figure 2.11, then the wind effect should also be taken into account by introducing the dynamic pressure term. The pressure p_{out} at the outdoor side of the opening is given by:

$$p_{out} = p_{ext} + \frac{1}{2}\rho_{ext}{v_{ext}}^2 \tag{2.26}$$

where p_{ext} and v_{ext} are the ambient pressure and wind velocity given by the weather conditions.

2.3.6 Duct

The duct is an element that can link two rooms, a room with outdoor or it can be used for the ducts of mechanical ventilation. In NEST the duct element is designed in a general way, so that it can be applied to simulate pipe lines for any application in general. It is implemented using two models:
First, the detailed model where the duct is discretised into a number of control volumes that take into account heat and mass transfer, shear stress and expansion/contraction phenomena. This approach gives us the ability to perform a detailed simulation of a duct and to have a full simulation of the fluid flow inside it.
Second, the simplified model where the duct is considered as an element that only applies pressure losses between its two connections. In this way, only the entring and the leaving flow rate is evaluated.

Detailed duct

The duct in this approach is discretized into a number of control volumes where continuity, momentum, energy and pollutants equations of the fluid flowing through it are solved. The continuity, energy and pollutants equations are solved over a centered mesh where the pressure and temperature values are evaluated in the node of the main control volume. On the other side, the momentum equation is solved over a staggered mesh where the velocity values are evaluated at the faces of the centered control volumes, as shown in Figure 2.12.

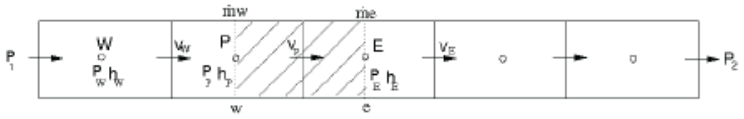

Figure 2.12: Detailed duct discretization.

The continuity, energy and pollutants equations over each control volume of the duct are the same as described in the room section 2.3.2. By considering the local shear stress in terms of friction factor, the momentum equation in the axial direction over the staggered mesh of the duct can be written as:

$$\frac{\delta m_P v_P}{\delta t} = \sum \dot{m}_e v_e - \sum \dot{m}_w v_w = (p_P - p_E)S - \frac{f}{4}\frac{|\dot{m}_P| v_P}{2S} A_p \tag{2.27}$$

where the subscripts w and e indicate the west and the east faces of the CV in the flow direction and W end E indicate the west and the east CV nodes, respectively. The friction factor f is evaluated as a function of the Reynolds number from the correlation of Churchill [42], S is the section area, and Ap is the surface area of the duct. The continuity and momentum equations are coupled and solved by means of SIMPLE solver (Semi Implicit Method for Pressure Linked Equations) [43].

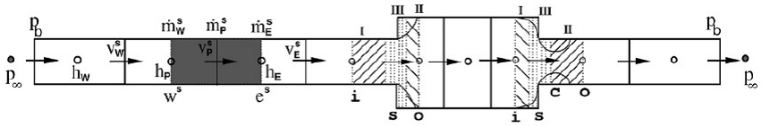

Figure 2.13: Expansion/contraction in a duct.

In this model the sudden expansion/contraction phenomena across the boundary of the duct when it is linked with a room, fan or with another duct is taken into account, the momentum equation across the expansion/contraction can be written in terms of mass flow rate in a general form as [44]:

$$\dot{m} = \frac{N\Delta p + H + \frac{l\dot{m}^o}{\Delta t}}{M} \tag{2.28}$$

where $N = S^s$, $H = max(\dot{m}_w, 0)v_W + max(-\dot{m}_e, 0)v_E + {v_s}^o \frac{m^{Io} + m^{IIo}}{2\Delta t}$ and M is equal to all transient, convective and shear stress terms for the zone I, II and III shown in Figure of duct expansion 2.13.

When the duct is connected to a room, The evaluated mass flow using (2.28) is given as an input to the room element in order to satisfy the mass conservation in equation (2.14).

Simplified duct

This approach consists on modelling the duct as an element that applies pressure losses between its two connections where the total pressure loss is the sum of friction, fittings and hydrostatic losses. Friction losses represent the resistance to the airflow due to the viscous shear stresses, the roughness of the internal duct walls and the geometry form [45]. It is calculated using Darcy-Weisbach equation [45] as:

$$\Delta p_{fric} = f_D \frac{L}{D_H} \frac{1}{2} \rho v^2 \tag{2.29}$$

where the Darcy friction factor f_D depends on the characteristics of the duct (hydraulic diameter and roughness height) and the characteristics of the flow regime (laminar or turbulent). In NEST it is evaluated using Churchill correlation [42].
In addition to the friction losses, additional minor losses due to entries and exits of the air, fittings, valves and bends are considered. These losses represent an additional energy dissipation in the flow and a pressure drop that can be calculated as [40]:

$$\Delta p_{fit} = \xi \frac{1}{2} \rho v^2 \tag{2.30}$$

where the coefficient of pressure loss ξ is given by the manufacturers or by formulations in catalogues [46].
The hydrostatic loss represents the pressure drop when there are differences in elevation from the inlet end to the outlet end of the duct segment and it is zero in horizontal ducts.

$$\Delta p_{hydro} = \rho g \Delta h \tag{2.31}$$

where Δh is the vertical elevation or drop.
Finally, the total pressure losses in a duct system is evaluated as the sum of friction, fittings and hydrostatic losses. Substituting the air velocity in equations (2.29) and (2.30) by the mass flow rate, the total pressure drop in a duct can be written as:

$$\Delta p_{tot} = \Delta p_{fric} + \Delta p_{fit} + \Delta p_{hydro} = \left(f_D \frac{L}{D_H} + \sum \xi \right) \frac{1}{2} \rho \left(\frac{\dot{m}}{\rho A} \right)^2 + \rho g \Delta h \tag{2.32}$$

The mass flow rate through a duct is determined from equation (2.32) as a function of the pressure difference in both sides of it. When it is connected to a room or a

ventilation box, this mass flow rate is given as an input to these elements in order to satisfy the mass conservation inside them in equation (2.14). When it is connected to an outdoor element the ambient pressure is given as a boundary condition to the duct.

2.3.7 Ventilation box

A ventilation box is an element that model the mechanical ventilation system, it is modeled as a room element that contains one or more fans and it can be connected with several ducts. Different mechanical ventilation systems exist in buildings, the most used ones and implemented in NEST library are the single flux system (or exhaust system) where the air is only extracted from the building and the double flux system where the air is extracted and injected in the same time. In both cases, one or several fans are used to create a pressure gradient in the ventilation box forcing a depression or an overpressure to force the air circulation in the house.
A fan is characterized by its performance curve, its efficiency and its pressure drop coefficient. These parameters are usually provided by the manufacturers. The performance curve of a given fan shows the relationship between the air flow rate that can deliver and the pressure gradient generated for each rate. This curve is modelled in NEST as a polynomial function of the mass flow rate $\Delta p = f(\dot{m})$.

Single flux system

In a single flux system, the air is extracted from the building by a centralized exhaust fan. The building is put into depression and then the air is forced to flow from outside to inside the building by infiltration through the openings as shown in Figure 2.14. This system allows the extraction of pollutant air from the rooms. However it increases infiltrations, increases pollutant coming from outdoor and increases the thermal losses as the heated/cooled air in the room is extracted and rejected to outside without any thermal recovery.

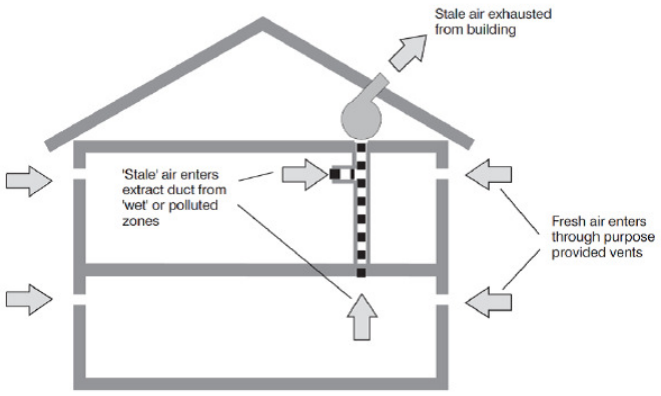

Figure 2.14: Exhaust mechanical ventilation system.

Double flux system

The mechanical ventilation with a double flux system combines the injection and the extraction of air in the building. It is composed of two independent fans, one for the injection of clean air and the other for the extraction of indoor poor air, as shown in Figure 2.15.
This system allows the control of the injected air flow in the building, the air flows through a thermal recovery unit where it can be pre-heated or pre-cooled before its injection. A part form the thermal energy of the extracted air is recovered using a heat exchanger. It allows to filter the injected air from pollutants. This system guarantees a high quality of ventilated air, reduce infiltrations and increase the energy performance in the building.

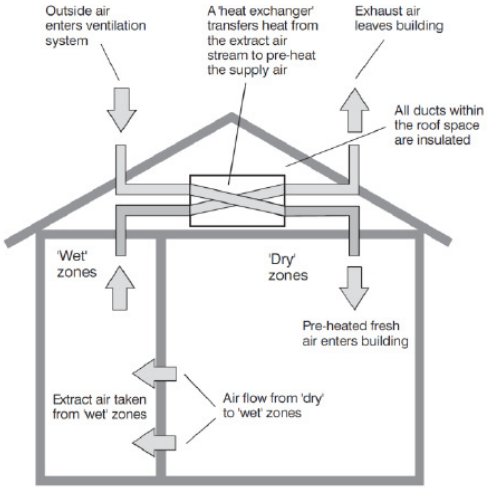

Figure 2.15: Double flux mechanical ventilation system.

2.3.8 Outdoor

The outdoor element provides a database of weather conditions during the simulation of the building. It provides ambient conditions of temperature, solar radiation, humidity, pressure, wind speed and CO_2 concentration. Wind speed and solar irradiation on the façades are evaluated depending on the orientation and the slope of each one. The meteorological data is obtained from Meteonorm software [47] then the data are interpolated during the simulation every time step.

2.3.9 Occupants

NEST software includes occupants elements to take into account heat, moisture and CO_2 generation due to their presence and activities. The amounts of heat and CO_2 generated by the occupants are introduced as a source term in the energy and CO_2 balance equations in the room.
During the simulation of a building, the dynamic behaviour of occupants is taken into account, they can change their activities (sleeping, reading, taking shower..), move from one room to another, leave the building and create events (open doors or windows, switch on ventilation systems, cooking, etc.) which can cause variation in the building performance simulation.

The dynamic behaviour is achieved by means of schedule databases. The software is continuously updating these database every time step for detecting any changes or new events in the building.
The metabolic rate of different occupants activities and the CO_2 generation rate per person are presented in Tables 2.2 and 2.3.

Activity	**Metabolic rate (W)**
Sleeping	83
Seated relaxed	104
Standing, sedentary activity (office,studying)	126
Shaving, washing and dressing	180
Cooking, washing dishes	261
Washing by hand, ironing	306
Gymnastics	574

Table 2.2: Metabolic rate of different occupants activities.

Activity	CO_2 **emission** (m^3/h)
Sleep	0.013
Resting or low activity work	0.02
Normal activity work	0.08-0.13
Hard activity work	0.33-0.38

Table 2.3: CO_2 generation rate per person.

2.3.10 Radiator

The radiator element is used for heating specific zones in the building where the heat power is obtained from a boiler. The heat generated by a radiator is introduced as a heat source term in the energy balance of the room element and it is computed iteratively using the following two equations:.

$$\dot{Q} = \dot{m} c_p (T_{wi} - T_{wo}) \tag{2.33}$$

$$\dot{Q} = \dot{Q_{50}} \left(\frac{\Delta T}{50} \right)^n \tag{2.34}$$

where $\dot{m}$ is the water mass flow rate given by the boiler (it is assumed the same mass flow rate for all radiators in the house), c_p is water heat capacity, T_{wi} is water temperature at the entrance of the radiator and is given by the boiler, T_{wo} water

temperature at the exit of the radiator, $\dot{Q_{50}}$ is the heat emitted by the radiator according to the standard UNE EN-442 [**?**] test and is found in radiators catalogs, n is the characteristic curve coefficient and found in the catalogs too and ΔT is computed as:

$$\frac{\Delta T_{out}}{\Delta T_{in}} = \frac{T_{wo} - T_{amb}}{T_{wi} - T_{amb}} \tag{2.35}$$

$$\frac{\Delta T_{out}}{\Delta T_{in}} \geq 0.7 \quad \text{then} \quad \Delta T = \frac{T_{wi} + T_{wo}}{2} - T_{amb} \tag{2.36}$$

$$\frac{\Delta T_{out}}{\Delta T_{in}} < 0.7 \quad \text{then} \quad \Delta T = \frac{T_{wi} - T_{wo}}{\ln(\frac{\Delta T_{in}}{\Delta T_{out}})} \tag{2.37}$$

where T_{amb} is the ambient temperature, while the inlet temperature is provided by the boiler, the outlet temperature is an unknown. The system of equations with the T_{wo} and $\dot{Q}$ as unknowns is solved iteratively.

2.3.11 Boiler

The boiler element connects with the radiators of a building and provides them with heat power. Based on the temperature of a reference room in the building, the boiler starts operating when the temperature of that room is below a set-point value. The same mass flow rate of heated water is given to all the radiators. While it takes some time to warm up, during this period, the temperature at the entrance of the radiators grows linearly with the time.

2.3.12 Controller

The controller is responsible for controlling the boiler and the mechanical ventilation set point temperature and fan speed, respectively. During the simulation, the controller updates these set points values according to a schedule related to the occupants presence. Other external controller software that works based on complex and advanced routines can be also embedded into NEST software.

2.4 Numerical resolution

The different elements of buildings, described in the previous section, are located in a sub-library of low level code in order to be transparent and easy to use by any user. On the other side, the resolution of the overall model of a building (composed of different elements) is done in a sub-library of high level code. The resolution is based on a block-Jacobi method where every element is solved in an independent

way according to its own physics, model and scale. Once all the elements have been iterated, the program synchronize their inputs/outputs and exchange data with their neighbouring (connected) elements. This process is repeated till the convergence of all the elements is achieved. Then the program checks for any new events, changes in the schedules of openings, occupants or control systems before moving to the next time step. The global resolution algorithm of the software is summarized in Figure 2.16, where ϕ represents all the solved variables of temperature, pressure, humidity and concentrations.

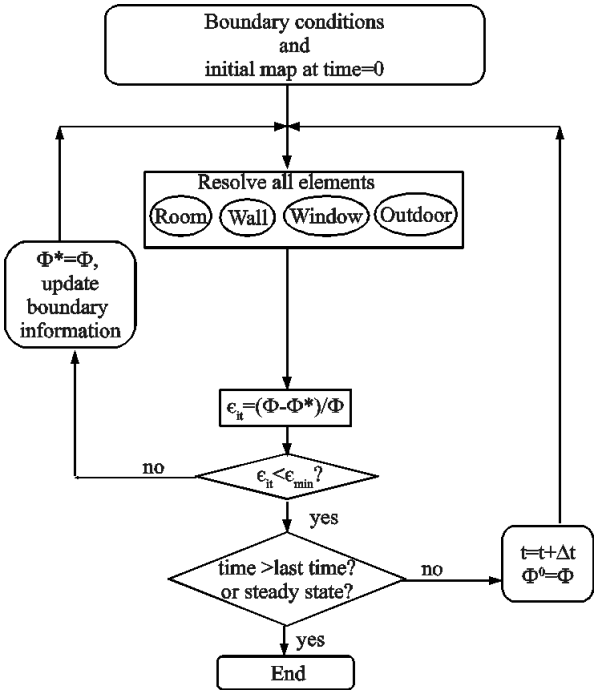

Figure 2.16: NEST-Buildings global algorithm.

The modular approach used in NEST provides an efficient and practical way to perform buildings simulation, since it allows a high degree of freedom, a rapid set up of any case and a flexible implementation of new elements and models.

The heat, moisture and pollutants transfer in a whole building are governed by transient diffusion-convection and balance equations, as seen in the wall, room and

detailed duct elements, then the resulting system of equations to solve temperature, humidity and pollutant concentrations is linear and it is solved, in NEST, by means of linear Jacobi solver [48].
However, the mass flow equations through openings and ducts are expressed function of the pressure gradient. Then in order to solve the airflow network inside a building, the pressure variable has to be solved in the rooms, openings and ducts elements. It is solved by means of SIMPLE [43] or Newton-Raphson [49] methods.
The SIMPLE method takes advantage of the modular approach of NEST and couples the mass flow rates and the mass conservation equations inside each element of rooms, openings and detailed ducts. By iterating all of them, the pressure is solved at each iterated element one by one in order to satisfy the mass conservation. It is a stable method to solve the airflow and avoid convergence problems, it provides a high level of details when solving the air flow inside the ducts, as shown in the detailed approach in section 2.3.6. However it requires a small time step and a high number of iterations, due to the difficulty in the propagation of information, which leads to a high computational time, especially when simulating a complex building with many rooms and ducts.
The disadvantage of the propagation of the information in the modular approach of NEST platform has been identified when solving airflow network in buildings: if a large cloud moves in front of the sun, there are some rooms that begin to cool down and this effect is propagated to the other rooms of the building progressively, first the neighbor rooms and then, to the others. The NEST modular approach can capture the physics of this thermal process since each element is connected to their physical immediate neighbors. Otherwise, if a window is opened, a heavy current of air appears and there is a door that ends up slamming on the other side of the house. This is because the air is incompressible and, due to mass conservation, this change of mass flow is instantaneously transmitted to all house. This means that modular approach is not ideal to solve the airflow in buildings because the communication through the rooms, even those not located far from each other should be fast. This inconvenient does not appear in heat, moisture and pollutant transfer, because in a building there is more inertia in these phenomena, as in the example of the cloud. Then, in order to optimize the resolution speed and maintaining the same accuracy, instead of solving the airflow at each element by relying on the modular approach of NEST like the SIMPLE method, it is proposed to use a monolithically approach where all the mass flow and continuity equations of these elements are gathered and solved in once inside only one element (called airflow element). The Newton-Raphson (NR) solver is used to solve simultaneously the system of equations of this airflow element. The mass flow equations through openings and the simplified ducts are non-linear equations as they are expressed in power function of the pressure. Then applying the mass balance inside all the rooms of building leads to a non-linear system of

equations with the pressure as an unknown. The same as described by Feustel [50], the Newton-Raphson method has shown to be efficient to solve this non-linear system of pressure equations inside a building and reduces the computational time of the simulation.
Table 2.4 shows the comparison of the computational time using the two described methods to simulate the airflow in a house having 12 rooms and a system of 5 ducts used for an exhaust mechanical ventilation system. The house will be studied later in chapter 4.

Solver used	**number of CPUs**	**computational time of the simulation of one week**
SIMPLE for rooms and ducts	16	83 h
SIMPLE for rooms and NR for ducts	4	5.5 h
NR for rooms and ducts	4	20 min

Table 2.4: Computational time for the simulation of one week of a building case.

The computational time is very important in buildings simulation, since long periods need to be simulated in order to analyse well the building performance. The simulated periods in buildings can reach one year or more in some cases, then it is essential to have a fast and reliable simulation tool. The Newton-Raphson solver is adopted by default in NEST, for the resolution of airflow inside a building simulation. However, the SIMPLE solver can be used also to simulate specific cases where it is important to study and analyse in detail the airflow through ducts.

2.5 Verification and validation

All the described elements in the previous section have for objective the resolution of airflow, heat and mass transfer inside the building envelope and the indoor spaces. In order to ensure the reliability of these basic models in NEST, the software has been validated and verified with experimental and analytical cases, respectively, and by comparison with other simulation tools. The test cases are chosen from the literature in a manner to be significant, simple, easy to run and cover all the phenomena for the assessment of building simulation.
The building envelope has been verified and validated with cases considering, first, only the moisture transfer, then the combined heat and moisture transfer through one layer and through a composite wall and finally with the combined heat, air and moisture transfer. The room and its envelope has been validated with cases simulating independently heat, moisture and VOC pollutants transfer inside it. The airflow in rooms has been verified and validated with cases testing the wind and stack effects

for different rooms configuration for both one-way and double-way openings.

2.5.1 Isothermal moisture transfer in a wall

The HAMSTAD benchmark exercise #2 [16] is a one dimensional case with isothermal moisture transfer in a single layer exposed to air with relative humidity of 65% on one side and 45% on the other side, while the temperature is held constant at 25^oC. The structure is perfectly airtight having a thickness of $20cm$ and initial conditions of 20^oC and 95% of relative humidity. The case allows the simulation of the drying process during time inside the wall.

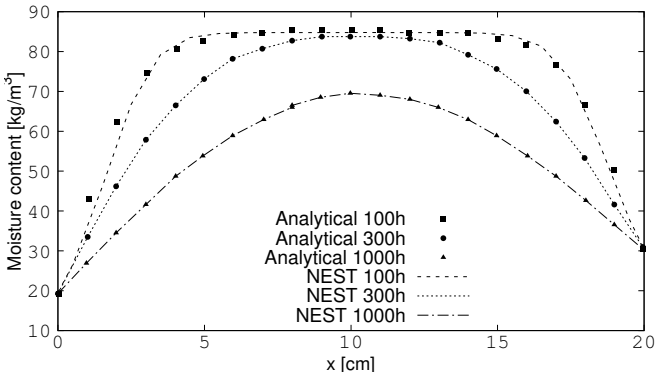

Figure 2.17: Moisture content profiles of the wall layer at 100, 300 and 1000 hours in isothermal moisture transfer case.

Figure 2.17 shows the moisture content profiles of the wall after three different periods of time during the transient simulation, where the moisture movement is caused by the lower values of relative humidity at both surfaces. The results show that the numerical model is able to predict very well the transient moisture transfer in the wall with a relative difference below 1.2%.

2.5.2 Heat and moisture transfer in a wall

The heat and moisture transfer through a single layer of concrete wall, studied my Maalouf [18], is simulated. A periodic variation of temperature and relative humidity similar to the summer weather condition are considered at outdoor condition. The external thermal convection coefficient is $25W/m^2K$ while the indoor temperature, relative humidity and thermal convection coefficient are set to 24^oC, 50% and $5W/m^2K$, respectively. Wall thickness is fixed to $20cm$ and initial walls temperature

and volumetric moisture content are 20^oC and $5 \cdot 10^{-3} \frac{m^3}{m^3}$, respectively. The concrete wall is simulated for a period of one year. Results of the moisture content in the internal and external surfaces and in the middle of the wall during time are shown in Figure 2.18.

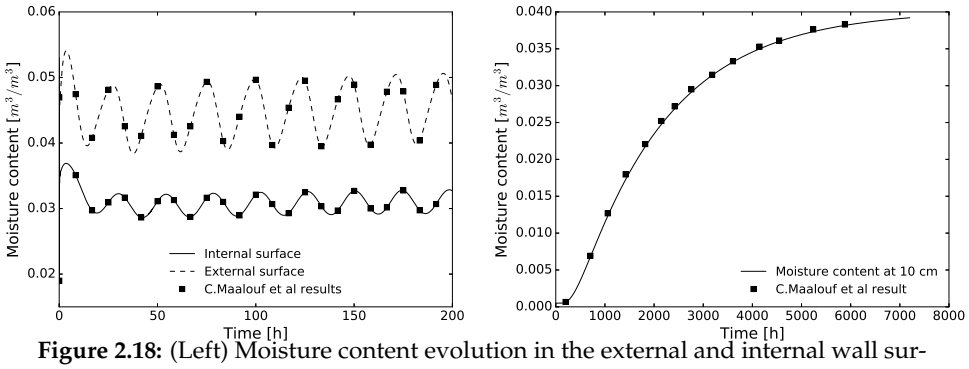

Figure 2.18: (Left) Moisture content evolution in the external and internal wall surfaces. (Right) Moisture content evolution in the middle of the concrete wall.

A good agreement is observed comparing with results obtained in [18]. The moisture content on the internal and external surfaces reach a periodic state in few days as shown on the left side of Figure 2.18, however it needs about six months to reach a steady state at a depth of $10cm$ inside the concrete material.

2.5.3 Heat, air and moisture transfer in a wall

The benchmark case HAMSTAD #3 [16] deals with heat, air and moisture transfer through a single layer wall of thickness $20cm$. The moisture transfer is driven mainly by the airflow convection and by the moisture and temperature gradients across the wall. The simulation time is 100 days: during the first 20 days there is air exfiltration (air flowing from inside to outside) with a constant pressure difference of $30Pa$ at both sides of the layer followed by infiltration (air flowing from outside to inside) where the pressure difference changes linearly and remains at $-30Pa$ during the next 80 days. The wall surfaces are exposed to air with relative humidity of 70% on the interior side and 80% on the exterior side, while the temperatures on the interior and exterior sides are 20^oC and 2^oC, respectively. Figure 2.19 shows the temperature and moisture distribution during time in the middle of the wall layer.

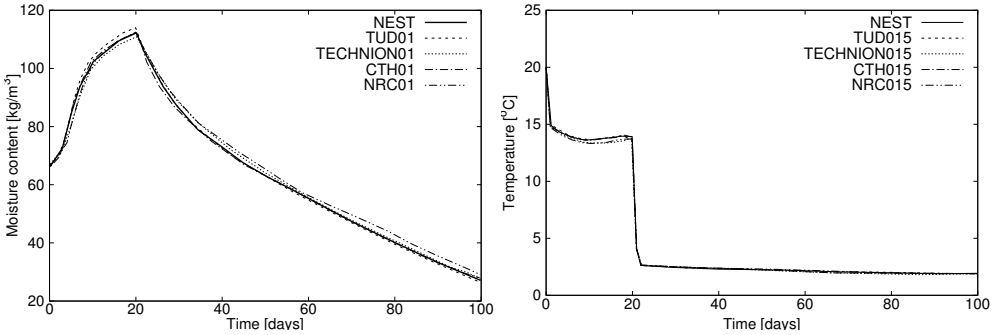

Figure 2.19: (Left) Moisture content evolution in the wall centre. (Right) Temperature evolution in the wall centre.

NEST results agree very well with the other four numerical solutions referenced in [16]. The wall exterior surface is water vapor tight but allows the dry air convection through it, then during the period of exfiltration, the wall receives humid air from the interior (at 70%) and the moisture content inside it increases up to 96%. During the period of infiltration the exterior surface doesn't allow the water vapor transfer inside it then the wall is dried out.

2.5.4 Heat and moisture transfer in a composite wall

The benchmark case #4 (Hagentoft, 2002) [16] deals with heat, air and moisture transfer in a composite wall having a hygroscopic finish. The wall is subjected to changes in heat and moisture loads at its surfaces where severe climatic load is imposed. It represents different phenomena of heat, air and moisture transfer generated by heating, cooling, alternating drying and wetting due to rain load along with fast liquid transfer properties of the first layer. These conditions allow a very good case for checking the heat, air and moisture transfer model. The description of climatic conditions are presented in [16].

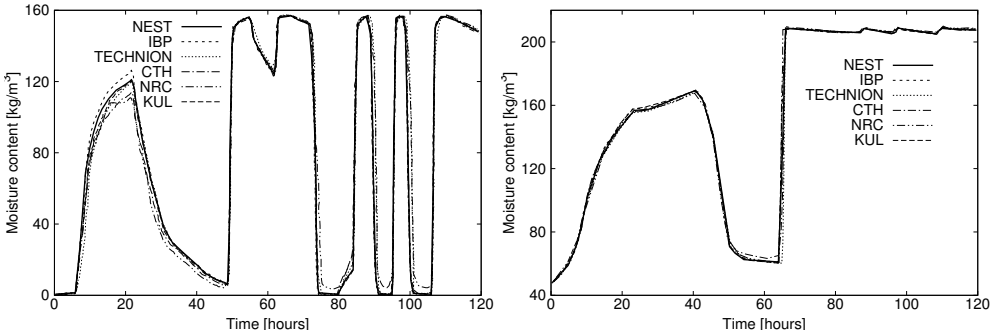

Figure 2.20: External side (left) and internal side (right) moisture contents evolution.

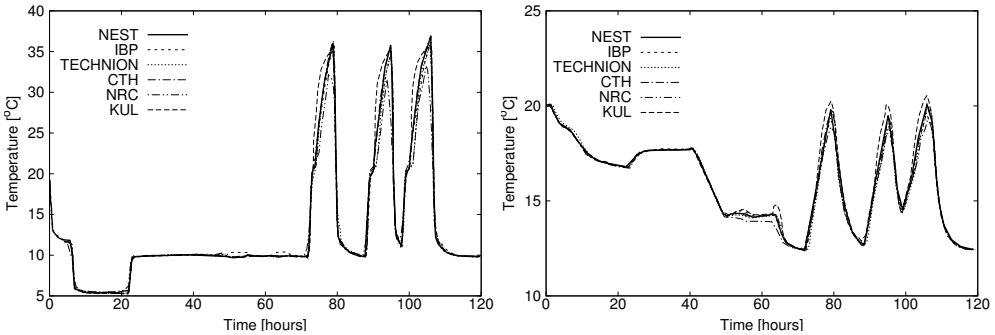

Figure 2.21: External side (left) and internal side (right) temperatures evolution.

Figure 2.20 shows the moisture evolution at the interior and exterior surfaces, while Figure 2.21 shows the temperature evolution at the interior and exterior surfaces. It can be seen that the external wall layer has a faster moisture transfer and response to the changing weather conditions, while the internal wall layer reached the moisture saturation only after 60 hours of simulation, but even though it's still isolating well the temperature. All comparative results show a good agreement as compared with other moisture transfer tools referenced in [16].

2.5.5 Moisture transfer in a room

A simplified building in a rectangular box shape with walls having thickness of 15cm of aerated concrete is tested by Bednar [51] under isothermal conditions and moisture transfer until cyclic steady state. The room envelope exchanges moisture with outdoor and an internal moisture generation of 500 g/h between 9:00h and

17:00h is considered. Two different cases are simulated: case 0A where heat and moisture transfer through the walls are not considered and case 0B where heat and moisture transfer through the walls are considered. Initial and boundary temperatures and relative humidity rates are fixed to 20C and 30%.

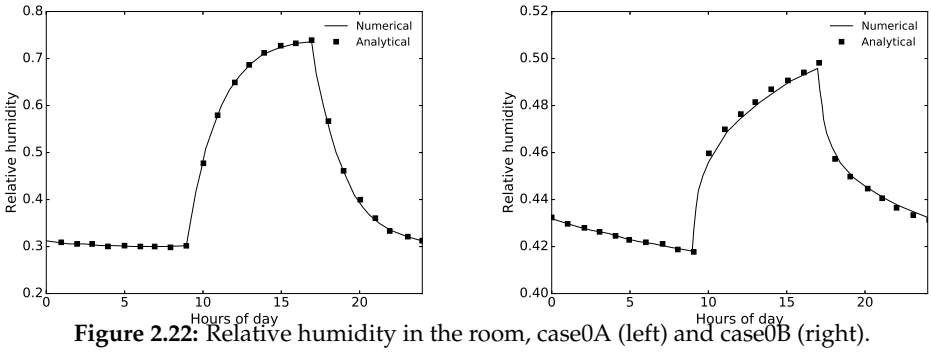

Figure 2.22: Relative humidity in the room, case0A (left) and case0B (right).

Figure 2.22 shows the relative humidity over the day without and with HAM transfer through the walls. It can be seen that when the wall are considered and linked with the room, they absorb the water vapour and reduce the relative humidity inside the room. Good agreement with analytical solution is observed with a maximum average relative error equal to 1.5% for the case 0B.

2.5.6 BESTEST

The BESTEST qualification cases in free-floating mode for lightweight 600FF and heavyweight 900FF building structure published by Judkoff and Neymark [52] is presented. It is a case simulating the transient thermal energy inside a building in Denver, Clorado U.S, with varying ambient condition. The building has a shape of a rectangular box with two windows facing south. A fixed internal heat gain and air change rate are 200W and $ACH = 0.5$, respectively, during the simulation period. A detailed description of the geometry and the outdoor conditions are presented in [52].

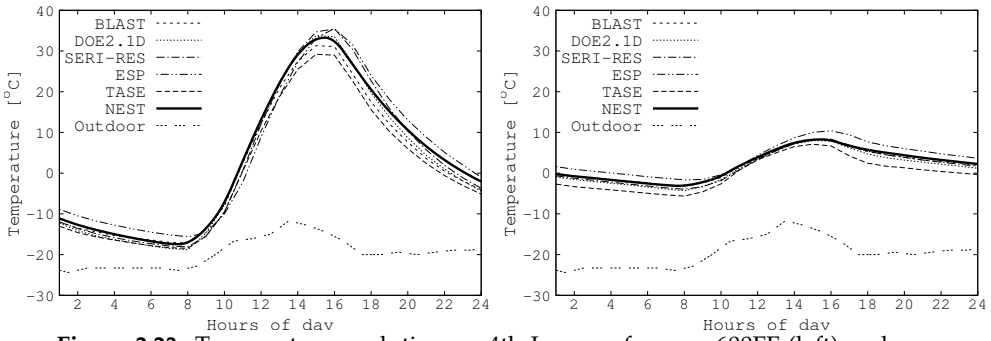

Figure 2.23: Temperature evolution on 4th January for case 600FF (left) and case 900FF (right).

Figure 2.23 shows the indoor temperature on 4th January for lightweight and heavyweight building structures. It can be seen that the results agree very well with the other building simulation tools. This test allows a collective verification of the energy model in elements like walls, room, window glazing allowing solar radiation and using the outdoor database model.

2.5.7 Pollutant transfer in a room

The implemented model for the pollutant transfer through walls and inside rooms is validated against the experiment data of Yang [23]. The case consists on a small chamber having a volume of 50 liters (0.212m x 0.212m x 0.0159m) with a pollutant emitting material inside. In this case the pollutant is a mixture of VOCs (hexanal, α-pinene, camphene and limonene) so the Total Volatile Organic Compound $TVOC$ is computed. Two particle boards PB1 and PB2 are tested one at a time for 96 hours and 840 hours, respectively. The initial concentration of $TVOC$ in these two particle boards is $5.28 \cdot 10^7 \mu g/cm^3$ and $9.86 \cdot 10^7 \mu g/cm^3$, respectively, while the initial $TVOC$ concentration of the chamber is zero. For both particle boards the diffusion coefficient for $TVOC$ is $7.65 \cdot 10^{-11}$. Air change rate of $1h^{-1}$ is maintained during the tests.

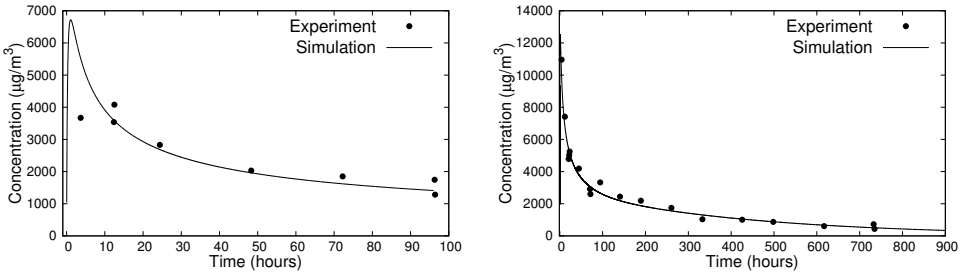

Figure 2.24: Evolution of pollutant concentration in the room using PB1 (left) and PB2 (right).

The Figure 2.24 shows the evolution of the pollutant concentration in the room during time with both particle boards. It can be seen that, after the first few hours, the numerical values show a good agreement with the measured values for both particle boards under consideration. The initial period corresponds to the high emission rate due to the high concentration of the $TVOC$ near surface and zero room air concentration. Beyond the initial period the material dries and the diffusion of $TVOC$ plays a more significant role. The numerical results show a good agreement comparing with the measured data where the maximum average of relative error is equal to 14.2% for the case using PB1.

2.5.8 Air flow through one-way opening

The ventialtion inside rooms having different windows modeled using one-way opening approach have been tested and validated by the comparison with the analytical results of six different tests cases described below [53]:

- Test 1. Monowind: wind action in a room having two orifices located in the same height.
- Test 2. Monostack: air circulation due to only stack effect inside a room having two orifices located at different heights.
- Test 3. Monows: combines tests 1 and 2, it shows the effect of stack and wind forces on air flow inside a room.
- Test 4. Three zones building 1: wind effect in the airflow inside three rooms having orifices at different heights.
- Test 5. Three zones building 2: thermal stratification effect in the airflow inside the same three rooms configuration.
- Test 6. Three zones building 3: combines tests 1 and 2 where the combined effects of wind and temperature combined have been tested.

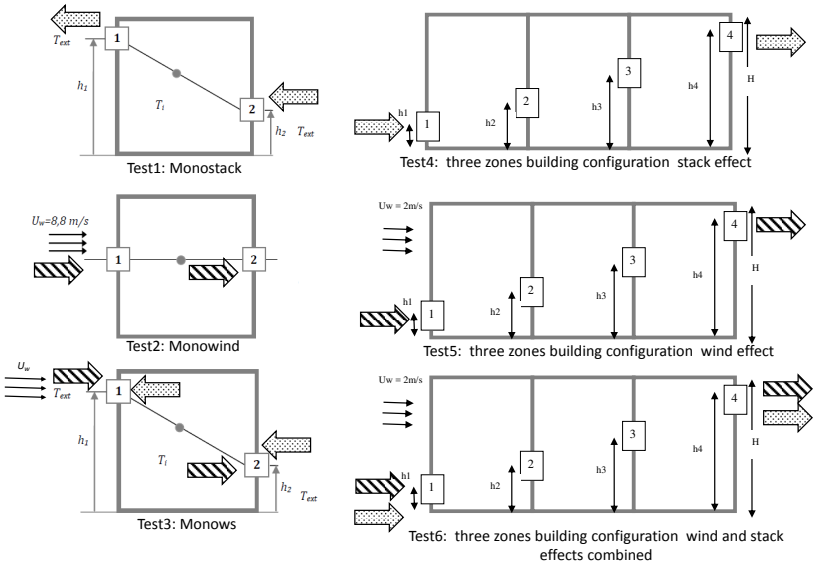

Figure 2.25: Test cases configurations to validate airflow through one-way opening.

Figure 2.25 illustrates the sketch of the different simulated cases and the table 2.5 shows the numerical results of the mass flow rate for each test case compared with the analytical result.

Table 2.5: Comparison between numerical and analytical results of mass flow rates through one-way opening.

Tests	Analytical	NEST	Relative error in %
1	0.07541	0.07540	0.01
2	0.00455	0.00453	0.40
3	0.06987	0.06988	0.01
4	0.08431	0.08430	0.01
5	0.06655	0.06640	0.22
6	0.11038	0.11030	0.07

A good agreement is obtained with a maximum relative error of 0.4%. It can be observed from test 3 that the mass flow due to thermal stratification (dotted arrow) and the mass flow due to wind force (striped arrow) are combined and decrease the

total mass flow since the two forces are acting against each other. However, in the test 6 the two forces are combined and increase the total mass flow rate in the rooms.

2.5.9 Airflow inside three floors building

A verification case of a building with 3 floors connected with each others and all of them connected to an enclosed stairwell is presented in COMIS [53]. This test case allows the testing of the combined wind and stack effects through the one-way openings in a case more close to the reality. A section of the building is shown in Figure 2.26.

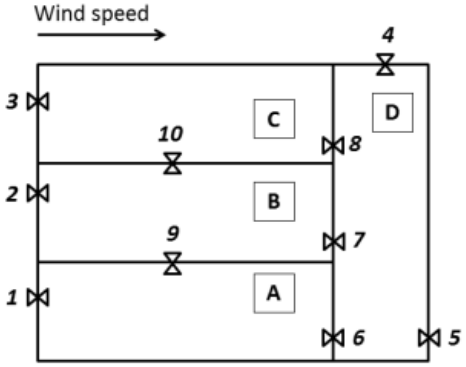

Figure 2.26: Building configuration for the airflow inside three floors building case.

Each floor (A, B and C) has a volume of $150m^3$ and the stairwell (D) has a volume of $135m^3$. The air circulates in the building through the small openings numbered from 1 to 10, as shown in Figure 2.26. Atmospheric pressure, outdoor temperature and wind speed at the roof height are $101325Pa$, 10^oC and $2m/s$, respectively.
The mass flow rates through the different openings are compared with results of other building simulation tools [53] and shown in the Figure 2.27.

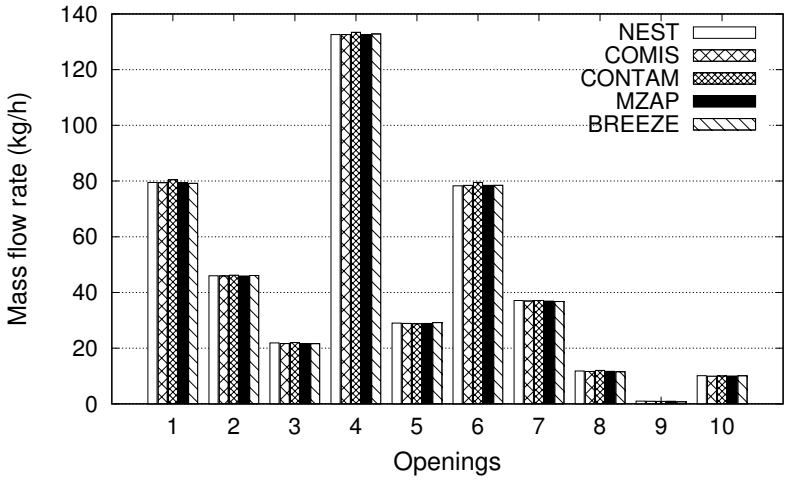

Figure 2.27: Comparison of mass flow rates obtained with NEST with results of other simulation tools.

The results obtained using NEST are in range comparing to the results obtained using other simulation tools. The mass conservation of air is satisfied inside the building as the sum of the incoming mass flow rates from different openings is equal in opposite to the sum of the outgoing mass flow rates.

2.5.10 Airflow through double-way opening

The double-way opening model has been validated comparing the results of a single side natural ventilation test (a room that has only one large opening) with the predictions of different simulation tools (COMIS, Passport Air, AIRNET, BREEZE, ESP and NORMA) [53] where a total of 23 tests are simulated. The first four tests are from PASSYS test cell experiments where the floor area and the volume of the single room are $8.6m^2$ and $28.3m^3$, respectively. The surface of the single large opening is $2.24m^2$ and the height $2.2m$. The mean climatic data during the experiments is given in [53]. The rest of the tests are from NOA experiments where the floor area of the room is $13.6m^2$, the volume $61.1m^3$ and the total surface of the window is $2.41m^2$. The window is divided into 5 parts where different parts are open for each test case. The mean climatic data and the open parts of the window for each experiment performed in NOA building are given in [53]. The predicted results of the mass flow rate in m^3/h through the large opening for each experiment compared with the results obtained with other simulation software [53] are shown in the Figure 2.28.

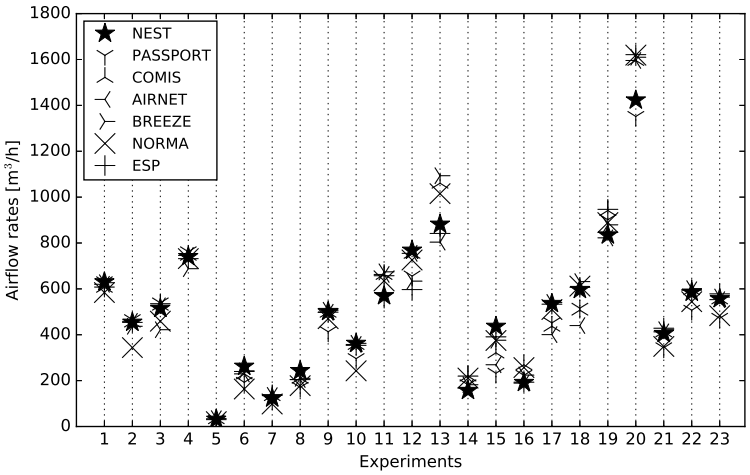

Figure 2.28: Air flow rate through large opening.

The simulation of large opening in NEST-Buildings shows results within the range of the ones obtained with other simulation tools. Experiments 11, 20, 22 and 23 correspond to a total opened window, using its maximum area, however the air flow rate is in its maximum only in the experiment 20, this is due to the high gradient of temperature between interior and exterior sides of the window for this experiment. The airflow is mainly driven by thermal stratification, the more is the temperature gradient the more is the mass flow rate through the large opening.

2.6 Conclusions

In the context of developing a modular, parallel and object-oriented tool for the simulation of multi-physics in general and buildings in particular, a big effort has been done to model and implement all the possible physical phenomena inside buildings in order to reproduce the reality with the a high level of details.
A building in NEST is modelled as a collection of elements like walls, rooms, openings, outdoor, etc. able to combine and solve airflow, heat, moisture and pollutants transfer through the building envelope and in the indoor space. In the first part of the chapter, all implemented elements in buildings library have been detailed. Then the resolution of the overall building system and the solvers used in NEST have been described. In the second part of the chapter, the developed software has been validated and

verified with a test suite including a collection of significant, simple and fast to run cases for the validation of airflow, heat, moisture and pollutants transfer in the whole building. There is a lack of references including test cases of all the building simulation phenomena altogether, so the test suite presented in this chapter can be used as a reference for the validation of new building simulation tools.
Satisfactory results have been found comparing to other numerical simulation tools during the validation and the verification process. The application of the simulation tool in real cases will be presented in the next chapters.

2.7 Nomenclature

A	Wall surface area	m^2
A_s	Opening section area	m^2
A_d	Duct section area	m^2
c_{p0}	Specific heat capacities of the material	$J/kg \cdot K$
$c_{p,a}$	Specific heat capacity of air	$J/kg \cdot K$
C_{co_2}	CO2 concentration	ppm
C_{voc}	VOC concentration	mg/m^3
C_d	Discharge coefficient	$-$
C	Flow coefficient	$m^3/s \cdot Pa^n$
D_{voc}	VOC diffusivity	m^2/s
D_H	Hydraulic diameter	m
f_D	Darcy friction factor	$-$
g	Gravity acceleration	m/s^2
g_m	Total moisture flow rate	$kg/m^2 \cdot s$
$g_{m,l}$	Water liquid flow rate	$kg/m^2 \cdot s$
$g_{m,v}$	Water vapor flow rate	$kg/m^2 \cdot s$
g_{air}	Mass airflow rate through wall structure	$kg/m^2 \cdot s$
h_n	Height of the neutral plan inside double-way opening	m
H	Height of the opening	m
H_{i-j}	Height of the opening relative to the ground of room i connecting room j	m
H_{Pi}	Height of the CV node relative to the ground in room i	m
k_l	Liquid permeability	$kg/m \cdot s \cdot Pa$
L	Duct length	m
m_P	Mass of air contained in a room	kg
$\dot{m}$	Air mass flow rate	kg/s
n	Exponent of flow equation	$-$
p_v	Vapor partial perssure	Pa
p_s	Suction pressure	Pa
p_{sat}	Saturation pressure	Pa
p_i	Pressure in the room i	Pa
p_{Pi}	Pressure in the control volume node P of the room i	Pa
p_{ext}	Pressure of the ambient air	Pa
T	Temperature	K
v_{ext}	external wind velocity	m/s
W	Width of the opening	m
w	Moisture content	kg/m^3
x	Humidity ratio	kg/kg

Greek symbols

α_i	Heat transfer coefficient at the wall surface i	$W/m^2 \cdot K$
β_i	Mass transfer coefficient at the wall surface i	s/m
$\beta_{voc,i}$	VOC transfer coefficient at the wall surface i	s/m
δ_p	Water vapor permeability	$kg/m \cdot s \cdot Pa$
λ	Thermal conductivity	$W/(m\,K)$
ξ	Pressure loss coefficient	$-$
ρ	Density of the air	kg/m^3
ρ_i	Density of the air in the room i	kg/m^3
ρ_0	Material density	kg/m^3
ϕ	Relative humidity	$-$

Subscripts

v	Water vapor
l	Liquid water
P	Control volume node
k	node at the Control volume side

Constants

R	General gas constant	$8.314 J/mol \cdot K$
M_w	Molar water mass	$0.018 kg/mol$

References

[1] J. Grunewald. *Documentation of the numerical simulation program DIM3.1. Theoretical fundamentals*, volume 1. 2000.

[2] A. Holm, H.M Kunzel, and K. Sedlbauer. *The hygrothermal behaviour of rooms: combining thermal building simulation and hygrothermal envelope calculation*. 2003. In: Proceedings of 8th International IBPSA Conference, Eindhoven, Netherlands.

[3] A. S. Kalagasidis, C. Rode, and M. Woloszyn. *HAM-Tools - a whole building simulation tool in Annex 41*, volume 1. 2008.

[4] H. Karlsson, Kalagasidis A. S., and Hagentoft C.E. *Development of a Modular Toolbox in Simulink for Dynamic Simulations of VOC-Concentration in Indoor Air.*, volume 1. 2005. The 9th International IBPSA Conference, Montreal, Canada.

[5] M. Woloszyn and C. Rode. *IEA Annex 41, MOIST-ENG Subtask 1 Modelling Principles and Common Exercises*, volume 1. 2007.

[6] Fluent. `/http://www.ansys.com/Products/Simulation+Technology/Fluid+Dynamics/ANSYS+FluentS`; 2012.

[7] Comsol. `/http://www.comsol.com/S`; 1998.

[8] P.V. Megri and F. Haghighat. Zonal modeling for simulating indoor environment of buildings: review, recent developments, and applications. *HVAC&R Research*, 13:887–905, 2007.

[9] Lawrence Berkeley National Laboratory and Ayres Sowell Associates Inc. *SPARK 2.0 reference manual*. 2003.

[10] H.E. Feustel. COMIS an international multizone air-flow and contaminant transport model. *Energy and Buildings*, 30:3–18, 1999.

[11] W.S Dols and G.N Walton. *CONTAMW 2.0 User Manual: Multizone Airflow and Contaminant Transport Analysis Software*. 2002. US Department of Commerce, Technology Administration, National Institute of Standards and Technology.

[12] G.N. Walton. AIRNET a computer program for building airflow network modeling. *NISTIR 89-4072*, 1989.

[13] J.H. Klote and J.A. Milke. Design of smoke management systems. *American Society of Heating, Refrigerating and Air-Conditioning Engineers*, 1992.

[14] *BREEZE 6.0 User Manual*. Building Research Esrablishment, Wutford, UK, 1994.

[15] P.A. Strachan, G. Kokogiannakis, and I.A. Macdonald. History and developement of validation with ESP-r simulation program. *Building and Environment*, 43:601–609, 2008.

[16] C.E. Hagentoft. *HAMSTAD-final report: methodology of HAM modelling*. Chalmers University of Technology, Gothenburg, Department of Building Physics, 2002.

[17] M.V. Belleghem, M. Steeman, A. Willockx, A Janssens, and M.D. Paepe. Benchmark experiements for moisture transfer modelling in air and porous materials. *Building and Environment*, 46:884–898, 2011.

[18] C. Maalouf, D. Tran, M. Lachi, E. Wurtz, and T.H. Mai. Effect of moisture transfer on thermal inertia in simple layer walls. *International Journal of Mathematical Models and Methods in Applied Sciences*, 5, 2011.

[19] P. Talukdar, O.F. Osanyintola, S.O. Olutimayin, and C.J. Simonson. An experiemental data set for benchmarking 1-D, transient heat and moisture transfer models of hygroscopic building materials. *International Journal of Heat and Mass Transfer*, 50:4527–4539, 2007.

[20] *Standard Method of Test for the Evaluation of Building Energy Analysis Computer Programs*. Atlanta, GA: American Society of Heating, Refrigerating, and AirConditioning Engineers, 2001.

[21] H.S.L.C. Hens. IEA-ECBCS annex 41 whole building heat, air, and moisture response. volume 115 part 2, pages 88–94, 2009.

[22] J.M. Furbringer, C.A. Roulet, and R. Borchiellini. Evaluation of COMIS. *IEA Annex 23: Multizone Air Flow Modelling*, 1996.

[23] X. Yang, Q. Chen, J.S. Zhang, R. Magee, J. Zeng, and C.Y. Shaw. Numerical simulation of VOC emissions from dry materials. *Building and Environment*, 36:1099–1107, 2001.

[24] H. Huang and F. Haghighat. Modelling of volatile organic compounds emission from dry building materials. *Building and Environment*, 37:1127–1138, 2002.

[25] T. Cheng, Y. Jiang, Y. Xu, and Y. Zhang. Mathematical model for simulation VOC emissions and concentration in buildings. *Atmospheric Environment*, 36:5025–5030, 2002.

[26] J. Xiong, C. Liu, and Y. Zhang. A general analytical model for formaldehyde and VOC emission/sorption in single-layer building materials and its application in determining the characteristic parameters. *Atmospheric Environment*, 47:288–294, 2012.

[27] P.A. Strachan and P.H. Baker. Outdoor testing, analysis and modelling of building components. *Building and Environment*, 43(2):127 – 128, 2008.

[28] F. Tariku, K. Kumaran, and P. Fazio. Transient model for coupled heat, air and moisture through multilayered porous media. *International Journal of Heat and Mass Transfer*, 53, 2010.

[29] A.S. Kalagasidis. *An Integrated Simulation Tool for Heat, Air and Moisture Transfer Analyses in Building Physics*. PhD thesis, Chalmers University of Technology, 2004.

[30] H.M. Kunzel. *Simultaneous heat and moisture transfer in building components: one and two dimensional calculation using simple parameters*. PhD thesis, University of Stuttgart, Germany, 1995.

[31] H.M. Kunzel. *IEA ANNEX 24 Heat, Air and Moisture Transfer Through New and Retrofitted Insulated Envelope Parts*. 1994.

[32] J.R. Howell and R. Seigel. *Thermal radiation heat transfer*. Taylor and Francis, 2001.

[33] M. Jacob. *Heat transfer*, volume 1. John Wiley and sons Inc, 1957.

[34] F. Tariku, K. Kumaran, and P. Fazio. Integrated analysis of whole building heat, air and moisture transfer. *International Journal of Heat and Mass Transfer*, 53, 2010.

[35] R. Siegel and J.R. Howell. *Thermal radiation heat transfer*. Taylor and Francis, 2002.

[36] R.H. Perry and Green D.W. *Perry's chemical engineers' handbook*. McGraw-Hill Professional, 1999.

[37] D. Kiel and D. Wilson. Gravity driven flows through open doors. 7th AIVC Conference, 1986.

[38] H. Feustel. *Fundamentals of the multizone air flow model - COMIS. Technical Note AIVC 29*. Air Infiltration and Ventilation Centre, 1990.

[39] F. Allard and Y. Utsumi. Airflow through large openings. *Energy and Buildings*, 18:133–145, 1992.

[40] J. Koffi. *Analyse multicritere des strategies de ventilation en maisons individuelles*. PhD thesis, Ecole doctorale Sciences pour l'Environnement et le Developpement Durable (SEDD), 2009.

[41] Walton G.N. *AIRNET - A computer program for building airflow network modeling*. U.S.Department of Commerce - National Institute of Standard and Technology, April 1989.

[42] S.W. Churchill. Friction-factor equation spans all fluid-flow regimes. *Chemical Engineering*, 84:91–91, 1977.

[43] S.V. Patankar. *Numerical Heat Transfer*, volume 1. Hemisphere publishing corporation, 1980.

[44] R. Damle, J. Rigola, C.D. Perez-Segarra, J. Castro, and A. Oliva. Object-oriented simulation of reciprocating compressors: Numerical verification and experimental comparison. *International Journal of Refrigeration*, 34(8):1989 – 1998, 2011.

[45] Brown and Glenn. *The Darcy-Weisbach Equation*. Oklahoma State University Stillwater, 2000.

[46] I.E. Idelcik. *Momento des pertes de charge-Coefficients de pertes de charge singulieres et de pertes de charge par frottement*. Centre de Recherches et d'essais du Chatou. Eyrolles, Paris, 1969. Translated from Russian by M. Meury.

[47] METEONROM 7.1. `https://meteotest.ch/produkt/meteonorm`, 2016. Meteotest Fabrikstrasse 14, CH-3012 Bern, Switzerland.

[48] R. Barrett, M. Berry, T.F. Chan, J. Demmel, J. Donato, J. Dongarra, V. Eijkhout, R. Pozo, C. Romine, and H. Van der Vorst. *Templates for the Solution of Linear Systems: Building Blocks for Iterative Methods, 2nd Edition*. SIAM, 1994.

[49] M.K. Herrlin and F. Allard. Solution methods for the air balance in multizone buildings. *Energy and Buildings*, 18:159–170, 1992.

[50] H.E. Feustel and J.A. Dieris. A survey of airflow models for multizone structures. *Energy and Buildings*, 18:79–100, 1992.

[51] T. Bednar and C.E. Hagentoft. *Analytical solution for moisture buffering effect validation exercises for simulation tools*. Nordic Building Physics Symposium, 2005.

[52] R. Judkoff and J. Neymark. *Building energy simulation test (BESTEST) and diagnostic method*. Golden, Colorado 80401-3393: National Renewable Energy Laboratory, 1995.

[53] J.M. Fubringer, C.A. Roulet, and R. Borchiellini. *Evaluation of COMIS. IAE-ECBCS Annex 23: Multizone Air Flow Modelling*. 1996.

3

Hygrothermal simulation. Application of NEST to public buildings

3.1 Introduction

Most building materials are porous and moisture can exist and cause significant effects in material durability, thermal performance and indoor air quality. For this reason it is important to take into account the moisture transfer during the design of new buildings when selecting construction materials and during the retrofitting of existing buildings in order to fix the damage caused by humidity and maintain a good thermal and moisture resistance. A satisfactory retrofit solution is the one that last longer, respond well to the building surrounding and climate and maintain the indoor comfort and air quality [1].
In this context, NEST software has been used to simulate and analyse the hygrothermal behaviour of different public buildings located in different climate conditions before their retrofitting. The idea is to retrofit these old buildings with efficient strategies using passive design, renewable heating&cooling sources and better insulating materials for buildings envelope.
In the first stage, NEST software has been used to simulate and analyse the hygrothermal behaviour of different representative rooms of the four different public buildings located in distinct locations in Europe: two hospitals in Spain, a university in UK and a school in Sweden. The numerical simulations allow to study materials durability,

energy and indoor air quality performance in these buildings, identify their weak points and predict the performance by considering the retrofitting solutions.
Most of the simulation tools and studies evaluate the building energy performance by studing only the thermal behaviour, using constant thermophysical properties and neglecting the impacts of moisture transfer. However, authors like Janssen et al. [3], Labat et al. [4] and Woloszyn et al. [5] highlight the importance of simulation of heat and moisture transfer in buildings and they ability to assess walls durability and performance. Furthermore, other investigations held by Haverinen et al. [6], Dales et al. [7] and Langmans et al. [8] point out that a high moisture level is a risk factor for a building energy performance, mould growth, and loss of the insulation properties of materials. On the other hand, the assumption of constant physical properties for buildings materials is not credible [9, 10] since the hygric properties can strongly influence the hygrothermal behaviour of the buildings envelope and consequently the energy efficiency inside them.
In this chapter, the representative rooms for the different demo sites are modelled and simulated using the hygrothermal models developed in chapter 2. They are first simulated in free-float mode where only natural ventilation are considered and then in HVAC mode where heating, cooling, humidification and dehumidification are considered. During the simulation of the first room of Terrassa, a detailed study is conducted and presented: the impact of the moisture on the heat transfer and in the hygrothermal behaviour of the room is investigated. The water condensation in the interior and exterior surfaces is checked and a sensitivity study of the materials properties has been conducted. In order to evaluate the rooms performance, the thermal and moisture load required to maintain the rooms at a comfort level using HVAC before and after the proposed solutions for retrofitting are evaluated and discussed.
A part of the results of this work has been done within the framework of the EU project RESSEEPE [2].

3.2 Demo sites modelling

NEST software has been used to simulate two representative rooms per each demo site. The rooms represent typical rooms from each of the public buildings (two hospitals, a university and a school). In order to avoid redundancy, only one room per demo site is presented: One room of one of the hospitals in Spain, one classroom of the school in Sweden and one classroom of the university in UK.

3.2.1 Rooms modelling

Each representative room is modelled as a collection of NEST elements described in section 2.3 of chapter2: The composite walls elements are connected with a room and outdoor elements. the windows as well are modelled using glass or multi-glass elements depending on the demo site and solar and thermal radiation are introduced using FSolD and RadBox elements, respectively. The room doors and windows are assumed to be closed, however air infiltration through them is taken into account.
The representative rooms are set initially to constant temperature and relative humidity fields of 23^{o}C and 50%, respectively. The numerical simulations use weather conditions of a typical year at each site obtained using Meteonorm [11] software through the outdoor element. The solar radiation is projected and evaluated in the different façades depending on their orientation. A symmetry boundary condition is used for the roof, floor and interior walls, where a zero heat and moisture fluxes at the symmetry plan are assumed.

3.2.2 Materials of buildings envelope

The materials used in the demo sites walls have been provided and their properties have been taken and evaluated from the NEST materials database. The database includes the hygrothermal properties of different common materials used in buildings construction, it is developed based on the literature from WUFI [12] and the International Energy Agency, Annex 24 [13]. The materials used to simulate the different demo sites are concrete, brick, mortar, plaster, wood fibre and glass.
Only the heat transfer is considered through the glass assuming a constant thermal conductivity of 0.917 $W/m \cdot K$. The rest of the materials are considered porous where thermal and hygric properties are defined. The thermal conductivity, water sorption, vapour and liquid permeability of the materials are not constant and they are evaluated function of the relative humidity as presented in Figure 3.1. Their dependency to the temperature variation is neglected. As it can be seen in Figure 3.1 the thermal conductivity increases when the humidity raises, the concrete has the highest conductivity while the wood fibre has the lowest one.

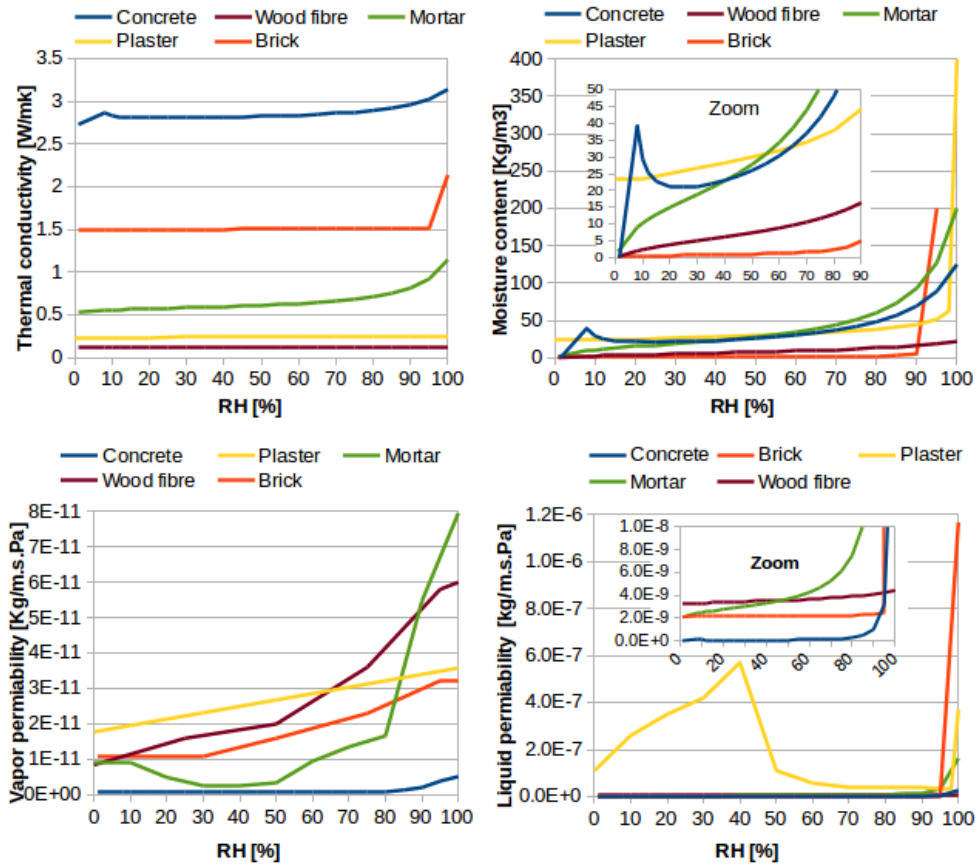

Figure 3.1: Material properties. (a) Top left: thermal conductivity. (b) Top right: moisture sorption. (c) Bottom left: vapour permeability. (d) Bottom right: liquid permeability.

The moisture content is important and more representative than relative humidity to analyse the water behaviour inside a material as it provides a direct meaning of the mass of moisture per unit volume of the dry material [13]. The relation between the moisture content and the relative humidity is called sorption curve and their representation for the simulated materials are shown in Figure 3.1 (b). The moisture content in the different materials vary function of the relative humidity in a non-linear way between the dry state and the fully saturated state when the pores are completely filled with water. In the dry state, the moisture is in adsorption and is

transported mainly in the vapour phase until 80% of relative humidity for mortar and concrete, 90% for brick and 98% for plaster, as shown in Figure 3.1 (b). After that, the moisture begins to condensate in the pores leading to saturation state, called capillary saturation and the moisture is transported more in the liquid phase. It can be seen that the plaster can reach a very high moisture content in capillary saturation while the wood fibre is more resistant to moisture and doesn't reach the saturation in high relative humidity.
Figures 3.1 (c) and (d) show the water vapour and liquid permeabilities. They give a measure of the passage of water vapour and water liquid, respectively, through the material and they represent the mass of water (vapour or liquid) transmitted through a unit area, in a unit time, induced by a unit pressure gradient.
All the rooms façades have an air cavity in their composite walls that are simulated using the same concept as for the composite glass in section 2.3.1. It is assumed as a room where heat transfer by natural convection and thermal radiation take place. The thermal radiation inside the air cavity is approximated as the heat transfer between two infinite opaque parallel plates [14, 15]. The heat convection coefficients between the cavity and the walls layers are assumed to be 1 W/m^2K.
It has been assumed a convection coefficient of 8 W/m^2K between the windows and the room, 3 W/m^2K for the convection between the interior walls and the room and 20 W/m^2K between the façades and the outdoor. The exterior and the interior mass transfer coefficients are evaluated as a function of the heat transfer coefficients using Lewis relation [16].

3.2.3 Standards and regulations

As the focus is on simulating and analysing the heat and moisture transfer in the different demo sites room, it is important to consider and take into a account the standards used in building as a reference line for the heat and moisture comfort levels. The indoor comfort is a complex concept that depends on many factors such us temperature, thermal radiation, relative humidity, season, clothing, activity levels, etc. [17]. To simplify the problem, the comfort in this study is reduced to the ranges of indoor temperature and relative humidity fixed by the standards. The standards in each country of the demo site buildings are described below. Standards were taken in 2013 when this work was performed.

Spanish regulation
The Regulation of Thermal Installations in Buildings (RITE) [18] introduces legal level constrains for temperatures and relative humidity in non-residential buildings such as offices. It recommends that the temperature should not drop below 21 ^oC in summer or exceed 26 ^oC in winter and the relative humidity should be between 30% and 70%.

In the particular case of an hospital, the Spanish standard UNE 100713:2005 [19] fixes the comfort ranges of temperature and relative humidity in their rooms, these ranges are presented in the table 3.4.

Location	Tmax	Tmin	RHmax	RHmin
All spaces	26	24	55	45
Operation rooms	26	22	55	45

Table 3.1: The temperature and relative humidity ranges in an hospital according to the Spanish standard UNE 100713:2005.

Swedish regulation
According to the Building Council Regulation in Sweden [20], buildings shall be designed so that heat and moisture does not cause discomfort, damage, bad smells or hygienic problems and microbial growth, which can affect human health. The minimum operative temperature in an occupied zone is estimated at 18 ^oC in habitable rooms and workrooms and 20^oC in sanitary accommodations, care premises, and in rooms for pre-school children, while a relative humidity of 75% is fixed as the critical moisture level.

UK regulation
The regulatory requirements for workplace temperatures, set by the Workplace (Health, Safety and Welfare) Regulations [21], state that the temperature of indoor workplaces should be at least 16^oC. No specific standards are prescribed by law for the relative humidity, however the ideal relative humidity considered for comfort is in the range of 55% to 65%.

3.3 Demo sites simulation

The hygrothermal behaviour in the rooms are simulated, analysed and discussed in this section. The heat and moisture in the representative rooms of hospital in Terassa, school in Skelleftea and university in Coventry have been simulated in free-float mode, where only natural ventilation is considered, for a period of one year under typical weather conditions and with a time step of 60 seconds. First, the performance of the rooms envelope is discussed by analysing the temperature and moisture at each layer. Second, the rooms response to the weather conditions, air infiltrations and walls buffering has been observed. After that the rooms are simulated by considering HVAC in the rooms and thermal and moisture loads required to maintain the indoor comfort level before and after the proposed solutions for retrofitting are evaluated.

In order to avoid redundancy, only during the first room of Terrassa, a deeper parametric investigation is conducted. The room is simulated by considering only heat transfer and then by considering the coupled heat and moisture transfer, as described by the models in section 2.3.1. Therefore the impact of moisture transfer on the thermal performance of the rooms and materials durability is discussed. Next, the condensation in the interior and the exterior layers of the rooms façades is evaluated and later a sensitive analysis of the walls hygrothermal parameters is done in order to analyse the effect of each one on the heat and moisture transfer though the wall and in the room.

3.3.1 Hospital in Terrassa

The representative room of Terrassa hospital, in Catalonia (Spain), is located in the 8th floor and it has a façade oriented south with a single glass window as shown in Figures 3.2, 3.3 and 3.4. The room façade is a composite wall made of brick, air cavity with porexpan, artificial stone and plaster. The artificial stone and the air cavity with porexpan are assumed to be mortar and empty air cavity, respectively.The interior walls are also composite walls made of brick material with a plaster finishing layer in both sides, the floor is made of concrete material with tiles layer in the top while the roof is a false ceiling made of gypsum plaster. The room's walls and their layers are shown in Figure 3.5. The toilet inside the room and its interior walls are not considered for the simulation.

Figure 3.2: The hospital demo site in Terrassa, Spain.

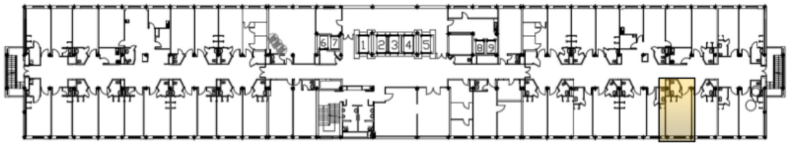

Figure 3.3: Terrassa hospital floor plan, Spain.

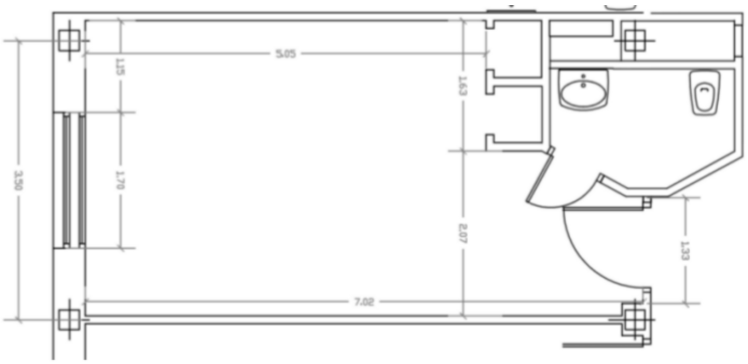

Figure 3.4: The prototype room plan of Terrassa hospital, Spain.

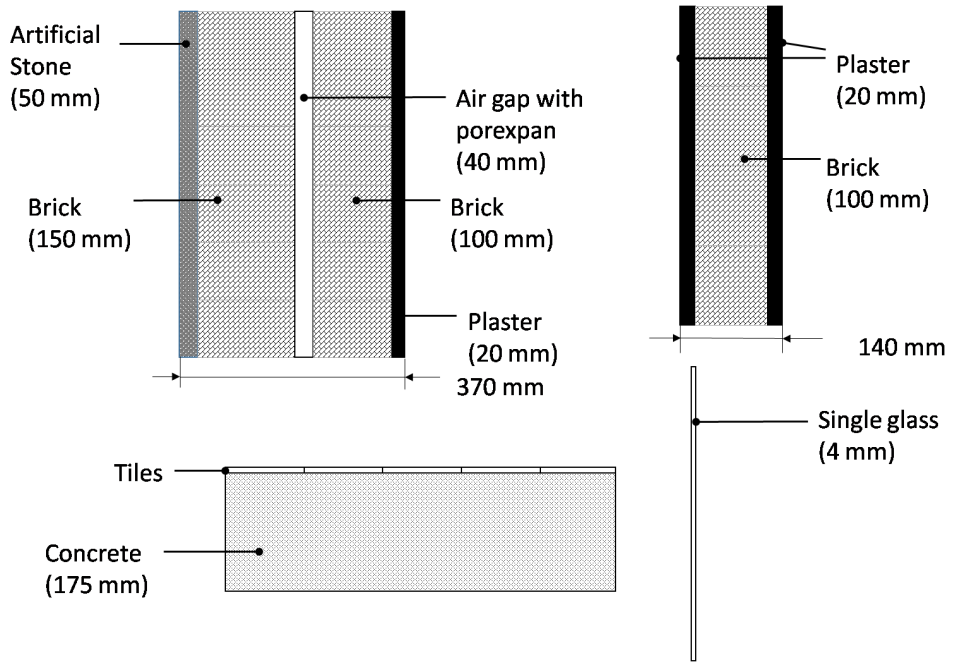

Figure 3.5: Room walls in Terrassa hospital demo site. Top Left: façade, top right: interior wall, bottom left: floor and bottom right: window.

Effect of moisture on the thermal performance

The moisture contained in the porous material affects its physical properties like the thermal conductivity , the sensible heat in the heat equation (2.11) by means of the $D_{T,v}$ coefficient and contribute to the latent heat due to water phase changes by means of the term that contains the $D_{\phi,v}$ coefficient in the same heat equation. So the dependency of moisture on the heat transfer can be observed through the model equations and should be taken into account.
In order to study the walls materials and the effect of moisture on the thermal insulation, the room is first simulated by only considering the heat transfer (without moisture) transfer and then by considering both heat and moisture transfer. All the interest will be in analysing the façade of the room since the other interior walls have a symmetric boundary condition and their contribution on the heat and moisture transfer in the room is not significant. Figures 3.6, 3.7, 3.8 and 3.9 show the temperature evolution in the room, in the interior and exterior surfaces of the façade and in

the centre of each interior layer, without and with the moisture model, during one week in February, May, August and November.

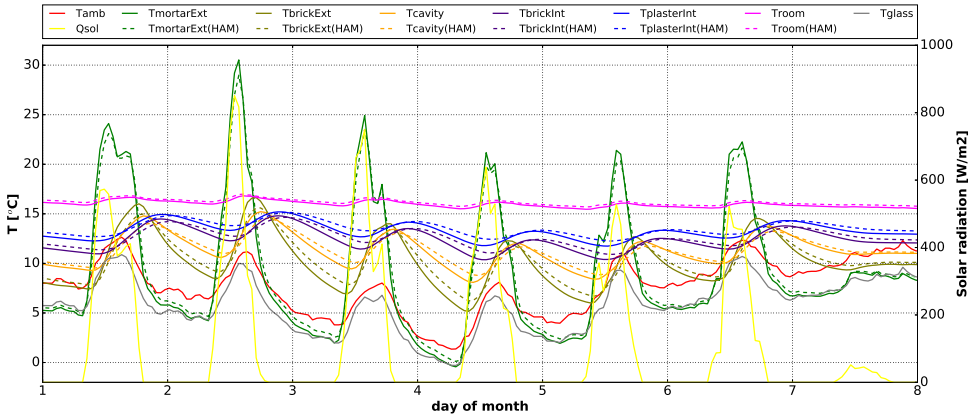

Figure 3.6: The temperature evolution in Terrassa room and in the layers of the façade wall during one week in February.

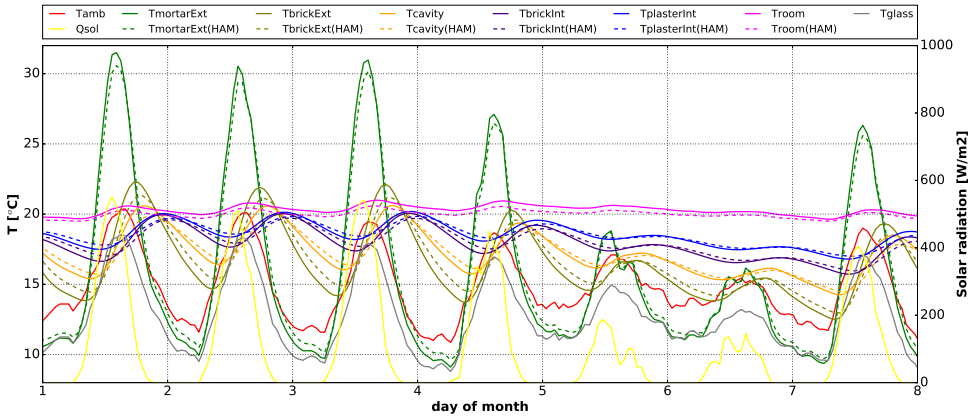

Figure 3.7: The temperature evolution in Terrassa room and in the layers of the façade wall during one week in May.

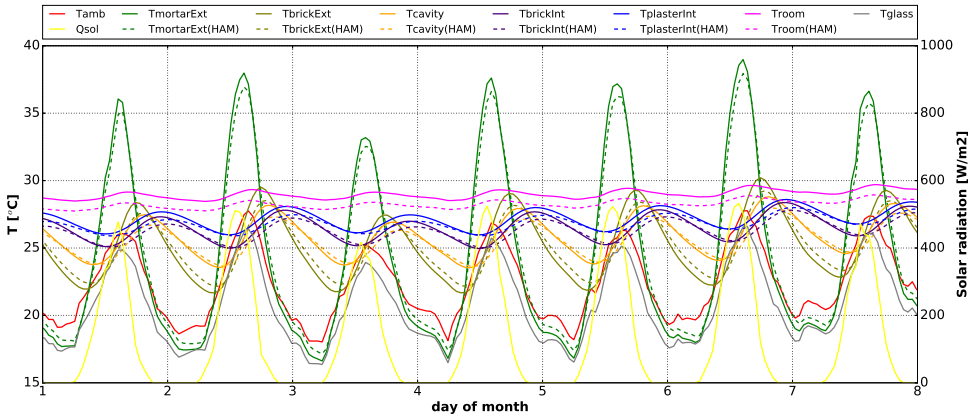

Figure 3.8: The temperature evolution in Terrassa room and in the layers of the façade wall during one week in August.

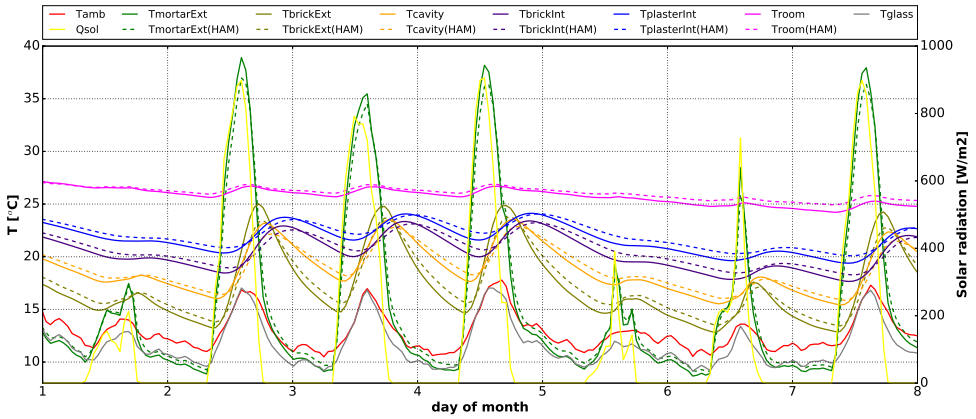

Figure 3.9: The temperature evolution in Terrassa room and in the layers of the façade wall during one week in November.

As it can be seen the exterior layer of the façade (TmortarExt) has a very oscillating temperature which goes from a minimum of 3^oC to a maximum of 42 ^oC. This is an expected behaviour as it is bearing directly all the variations of ambient temperatures (Tamb) and solar radiation (Qsol). The oscillation amplitude of temperature decreases from one layer to another in the façade and it is the lowest in the interior layer (TplasterInt). The air chamber (Tcavity) has the function of thermal insulation as it reduces significantly the heat transfer from the exterior layers (TmortarExt and

TbrickExt) to the interior ones (TbrickInt and TplasterInt), it has shown to be effective insulating the interior wall layers and reducing the oscillations due to the ambient conditions. The window glass has the lowest temperature in the façade, even lower than the ambient temperature, which is mainly due to its thermal radiation exchange with the sky. The single glass (Tglass) has shown to be the weakest part of the envelope since it doesn't provide any thermal insulation.
When the moisture model is taken into account, the temperature evolution in the room and in the wall layers has been showed in dashed lines in order the see the effect of moisture on the heat transfer. Variations on the temperature patterns have been observed, the temperatures in the layers (TbrickExt, Tcavity, TbrickInt and TplasterInt) and in the room have slightly increased in winter and decreased in summer, while the oscillation peaks of temperature in the exterior layer (TmortarExt) has slowly decreased during all the simulation. These variations are explained due to the latent heat of evaporation/condensation of water inside the walls: During winter season, as in February and November, the water vapour present in the wall doesn't have enough energy to remain in the vapour phase, so it condensates releasing its latent heat (exothermic process) that contributes to the heating of the wall material and then the temperature slightly rises. During summer, as in May and August, the water liquid retained in the wall has enough energy to evaporate and thus it absorbs the latent heat from the wall to change its phase (endothermic process) which leads to the cooling of the wall, as a consequence the temperature decreases. This contribution of moisture in the building performance has been also pointed out by several authors like Woloszyn [5], Hoseini [22] and Haba [10].

Moisture content

The consideration of moisture in the simulation doesn't only affect the heat transfer but it allows also the prediction and the analysis of the moisture contained in the envelope. In order to analyse and discuss clearly the moisture transfer, the moisture content parameter is presented for the materials as it provides a direct meaning of the mass of moisture per unit volume of the dry material. However in the air spaces like room or air cavity, the relative humidity is presented as it expresses in percentage the amount of water vapour relative to what the air can hold. As described in section 3.2.2, these two variables are related by the sorption curve depicted in Figure 3.1.
Figures 3.10, 3.11, 3.12 and 3.13 show the moisture content evolution in the centre of each solid layer of the façade wall and the relative humidity in the air cavity layer and in the room during February, may, August and November.

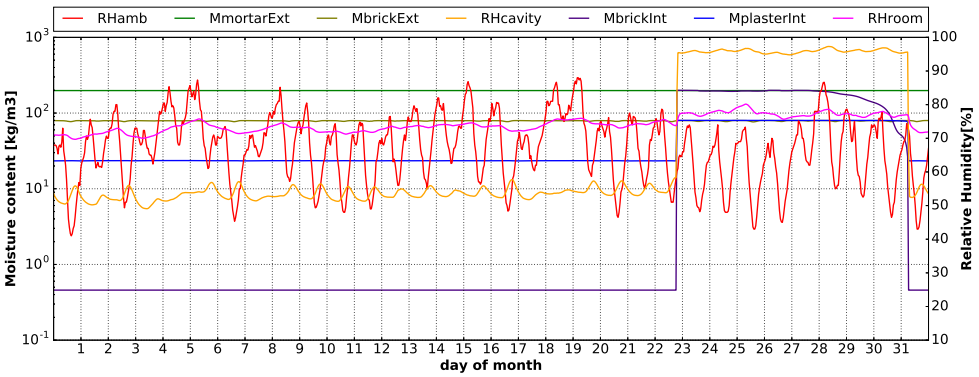

Figure 3.10: The relative humidity evolution in Terrassa room and the moisture contents in the layers of the façade wall during February.

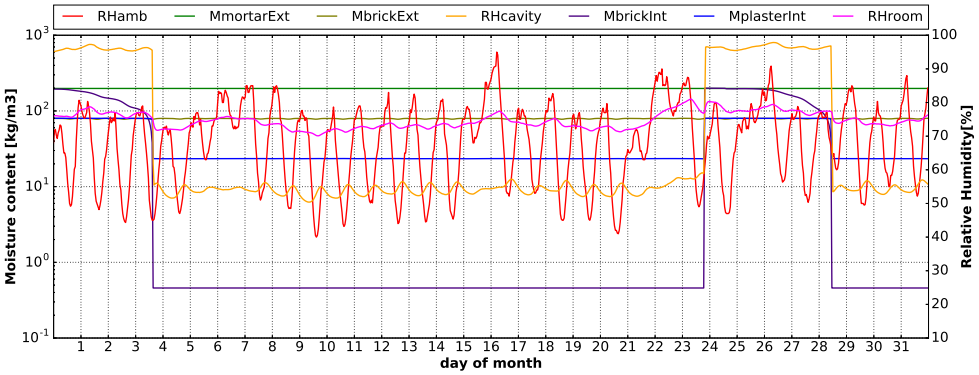

Figure 3.11: The relative humidity evolution in Terrassa room and the moisture contents in the layers of the façade wall during May.

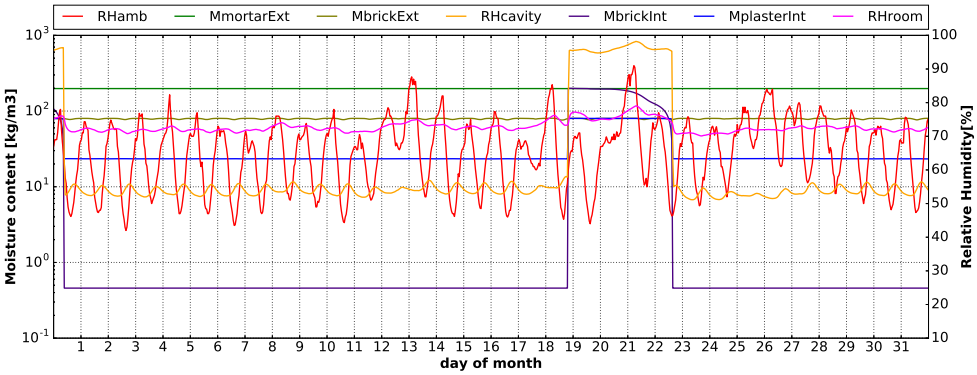

Figure 3.12: The relative humidity evolution in Terrassa room and the moisture contents in the layers of the façade wall during August.

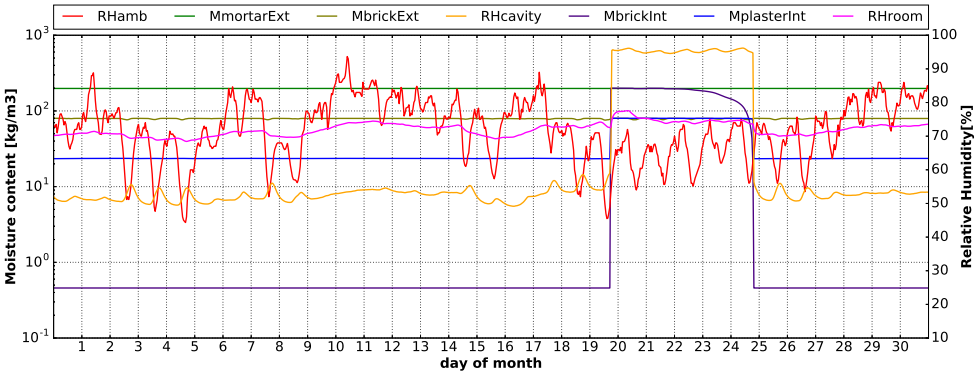

Figure 3.13: The relative humidity evolution in Terrassa room and the moisture contents in the layers of the façade wall during November.

The warm climate in Terrassa makes the air able to hold a high amount of water vapour even though the ambient relative humidity is not high. This is reflected in the exterior façade layer (MmortarExt) since it has the highest moisture content and it is always in capillary saturation state at $200 kg/m^3$. the state of the external layer affects the other wall layers, as a consequence the relative humidity in the air cavity increases up to 98%, the brick layer (MbrickInt) reach the capillary saturation at $200 kg/m^3$ and the interior layer plaster moisture content (MplasterInt) increases to $80 kg/m^3$, several days during the year which increase the risk of deterioration, provoke an increase in the indoor relative humidity and thus affects the indoor air quality. The air cavity has the function of moisture break in the wall to prevent liquid transmission, however it

was not able, all the year, to protect the interior layers (plaster and brick) from the high moisture content.

Water condensation

In this section, it has been checked whether water condensation occurs in the interior and exterior surfaces of the façade. The water vapour condensates into droplets when the temperature of the façade surfaces are below the dew point. The dew point is defined as the temperature at which the water vapour condensates to form liquid water. It is evaluated using Arden Buck equation [23] as:

$$T_{dew} = \frac{c\gamma}{b-\gamma} \tag{3.1}$$

where

$$\gamma = \ln\left(\frac{\phi}{100} e^{\left(\frac{b-T}{d}\frac{T}{c+T}\right)}\right); \qquad b = 18.678; \qquad c = 257.14^{o}C; \qquad d = 234.5^{o}C \tag{3.2}$$

where T and ϕ are the temperature and relative humidify of the air in contact with the surface. The difference between the temperature of surface and the dew point of air close to the surface defines the magnitude of moisture condensation.
When the temperature of the interior and exterior surfaces (TplasterInt and TmortarRxt) of Figures 3.6, 3.7, 3.8 and 3.9 drop below the dew point, the colour of the corresponding curves will change into light blue and light green, respectively, which gives an indication about the time and duration of water condensations in the corresponding surfaces. The water condensation has been observed several days in the exterior layer (TmortarExt), in 20 days in total during all the simulated year. On the other hand the condensation in the interior surface (TplasterInt) has been observed only one day in November, as shown in light blue in Figure 3.14 (d).
The dew point of the air near the interior and exterior surfaces under the influence of different outdoor condition (Two days from February, May, August and November) are depicted in Figure 3.14.
It has been observed that when the ambient temperature of air near the external surface (mortar) increases from figure (a) to (b), the duration and magnitude of moisture condensation in the surface (TmortarExt) are reduced. In the same manner, when the humidity of ambient air near the surfaces increases the duration and magnitude of moisture condensation are increased as shown from figure (c) to (d).
The water condensation in buildings envelope is an important agent for materials deterioration and mould formation, as a consequence it affects the thermal and moisture resistance of the wall which lead to high energy consumption. Furthermore, the condensation induces high indoor relative humidity that in addition to the mould growth affects the indoor air quality of the rooms and can cause discomfort and health

problems [17]. To prevent from this phenomena HVAC system is recommended to avoid condensation in the interior and hydrophobic materials is recommended to avoid water absorption by the exterior layer [24].

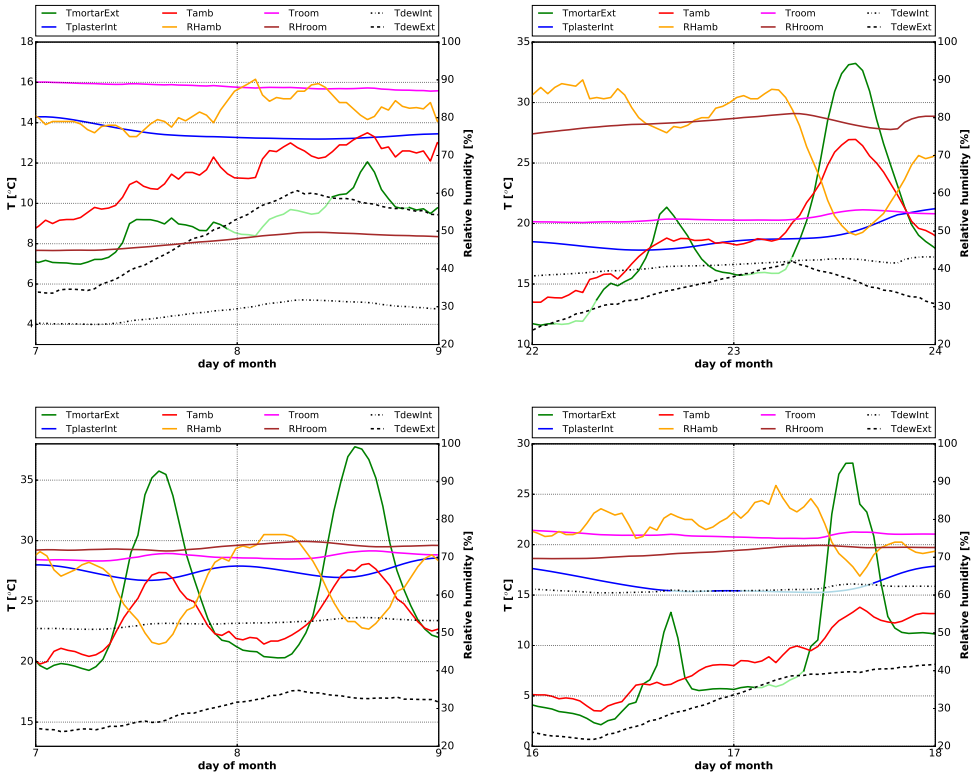

Figure 3.14: Condensation in the interior and exterior surfaces of the façade. Top left (a): February, top right (b): May, bottom left (c): August and bottom right (d): November.

Sensitivity analysis

In order to understand the importance and the influence of each parameter of the material properties on the hygrothermal behaviour, a sensitivity analysis is conducted by varying the hygrothermal parameter of the exterior layer (mortar) and analysing the effects on the interior layer (plaster) and the room.
Only the properties of the external layer are changed because the retrofitting of the building façade is expected to be done in the exterior surface.

Thermal conductivity, λ

The thermal conductivity is an important parameter and indicator of the materials thermal insulation. The energy used for space heating or cooling can be decreased by using low thermal conductivity materials [25]. Hence it is an important parameter to consider when selecting the construction materials. The thermal conductivity of the exterior layer (mortar), presented in section 3.2.2, has been decreased to 90%, 50% and increased to 50% by multiplying the property by 0.1, 0.5 and 1.5, respectively. The influence of the thermal conductivity of the exterior layer (mortar) on the hygrothermal behaviour of the interior surface (plaster) and of the room is shown in Figures 3.15 and 3.16.

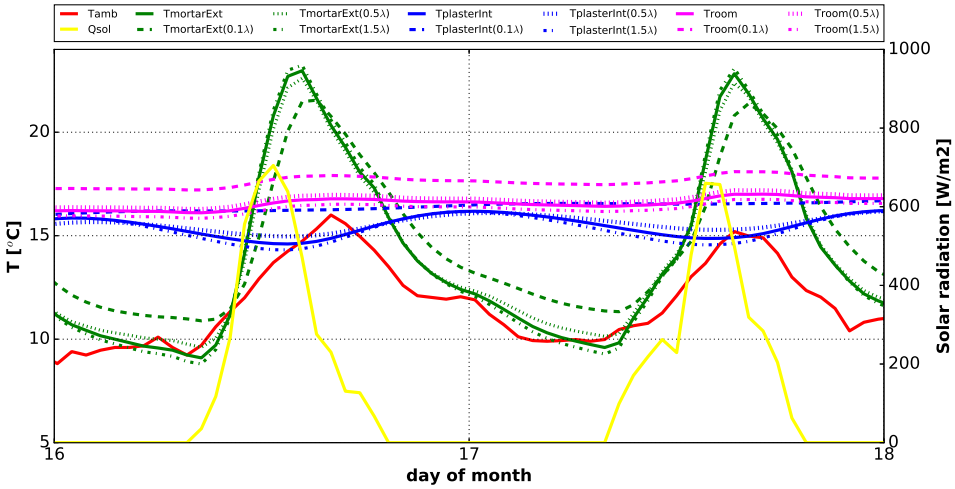

Figure 3.15: Effect of conductivity on thermal behaviour of Terrassa room.

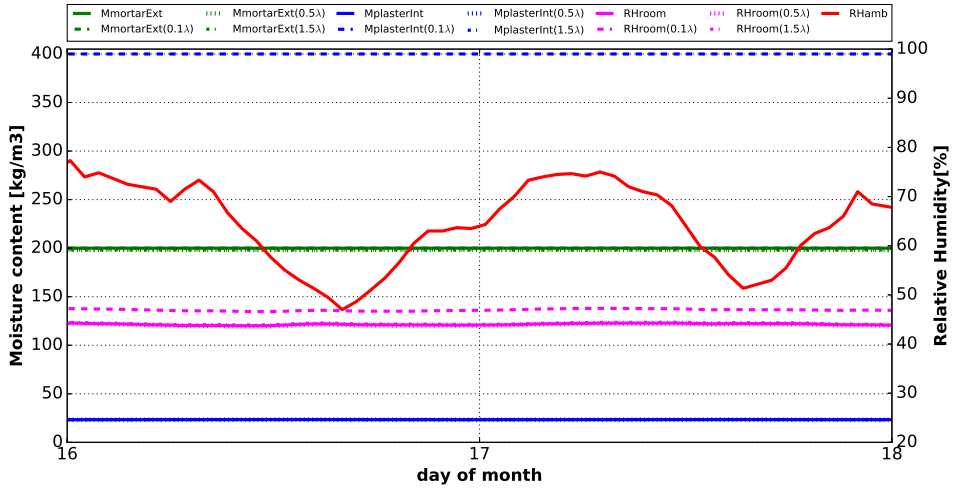

Figure 3.16: Effect of conductivity on moisture behaviour of Terrassa room.

As it can bee seen in Figure 3.15, the variation of the thermal conductivity of the exterior layer has a significant impact on the temperature of the interior layer and therefore in the room. The variation of $\pm 50\%$ has shown a slight effect on the temperature profiles, nevertheless decreasing the parameter by 90% affects significantly the temperature evolution in the exterior layer: its amplitude variation and time lag have decreased. As a consequence, the thermal diffusivity through the wall decreases leading to an increase in the temperature of the interior layer and in the room. The moisture content in the interior layer is affected and increases to the capillary saturation state ($400 kg/m^3$) as shown in Figure 3.16, which is mainly due to the rise of the temperature in this layer that affect the moisture diffusivity through the term D_ϕ in equation (2.5). Thus the relative humidity in room has slightly increased.
As described by the governing equations in section 2.3.1 of chapter 2, the heat and moisture are coupled phenomena. The moisture does not only affect the heat transfer but it is also affected by the variations of the temperature as seen for the interior layer. The insulation material is usually selected based on its thermal conductivity, however it is important also to consider the effect that thermal conductivity can have on the moisture transfer since it can contribute to a higher indoor humidity rates despite its good thermal insulation.

Moisture sorption, w

The moisture content in a material is related with the relative humidity inside it by

means of the moisture sorption curve, as explained in section 3.2.2. The sorption curve presented in section 3.2.2 has been multiplied by 0.5 and 1.5 to see the effect on the material. The influence on the hygrothermal behaviour of the interior surface (plaster) and of the room is shown in Figures 3.17 and 3.18.

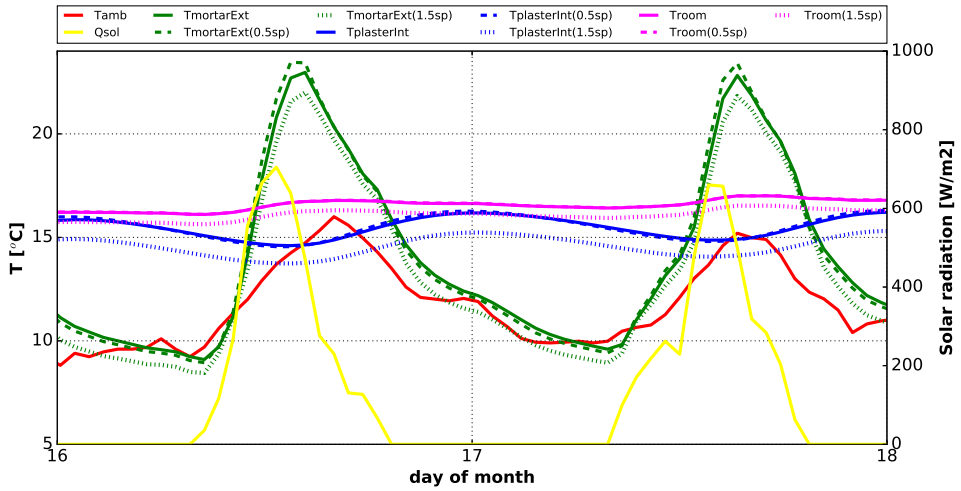

Figure 3.17: Effect of the variation of the moisture sorption on the thermal behaviour of Terrassa room.

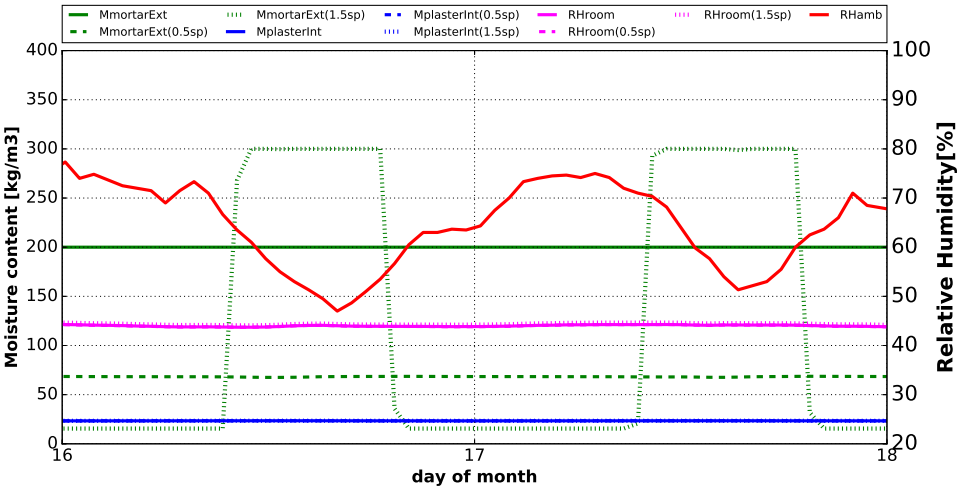

Figure 3.18: Effect of the variation of the moisture sorption on the moisture behaviour of Terrassa room.

A ±50% variation in the moisture sorption of the mortar layer has an effect of the temperature of this layer. For a 1.5xsorption, the moisture content in the mortar material is higher which leads to a decrease in the layer temperature, as shown in the Figure 3.17, as a consequence, the temperature has decreased in the interior layer and in the room.
When the moisture sorption increases, the material can hold more moisture in the porous for the same relative humidity values, this is can be seen in Figure 3.18 for the higher sorption value, where the material is in dry state during some periods and it is not always saturated in moisture. Despite the effect that moisture sorption has on the moisture transfer of the exterior layer, the moisture in the interior layer is not very affected and so the room relative humidity.
Similar effects of the moisture sorption in the material's hygrothermal behaviour have been observed by Maalouf [26], Rahim [27] and Collet [28] when studying different materials.

Water vapour permeability, δ_p

The water vapour permeability parameter has been widely investigated in many works [10,29,30]. The water wapour permeability of the exterior layer (mortar) has been multiplied by 10^3 and 10^{-3} in order to see an effect on the material. The influence of the parameter on the hygrothermal behaviour of the interior surface (plaster) and of the room is shown in Figures 3.19 and 3.20.

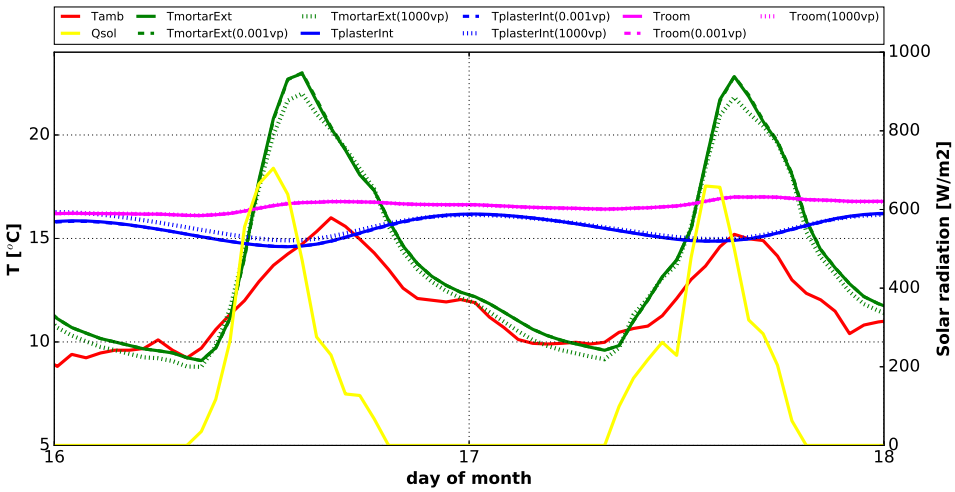

Figure 3.19: Effect of the variation of the vapour permeability on the thermal behaviour of Terrassa room.

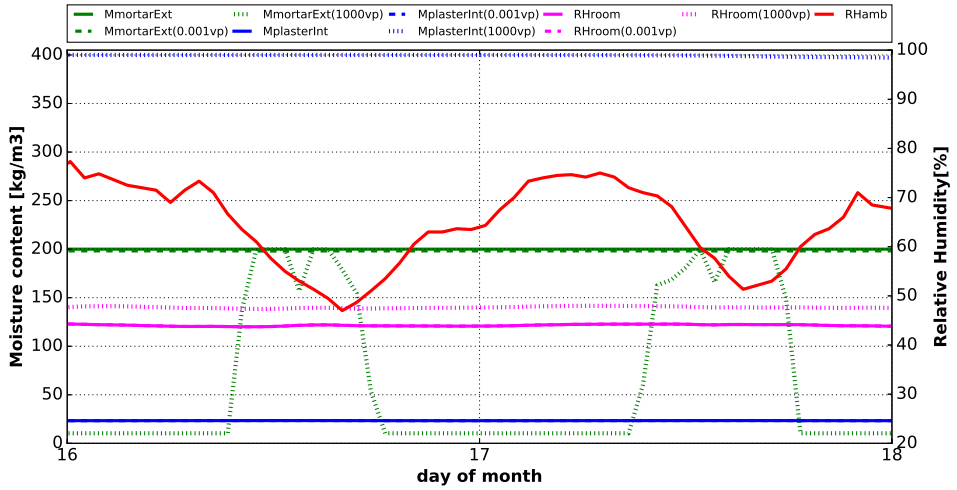

Figure 3.20: Effect of the variation of the vapour permeability on the moisture behaviour of Terrassa room.

The mortar has a low vapour permeability in low relative humidity as described in the material properties in section 3.2.2, so decreasing the parameter does not show any effect on the temperature and has only a slight effect on the moisture content of the exterior layer, as seen in Figures 3.19 and 3.20. Multiplying the parameter by 10^3 increases the latent heat diffusivity coefficients $D_{T,v}$ and $D_{\phi,v}$ in the energy equation (2.11) which lead to higher thermal diffusivity in the wall. As a consequence, the temperature slightly decreases in the exterior layer and increases in the interior one, as it is receiving more heat flux.
Not only the thermal diffusivity increases but also the moisture diffusivity through the coefficients D_ϕ and D_T in the moisture equation (2.5) which lead to a high water vapour transport through the wall, so the exterior layer dries and its moisture content decrease while the interior wall receive more water vapour that make it reach the saturation state. As a result the relative humidity in the room increases. The parameter has shown a strong influence in the heat and moisture content of the mortar layer, but not in the whole composite wall.

Water liquid permeability, k_l

The liquid permeability provides information about the magnitude of the sucked water liquid in the material. The water liquid permeability of the exterior layer (mortar) has been multiplied by 10^3 and 10^{-3} in order to see an effect on the material. The influence of the parameter on the hygrothermal behaviour of the interior surface

(plaster) and of the room is shown in Figures 3.21 and 3.21.

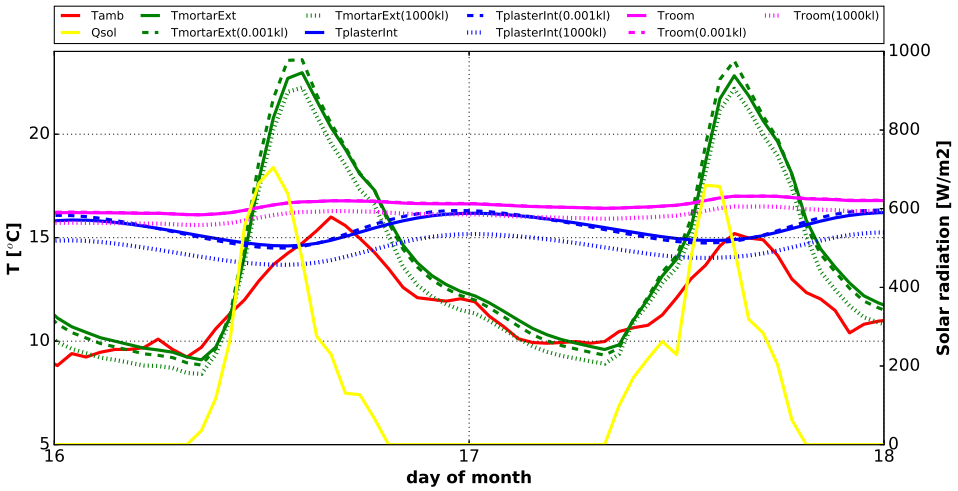

Figure 3.21: Effect of the variation of the liquid permeability on the thermal behaviour of Terrassa room.

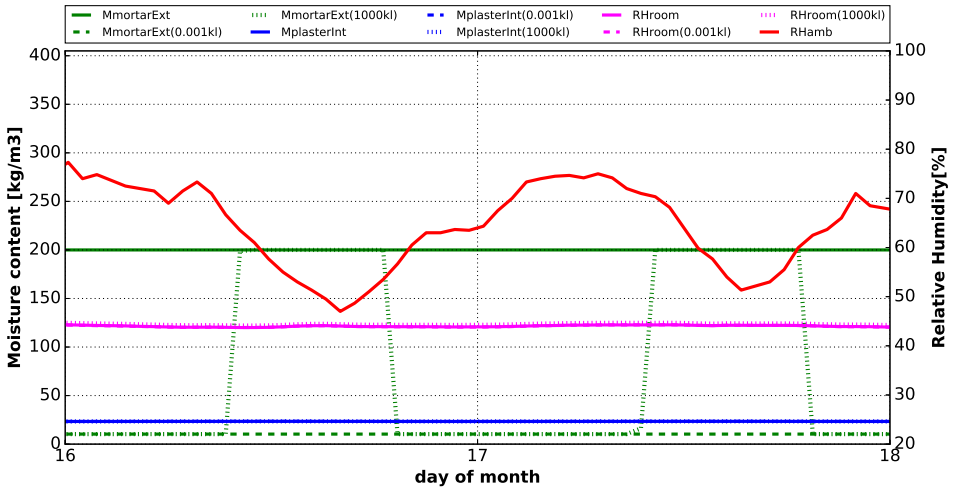

Figure 3.22: Effect of the variation of the liquid permeability on the moisture behaviour of Terrassa room.

The variation of the liquid permeability in the exterior layer affects its temperature. When this parameter increases the water liquid transport through the material in-

creases leading to a decrease on its temperatures and therefore in the temperature of the interior layer and in the room, as seen in Figure 3.21.
The liquid permeability affects the water liquid diffusivity in the material through the coefficients D_ϕ and D_T in the moisture equation (2.5). When it increases the moisture content in the mortar is decreased because the liquid has been transported from the material. Despite the high transport of water liquid in the exterior layer, the interior layer doesn't reach the saturation and is maintained at low moisture content, the water liquid may require more time to reach the interior layer especially in the presence of the air cavity in the façade layers, that acts like a break for the moisture liquid transfer.
When the liquid permeability is decreased, the water liquid transport is decreased and the moisture in the mortar is transported farther in the vapour phase, which leads to its drying and to a decrease in its moisture content.

Based on the conducted sensitivity analyses, in order to have a better thermal and moisture resistant material in the exterior layer, not only thermal conductivity should be considered while selecting the material but also the hygric properties. A lower moisture sorption decreases the capacity of the material to hold moisture. A higher vapour permeability leads to higher vapour transport, increases the drying process in the façade and therefore decreases the risk of deterioration. A lower liquid permeability reduces the liquid transport to the other materials and promote the vapour transport.

After the analysis of heat, moisture, condensation and sensitivity of the properties in free floating mode in the demo site room of Terrassa, the façade has shown to be efficient in providing thermal insulation except for the single glass window which demonstrate a low thermal performance. Regarding the moisture resistant, it is not enough, there is a risk of deterioration in the interior layer (plaster) and exterior (mortar) materials. It is recommended to change the single glass window to a multi-glass and reform the façade by using a better insulation material.
The proposed solutions for retrofitting were to substitute the existing window with a double glass and to use a super insulating aerogel mortar with a thermal conductivity 85% lower than the exterior layer mortar. The hygric properties of the aerogel material are not known. They will be assumed the same as the conventional mortar when carrying out the simulations in NEST to see the efficiency of these proposed retrofitting solutions.

HVAC and energy consumption

During the previous free-float simulations, the indoor temperature reaches a minimum of 15 ^{o}C in winter and a maximum of 33 ^{o}C in summer, while the relative

humidity is at a minimum of 38% and at a maximum of 82 %. The two variables are most of the time outside the ranges of comfort fixed by the Spanish standard. In order to compensate the differences, the hospital of Terrassa use a central HVAC system to heat/cool and dehumidify/humidify the air to the set point temperature and relative humidity of 23^0C and 50%, respectively, before its injection in the building rooms with a mass flow of 100 m^3/h. The room is re-simulated by considering the HVAC in the both cases, with and without the consideration of moisture and then by considering the insulation enhancements of double glass window and aerogel mortar. The annual thermal and moisture loads for the room are evaluated and presented in the following table.

	Heating	**Cooling**	**Dehumidification**	**Humidification**
Load (Heat simulation)	134.4 $kW \cdot h$	208.4 $kW \cdot h$	-	-
Load (HAM simulation)	111.7 $kW \cdot h$	217.0 $kW \cdot h$	62.3 $mg \cdot h$	18.2 $mg \cdot h$
Load after retrofitting (HAM simulation)	18.1 $kW \cdot h$	220.0 $kW \cdot h$	26.9 $mg \cdot h$	16.2 $mg \cdot h$

Table 3.2: Annual thermal and moisture load in Terrassa room

Due to the warm climate in Terrassa more cooling than heating is required during the year. The total thermal load by considering heat and moisture simulation is lower than the one evaluated by performing only heat simulation. Neglecting the moisture dependence to energy leads to an error in estimating the thermal load which can lead to a bad sizing of HVAC systems. Moreover, the moisture load give an idea about the amount of additional energy required for the dehumidification or humidification of the air which should be taken into account when evaluating the total energy consumption in the building. The accuracy of loads calculations by means of the coupled heat and moisture in buildings has been also pointed out by Maalouf [31] and Hoseini [22].
By considering the proposed enhancement for the building envelope insulation, the predicted energy consumption in the room has been decreased by more than 80% for heating, however the energy consumption for cooling has been increased due to the use of double glass window [32] that reduces the radiation and the heat loss from the room to the exterior. The total annual energy saving in the room is around 27%. The humidification and dehumidification loads have been reduced as well.
More attention should be given to the moisture in buildings since it has an impact of the thermal performance, it allows the evaluation of the moisture content and condensation in the materials and estimate the real thermal and moisture loads in the room.
The other hospital demo site is located in Sabadell (at 10 km from Terrassa), The simulation results have shown similar behaviour to ones of Terrassa since both sites

have similar weather conditions and structure. To avoid repetitions, Sabadell demo site will not be presented. In the rest of the demo sites (Sweden and UK) only the simulations of heat and moisture will be presented and discussed.

3.3.2 School in Skelleftea

The representative room of the school in Skelleftea, Sweden, is a classroom that has a south and east façades, as shown in Figure 3.24 and 3.25, five windows are located in the south façade, they are composed of triple glass. The façades are composite walls made of brick, wood fibre and plaster materials while the interior walls are only made of brick. The ground is made of concrete material (unknown finishing layer) and the roof a false ceiling of gypsum board. The room's walls and their layers are shown in the Figure 3.26.

Figure 3.23: School demo site in Skelleftea, Sweden.

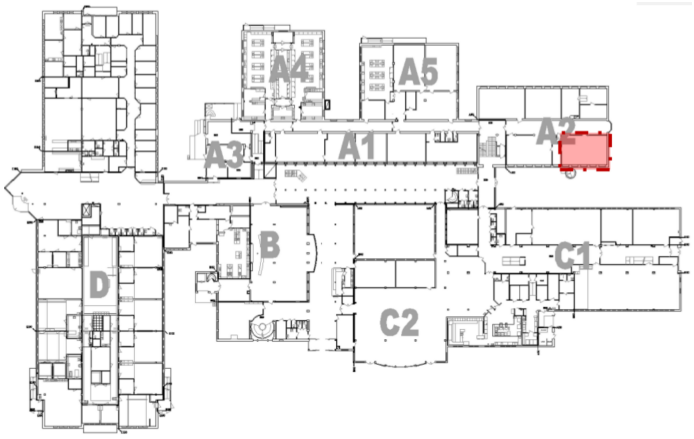

Figure 3.24: The school floor plan and room location in Skelleftea, Sweden.

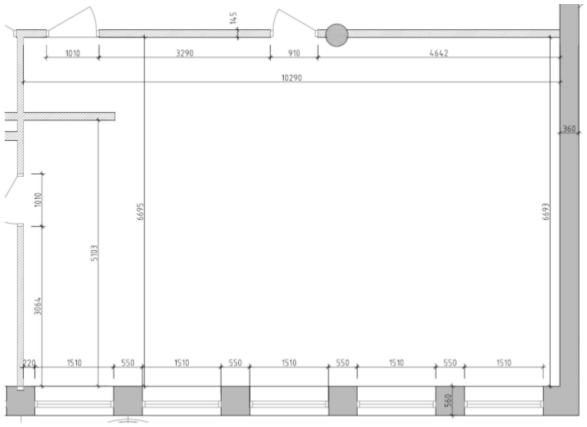

Figure 3.25: The representative room plan in Skelleftea school, Sweden.

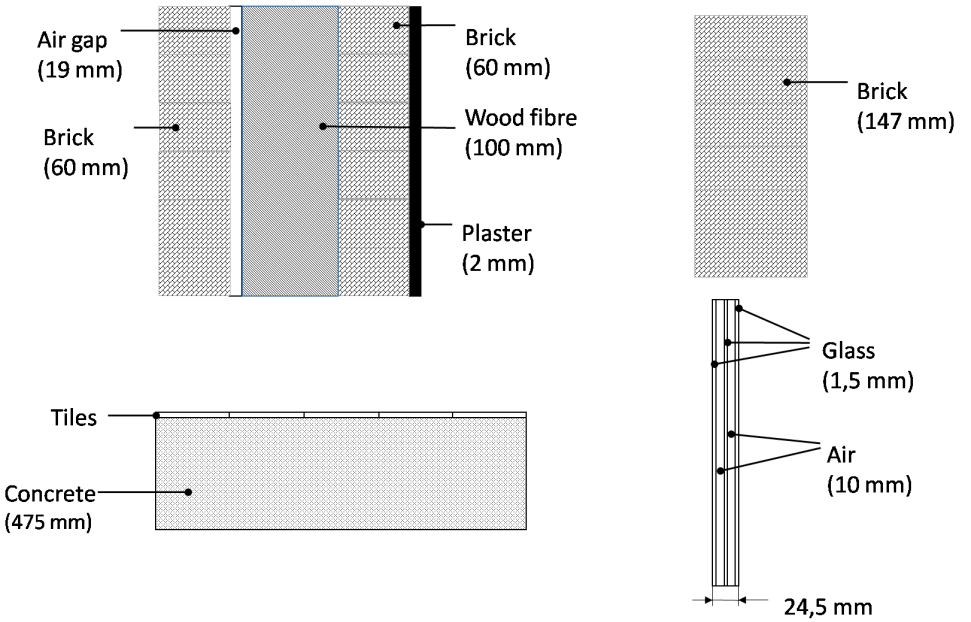

Figure 3.26: Room walls in Skelleftea school demo site. Top Left (a): façade, top right (b): interior wall, bottom left (c): floor and bottom right (d): Window

Room envelope

The temperature evolution in the interior and exterior sides of the south and east façades and in the centre of each interior layer of them are presented during one week in February, May, August and November in Figures 3.27, 3.28, 3.29 and 3.30, respectively, by using the coupled heat and moisture model.

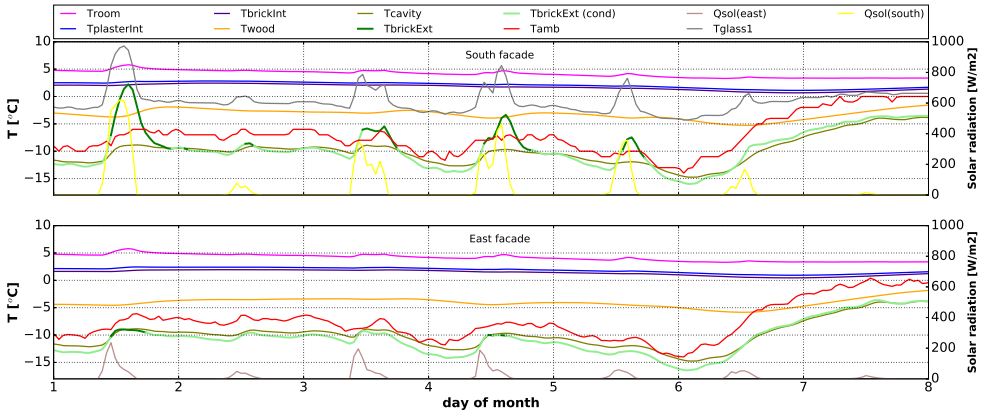

Figure 3.27: The temperature evolution in Skelleftea room and in the layers of the façades walls during one week February.

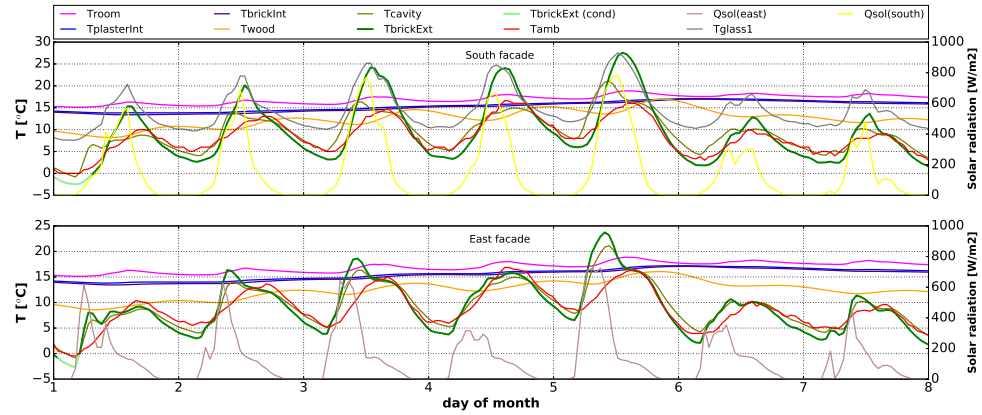

Figure 3.28: The temperature evolution in Skelleftea room and in the layers of the façades walls during one week in May.

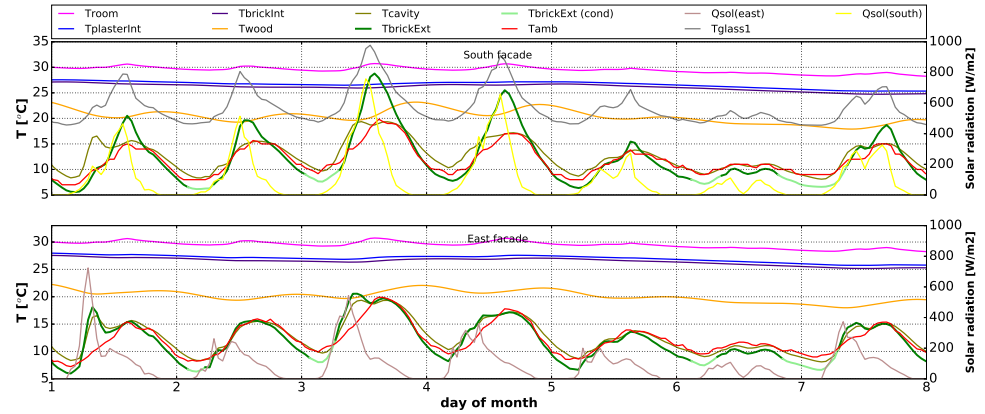

Figure 3.29: The temperature evolution in Skelleftea room and in the layers of the façades walls during one week in August.

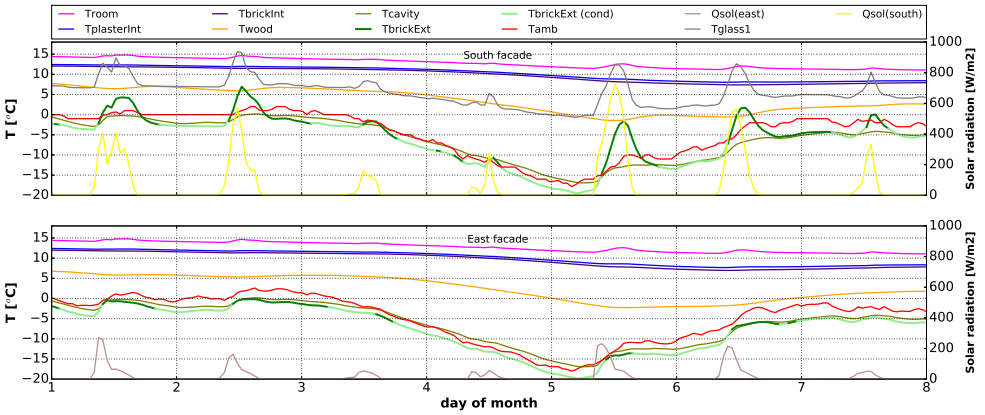

Figure 3.30: The temperature evolution in Skelleftea room and in the layers of the façades walls during one week in November.

Contrary to Terrassa, the air cavity function for thermal insulation is not enough in the cold weather of Skelleftea. The temperature in the air cavity (Tcavity) has a similar profile as the exterior layer (TbrickExt), both of them have a very low temperature similar to the ambient (Tamb) and reach -25^0C during winter as shown in February. However the wood fibre (Twood) layer has shown to be a very effective in providing thermal insulation, it has significantly reduced the heat transfer between the exterior layers (TbrickExt and Tcavity) and the interior layers (TbrickInt and TplasterInt). It

is a good material for the insulation but not enough considering the extremely cold weather. It is recommended so to use additional insulation materials to maintain a warmer temperature in the room.
The five windows in the south façade with triple glass each one have shown a good thermal insulation, despite the cold weather conditions, the interior glasses temperature goes from -8^oC in February (when the ambient temperature is -23^oC) to 38^oC in August (when the ambient temperature is 25^oC) . The use of multi glass window increases the heat gain due to solar radiation in the room and decrease the heat losses from the room to the outside due to sky radiation, it demonstrates a better thermal performance comparing to the single glass window in Terrassa.
There is no water condensation in the interior surface of the façades (TplasterInt), however the outdoor relative humidity is high during the winter and reaches 100% at very low temperatures as shown in February and November, which help the condensation to occur in the exterior surface of the façades (TbrickExt). This phenomena is more noticeable in the east façade than the south one due to its lower temperature. The condensation occurs in 9 months in total during all the simulated year which can lead to serious problems of deterioration and mould growth.
In addition, the high outdoor relative humidity in winter leads to a high moisture content in the exterior layer (MbrickExt) that reaches the water saturation state during February and November as shown in Figures 3.31 and 3.34. During summer, the outdoor relative humidity decreases, then the exterior layer (MbrickExt) contains less moisture than in winter season as shown in 3.32 and 3.33. In both seasons, the air cavity reduces the moisture transfer and the wood fibre board doesn't reach the saturation state during all the year, despite that the exterior layer (brick) is saturated or at high levels of moisture. The interior layers (MbrickInt and MplasterInt) are maintained at lower moisture contents and therefore a good moisture resistance in the façade is ensured.

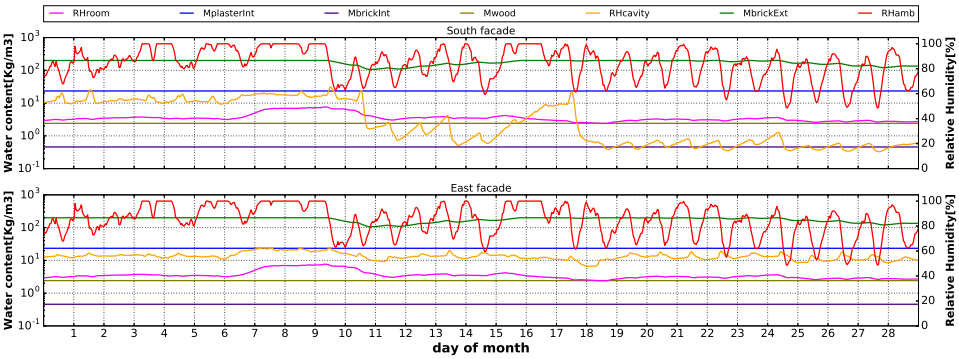

Figure 3.31: The relative humidity evolution in Skelleftea room and the moisture contents in the layers of the façade wall during February.

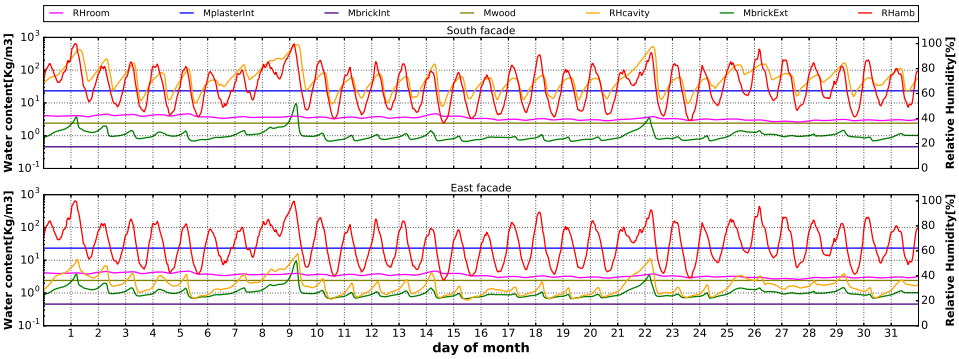

Figure 3.32: The relative humidity evolution in Skelleftea room and the moisture contents in the layers of the façade wall during May.

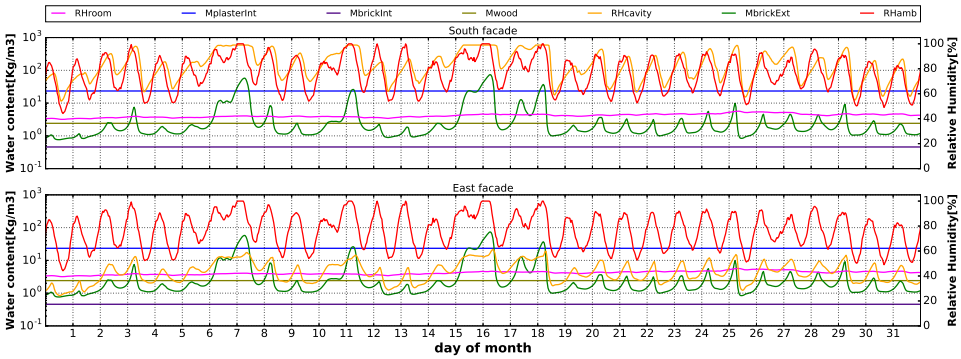

Figure 3.33: The relative humidity evolution in Skelleftea room and the moisture contents in the layers of the façade wall during August.

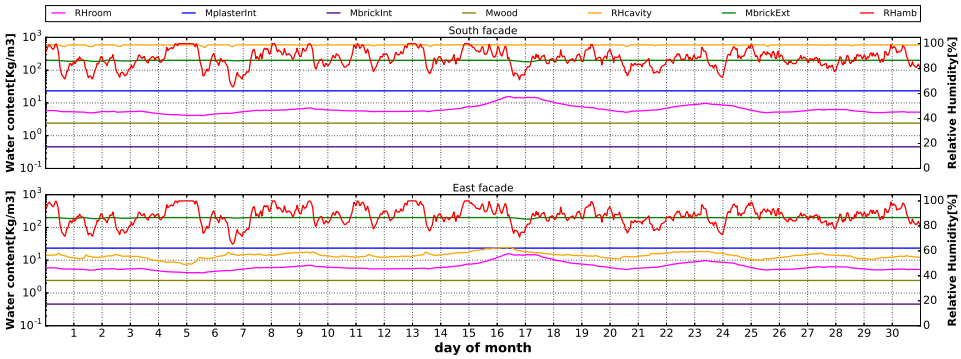

Figure 3.34: The relative humidity evolution in Skelleftea room and the moisture contents in the layers of the façade wall during November.

In the cold and dry climate of Skelleftea the room façades have shown to be efficient in providing moisture resistance but not enough for thermal insulation. Despite that the existing wood fibre layer and the triple glass windows have demonstrated good thermal performance, it is recommended to use additional thermal insulation material to reach a warmer room's temperature.
The proposed solution to enhance the insulation in the façades was using vacuum insulating panels (VIP) made of pressed silica as an additional layer in the exterior. The VIP is characterized by its low thermal conductivity (3.5 $mW/m \cdot k$) and high moisture resistance (low water sorption with a maximum moisture content of $32 kg/m^3$ in capillary saturation).

HVAC and energy consumption

The relative humidity in the room in free floating mode has a minimum of 38% and a maximum of 55% during all the simulation which is in the range of the Swedish standard. The room temperature has a minimum of 3^oC in winter and 30^oC in summer and need to be conditioned to maintain thermal comfort.
In the school of Skelleftea, a central HVAC system is used to heat, humidity and dehumidify the air at a set point temperature and relative humidity of 20^oC and 50%, respectively, before its injection in the building rooms with a mass flow rate of 300 m^3/h. The air is cold and dry in Coventry, neither cooling or dehumidification systems are used. The room is re-simulated by considering the HVAC without and with the proposed retrofitting solutions of VIP material and the annual energy and moisture loads are evaluated and presented in the following table.

	Heating	**Cooling**	**Dehumidification**	**Humidification**
Load	1579.0 $kW \cdot h$	-	-	688.0 $mg \cdot h$
Load after retrofitting	369.0 $kW \cdot h$	-	-	154.2 $mg \cdot h$

Table 3.3: Annual thermal and moisture load in Skelleftea room

As a consequence of the extremely cold weather conditions and the low thermal performance of the envelope, an important thermal load is required to maintain the room at a minimum of 20 ^oC. The indoor relative humidity was good, at around 40%, in free-float before using HVAC, however when the HVAC is used, the air containing low humidity becomes drier and therefore more humidification load is required to increase the humidity at the comfort level of 50%.
By considering the proposed enhancement for the building envelope insulation, the predicted energy consumption in the room has been decreased by more than 76%. Since less heating is used in the room, the air remain less dry and the humidification load has been reduced also by more than 77 %.The proposed solution of using VIP as an additional exterior layer seems to be effective as it contributes to a significant decrease in the thermal and moisture loads.

3.3.3 University in Coventry

The representative class room of Coventry, in England, is located in the first floor, it has a west façade with two single glass windows, as shown in the room plan 3.37. The exterior and the interior walls are made of brick while the roof and the floor are made of concrete material (no finishing materials were specified). The walls of the room and their layers are shown in Figure 3.38.

Figure 3.35: The university demo site in Coventry, UK.

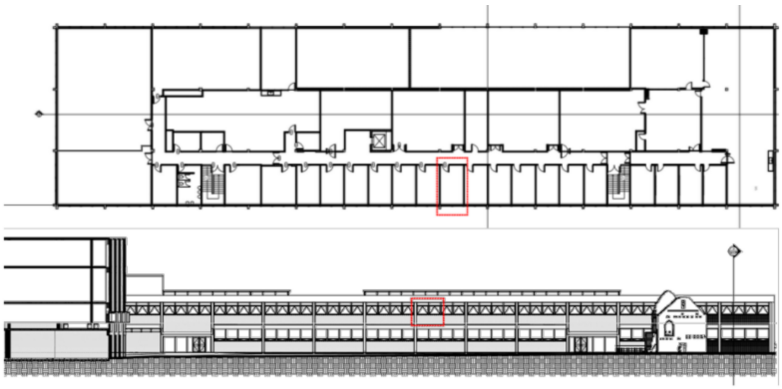

Figure 3.36: The university floor plan and room location in Coventry, UK.

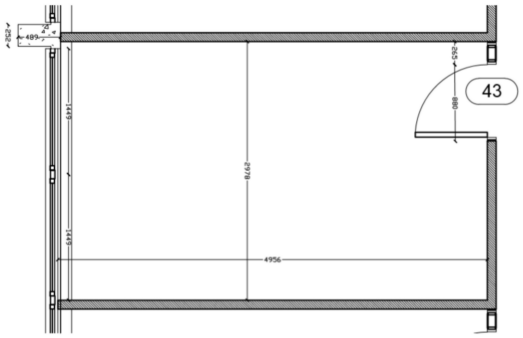

Figure 3.37: The representative room plan of Coventry, UK.

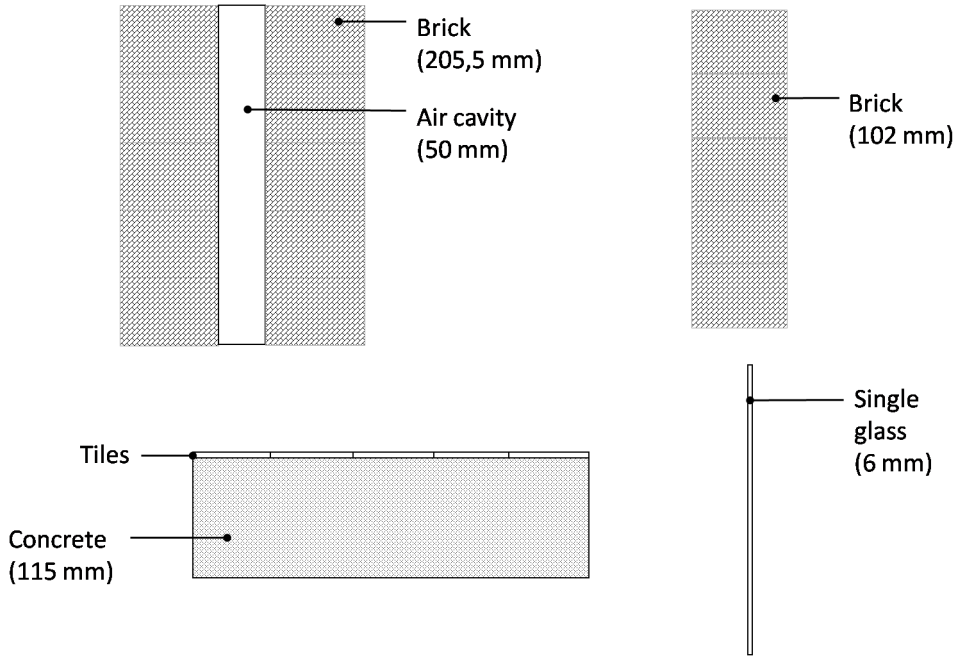

Figure 3.38: The room walls in Coventry university demo site. Top Left (a): façade, top right (b): interior wall, bottom left (c): floor and bottom right (d): Window.

Room envelope

The temperature evolution in the interior and the exterior side of the façade and in the air chamber layer during one week in February, May, August and November are presented in the Figures 3.39, 3.40, 3.41 and 3.42, using the heat and moisture model.

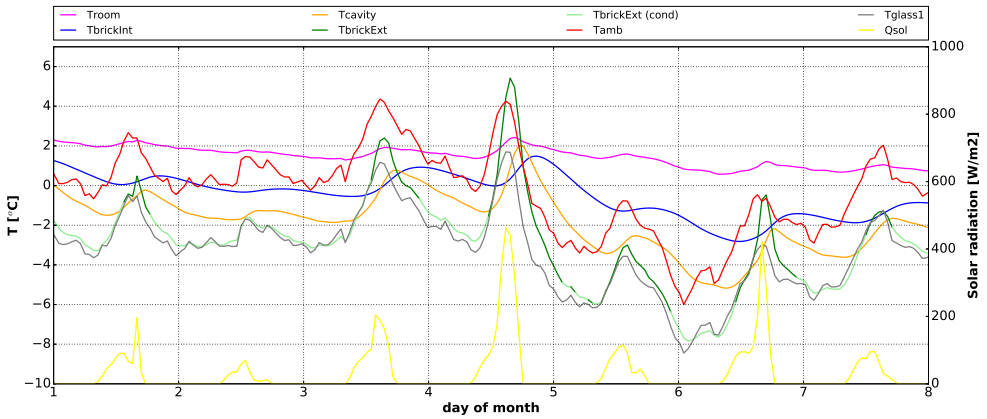

Figure 3.39: The temperature evolution in Coventry room and in the layers of the façades walls during one week in February.

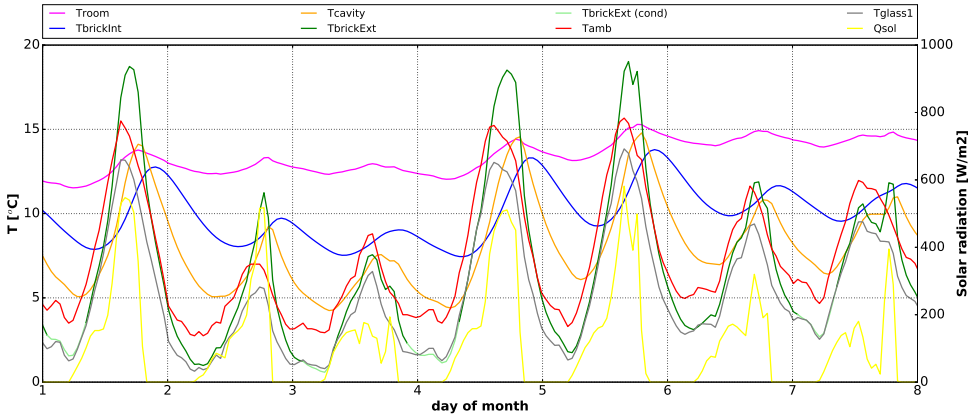

Figure 3.40: The temperature evolution in Coventry room and in the layers of the façades walls during one week in May.

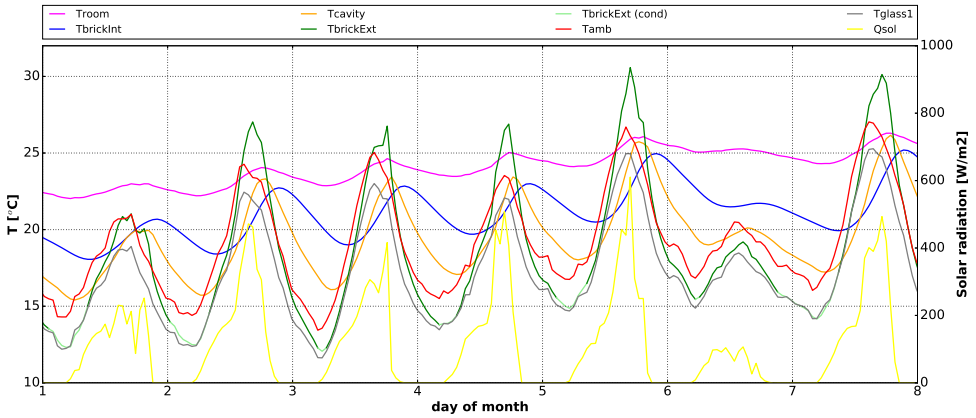

Figure 3.41: The temperature evolution in Coventry room and in the layers of the façades walls during one week in August.

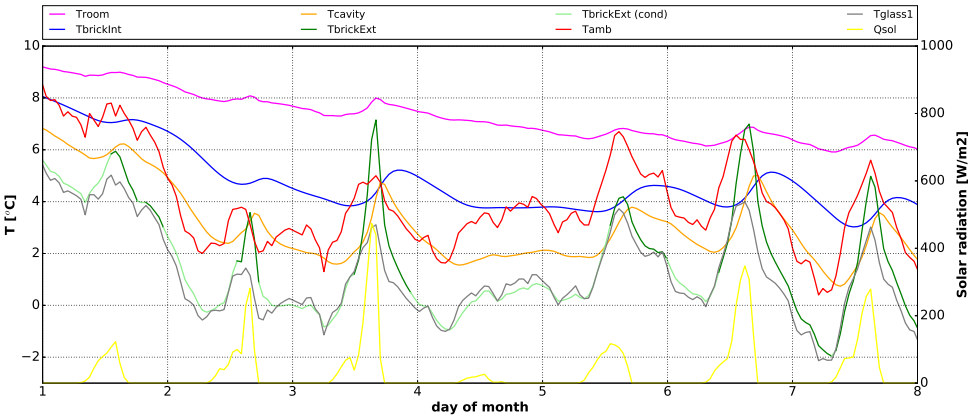

Figure 3.42: The temperature evolution in Coventry room and in the layers of the façades walls during one week in November.

The brick layers (TbrickExt and TbrickInt) and air chamber (Tcavity) are not enough to insulate the room especially in winter when their temperature are low and goes below zero sometimes, as shown in February when the ambient air temperature is -8^0C. The single glass windows (Tglass) have the lowest temperature in the façade, the same as in the case of Terrassa, the single glass demonstrates a low efficiency in thermal insulation, however the windows allow the transmission of solar radiation to the room which increase its temperature during the day, as shown in May and

August, when the room temperature has more oscillating behaviour.
There is no condensation observed in the interior side of the façade (brickInt), however water condensation occurs frequently in the exterior side almost during all the year which can lead to the deterioration of the material.
During winter the relative humidity of the ambient is high and the external layer of the façade (MbrickExt) is at high moisture content and sometimes reaches the saturation levels during February and November as shown in Figures 3.43 and 3.46. The air cavity (RHcavity) reduces the moisture transmission and the moisture decreases significantly at the interior layer (MbrickInt).

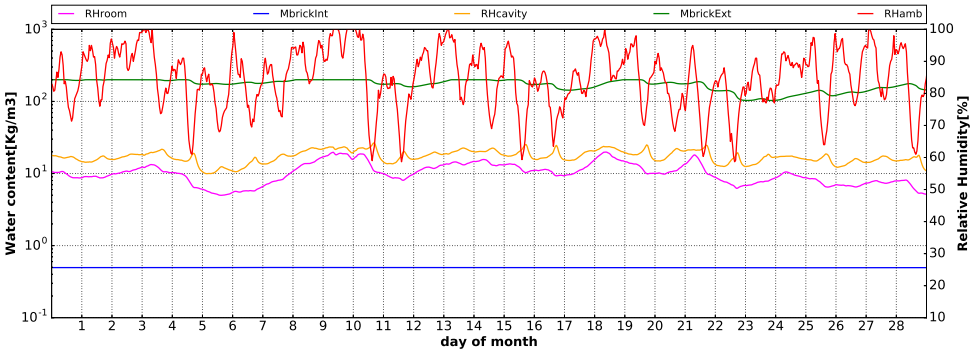

Figure 3.43: The relative humidity evolution in Coventry room and the moisture contents in the layers of the façade wall during February.

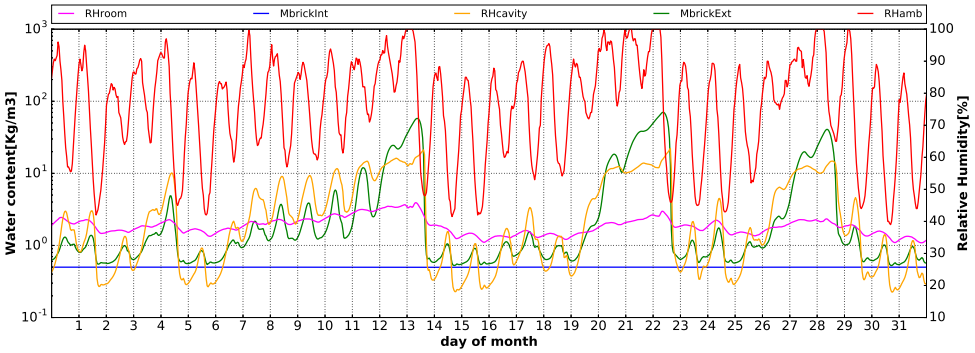

Figure 3.44: The relative humidity evolution in Coventry room and the moisture contents in the layers of the façade wall during May.

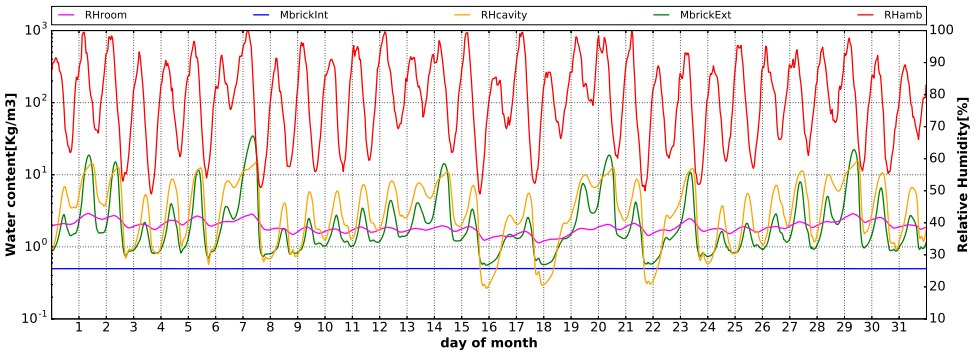

Figure 3.45: The relative humidity evolution in Coventry room and the moisture contents in the layers of the façade wall during August.

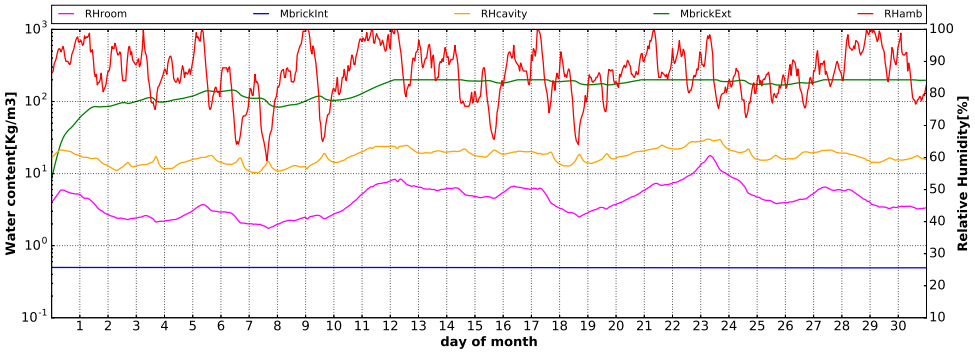

Figure 3.46: The relative humidity evolution in Coventry room and the moisture contents in the layers of the façade wall during November.

The façade wall ensures a good moisture resistance, however the thermal insulation is very low and need to be improved. The proposed solutions for retrofitting are the substitution of the single glass windows by double glass and installing additional VIP insulation material in the exterior side.

Indoor space and comfort level

The room temperature has a minimum of 0^oC and a maximum of 27^oC and it is below the range of UK standard almost during all the simulation time. On the other hand, the relative humidity is in the range of comfort level, it is between a minimum of 33% and a maximum of 60%. A central HVAC system is used to heat, humidify and

dehumidify the air to the set point temperature and relative humidity of 23^oC and 50%, respectively, before its injection in the building rooms with a mass flow rate of 100 m3/h. The air is cold and dry in Coventry, neither cooling or dehumidification systems are needed. The room is re-simulated by considering the HVAC without and with the insulation enhancements of double glass and VIP insulation and the annual energy and moisture loads are evaluated and presented in the following table.

	Heating	**Cooling**	**Dehumidification**	**Humidification**
Load	874.1 $kW \cdot h$	-	-	385.6 $mg \cdot h$
Load after retrofitting	373.3 $kW \cdot h$	-	-	333.1 $mg \cdot h$

Table 3.4: Annual thermal and moisture load in the room

An important thermal load is required to maintain the room at a minimum of 23 ^oC since the envelope has a low thermal performance. The same as observed in Skelleftea, the indoor relative humidity was good in free-float (between 33% and 60%), however when the HVAC is used to heat the room, the air containing low humidity becomes very dry and therefore more humidification load is required to increase the humidity at a comfort level to 50%.
By considering the proposed enhancement for the building envelope insulation of double glass and VIP material, the predicted energy consumption in the room is decreased by more than 57% for heating and by 13,6% for humidification. An important amount of humidification is required for the room which can be explained due to its small volume contradictory to Skelleftea case.
The proposed solutions for retrofitting have contributed to less thermal and moisture loads, however the energy saving is lower comparing to the case of Skelleftea.

3.4 Summary and conclusions

3.4.1 Effect of moisture

The importance of moisture simulation in buildings has been highlighted first, during the demo site simulation of Terrassa. The room has been simulated by first considering only the heat transfer model and second by considering both heat and moisture transfer model. It has been shown how the moisture presence in the materials has an impact on the heat transfer through them, it is mainly due to the effect of moisture on the thermal conductivity of the wall material and due to the effect of latent heat during the exothermic process of condensation and endothermic process of evaporation.
The effect on the heat transfer is not only observed in the materials but also in the indoor space. In the demo site of Terrassa the annual thermal load of heating

and cooling required to maintain thermal comfort in the room is 342.8 $kW.h$ when taking into account only heat transfer simulation and 328.7 $kW.h$ when taking into account both heat and moisture transfer simulation. Therefore performing only energy simulation in buildings can lead to significant errors in estimating thermal load and then the bad sizing HVAC systems [22]. Moreover, the moisture simulation allows the estimation of moisture load required to humidify and dehumidify the air, which is an additional factor to take into account when evaluating the total energy consumption in the building. Thus considering moisture simulation in buildings gives a higher accuracy for estimating the real energy consumption and allows a better sizing and optimization of HVAC systems.
By considering the heat and moisture simulation in buildings, the moisture content in the materilas and the relative humidity in the air cavities of the walls and rooms are solved and analysed, as presented at each demo site simulation. They are very important variables, first, to monitor the evolution of moisture in the materials and check whether they reach the capillary saturation state or not in order to prevent deterioration and avoid high moisture transfer. Second, they give information about the duration and magnitude of the water condensation that occurs in the façades surfaces in order to prevent deterioration and mould formation. Finally, the relative humidity is a good indicator of the indoor air quality and comfort level. In fact, a high indoor humidity increases the thermal sensations, it makes the temperature feels higher, as a consequence the human body (of the occupant) makes additional effort to cool itself down by increasing respiration and sweating which leads to an uncomfortable state. On the other side, a very low indoor humidity indicates that the air is dry, which can affect also the respiratory system and the skin. In both cases a high or low humidity cause a discomfort indoor environment. Then, it is important to monitor, identify the need and control the humidity levels by humidification or dehumidification in order to maintain a good comfort level.
Most of the buildings software consider and focus only on the energy and heat transfer simulation in buildings. However, using NEST software for the simulation of the representative rooms has proven the importance of the coupled heat and moisture transfer simulations in buildings.

3.4.2 Heat and moisture transfer in the envelopes

The simulation of heat and moisture transfer in the demo sites rooms using NEST has allowed to study and identify different problems in the thermal and moisture insulation in the rooms envelope. It has been observed that in warmer climates like in Terrassa, the room façades have better thermal insulation than moisture resistance. The warm air of Terrassa holds more moisture content that has been absorbed by the façades layers which led to the capillary saturation of its layers, as seen in the simulations. on the other side, in cold climates like in the case of Skelleftea and

Coventry, the rooms façades have better moisture resistance than thermal insulation. The cold air holds less water vapour so the air is drier and less moisture is absorbed by the façades layers, nevertheless due to the low ambient temperature more water condensation occurs in the exterior surfaces which can affect the materials durability. The weak points in the room envelope of each demo site have been predicted and identified. It is recommended to substitute the single glass windows with multi-glass and to use better moisture resistance materials in the site of Terrassa and a better thermal insulation materials in the sites of Skelleftea and Coventry. These recommendations should be considered and the materials should be selected depending on their thermal and hygric properties, as highlighted in the sensitivity analysis in section 3.3.1, in order to make an efficient retrofitting and prevent from the same problems in the future.
Different retrofitting solutions were proposed, such as replacing the single glass by double glass windows and retrofit the external layers of the façades by using external coat aerogel mortar or reinforcing layer of Vacuum insulation panels (VIP) . The selected materials, aerogel mortar and vacuum insulation panels (VIP), are classified as super insulating materials because of their low thermal conductivities. The expected efficiency of the retrofitting solutions at each demo site, in terms of energy consumption have been simulated and resumed in the next section.

3.4.3 Heat and moisture transfer in the rooms

In order to reach and maintain comfort levels of temperature and humidity as stated by the standards and evaluate the thermal and moisture loads of the rooms in their actual state, the demo sites rooms are re-simulated by taking into account HVAC. A conditioned air at the set point temperature and humidity is injected into each room in order to heat or cool and humidify or dehumidify the indoor air.
Figures 3.47 and 3.48 show the thermal and moisture loads required for each demo site room. It has been observed that in warmer climate (like in Terrassa), the indoor relative humidity is high due to high moisture transfer through the walls and then more dehumidification than humidification is required to maintain the humidity at set point value. However in colder climates (like in Skelleftea or Coventry), in the natural condition, free-float mode, when no HVAC is used, the indoor relative humidity is at good level, between 35% and 60%, but the temperature is below the set point temperature. When the HVAC is used to heat the corresponding rooms, the air containing low moisture becomes very dry, then more humidification load is required to increase the humidity level to 50%.
The simulation of demo sites rooms including HVAC is important for monitoring the energy consumption before and after the buildings retrofitting and to check the efficiency of the proposed solutions.

Figure 3.47 shows that retrofitting solutions in the warm climate of Terrassa (double glass window and aerogel mortar) has led to a total energy saving of 27%. The proposed enhancements were very efficient in winter since they reduce the heating up to 80% but not in summer because they contribute to more cooling load. More retrofitting solutions should be considered in order to reduce the energy consumption due to cooling. In the cold climates of Skelleftea and Coventry, the retrofitting solutions of VIP in Skelleftea and double glass and VIP in Coventry, have shown a significant energy saving in heating up to 76% in Skelleftea and 57% in Coventry. Figure 3.48 shows how the dehumidification need has been reduced to more than 50% in Terrassa, while the humidification required in the cold sites of Skelleftea and Coventry has been reduced to 77% and 13.6%, respectively. Which contribute also to more energy saving and higher air quality.

Figure 3.47: Thermal loads in the simulated rooms

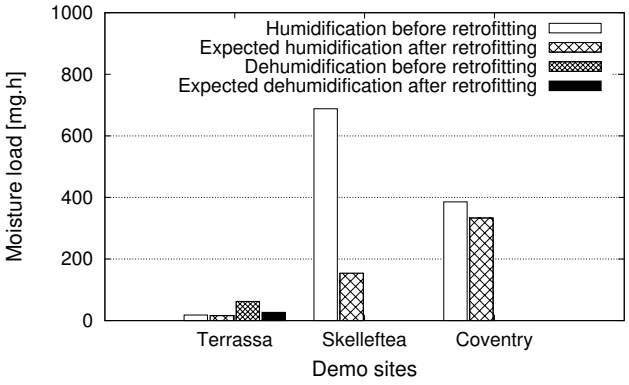

Figure 3.48: Moisture loads in the simulated rooms

During this work, the developed simulation software NEST has successfully employed for simulating, predicting and analysing the hygrothermal transfer in different public buildings. The building simulation tool has shown different capabilities and it can be used in other future work to compare the simulation with experimental data before and after retrofitting, to extrapolate the simulation and the analysis to the whole building and to use the software as a decision making tool to choose the best retrofitting solutions.

References

[1] J. Zhao, J. Grunewald, U. Ruisinger, and S. Feng. Evaluation of capillary-active mineral insulation systems for interior retrofit solution. *Building and Environment*, 115:215–227, 2017.

[2] *Retrofitting Solutions and Services for the enhancement of Energy Efficiency in Public Edification (RESSEEPE)*. `http://www.resseepe-project.eu`, 2013-2015. European project. Accessed: 2015-12-07.

[3] H. Janssen, B. Blocken, and J. Carmeliet. Conservative modelling of the moisture and heat transfer in building components under atmospheric excitation. *International Journal of Heat and Mass Transfer*, 50(1128-1140), 2007.

[4] M. Labat, M. Woloszyn, G. Garnier, and J. J. Roux. Dynamic coupling between vapour and heat transfer in wall assemblies: Analysis of measurements achieved under real climate. *Building and Environment*, 87(129-141), 2015.

[5] M. Woloszyn, M.M. Maxime Perier, B. Sid, T. Bejat, Y.A. Kedowide, C. Buhe, and E. Wurtz. Evaluation of the contribution of highly hygroscopic and vapour permeable walls to whole building performance. *Proceedings of BS2015: 14th Conference of International Building Performance Simulation Association*, 2015.

[6] U. Haverinen-Shaughnessy, M. Toivola, S. Alm, T. Putus, and A. Nevalainen. Personal and microenvironmental concentrations of particles and microbial aerosol in relation to health symptoms among teachers. *Journal of Exposure Science and Environmental Epidemiology*, 17(2):182–190, 2007. cited By 8.

[7] R.E. Dales, R. Burnett, and H. Zwanenburg. Adverse health effects among adults exposed to home dampness and molds. *American Review of Respiratory Disease*, 143(3 I):505–509, 1991. cited By 216.

[8] J. Langmans, R. Klein, and S. Roels. Hygrothermal risks of using exterior air barrier systems for highly insulated light weight walls: A laboratory investigation. *Building and Environment*, 56:192–202, 2012. cited By 24.

[9] F. Collet and S. Pretot. Thermal conductivity of hemp concretes: Variation with formulation, density and water content. *Construction and Building Materials*, 65:612–619, 2014. cited By 42.

[10] B. Haba, B. Agoudjil, A. Boudenne, and K. Benzarti. Hygric properties and thermal conductivity of a new insulation material for building based on date palm concrete. *Construction and Building Materials*, 154:963–971, 2017.

[11] METEONROM 7.1. `https://meteotest.ch/produkt/meteonorm`, 2016. Meteotest Fabrikstrasse 14, CH-3012 Bern, Switzerland.

[12] K. Lengsfeld and A. Holm. Entwicklung und validierung einer hygrothermischen raumklima- simulationssoftware wufi-plus. *Bauphysik*, 29(3):178–186, 2007.

[13] M.K Kumaran. *TASK 3: Material properties*. 1996. International energy agency, Energy Conservation in Buildings and Community Systems, IEA ANNEX 24.

[14] M. Jacob. *Heat transfer*, volume 1. John Wiley and sons Inc, 1957.

[15] Issam Sobhy, Abderrahim Brakez, and Brahim Benhamou. Analysis for Thermal Behavior and Energy Savings of a Semi-Detached House With Different Insulation Strategies in a Hot Semi-Arid Climate. *Journal of Green Building*, 12(1):78–106, 2017.

[16] N.G Mihajlo, H.D. Madhawa, B. William, and William M.W. A new method for the experimental determination of lewis' relation. *International Communications in Heat and Mass Transfer*, 33(8):929 – 935, 2006.

[17] P.O. Fanger. *Thermal comfort: Analysis and Applications in Envioronememental Engineering*, volume 1. United States: NcGraw-Hill Book Company, 1970.

[18] *Regulation on Indoor Heating and Air-conditioning Systems (RITE)*. 2008. Spain, Royal Decree 1027/2007.

[19] *Instalaciones de acondicionamiento de aire en hospitales*. 2005. UNE 100713:2005.

[20] *Sweden Green Building Council*. 2011. `https://www.sgbc.se/in-english`.

[21] *Workplace health, safety and welfare regulations*. 1992. `http://www.hse.gov.uk/pUbns/priced/l24.pdf`.

[22] A. Hoseini and M. Bahrami. Effects of humidity on thermal performance of aerogel insulation blankets. *Journal of Building Engineering*, 13:107–115, 2017.

[23] A.L. Buck. New equations for computing vapor pressure and enhancement factor. *J. Appl. Meteorol*, 20(1527-1532), 1981.

[24] S. You, W. Li, T. Ye, F. Hu, and W. Zheng. Study on moisture condensation on the interior surface of buildings in high humidity climate. *Building and Environment*, 125:39–48, 2017.

[25] D.M. Nguyen, A.-C. Grillet, T.M.H. Diep, C.N. Ha Thuc, and M. Woloszyn. Hygrothermal properties of bio-insulation building materials based on bamboo fibers and bio-glues. *Construction and Building Materials*, 155:852–866, 2017.

[26] C. Maalouf, D. Tran, M. Lachi, E. Wurtz, and T.H. Mai. Effect of moisture transfer on thermal inertia in simple layer walls. *International Journal of Mathematical Models and Methods in Applied Sciences*, 5, 2011.

[27] M. Rahim, O. Douzane, A.D. Tran Le, G. Promis, and T. Langlet. Characterization and comparison of hygric properties of rape straw concrete and hemp concrete. *Construction and Building Materials*, 102:679–687, 2016.

[28] F. Collet, J. Chamoin, S. Pretot, and C. Lanos. Comparison of the hygric behaviour of three hemp concretes. *Energy and Buildings*, 62:294–303, 2013.

[29] M. Rahim, O. Douzane, A.D. Tran Le, G. Promis, B. Laidoudi, A. Crigny, B. Dupre, and T. Langlet. Characterization of flax lime and hemp lime concretes: Hygric properties and moisture buffer capacity. *Energy and Buildings*, 88:91–99, 2015.

[30] P. De Bruijn and P. Johansson. Moisture fixation and thermal properties of lime-hemp concrete. *Construction and Building Materials*, 47:1235–1242, 2013.

[31] C. Maalouf, H. Boussetoua, T. Moussa, M. Lachi, and A. Belhamri. Experimental and numerical investigation of the hygrothermal behaviour of cork concrete panels in north algeria. *Proceedings of BS2015: 14th Conference of International Building Performance Simulation Association*, 2015.

[32] E. Cuce, P.M. Cuce, and C.-H. Young. Energy saving potential of heat insulation solar glass: Key results from laboratory and in-situ testing. *Energy*, 97:369–380, 2016.

[33] ASHRAE Standard 62.1. *Ventilation for Acceptable Indoor Air Quality*. 2016.

4

Airflow, heat and pollutant simulation. Application of NEST with dwelling control systems

4.1 Introduction

Since building thermal systems are major consumers of energy as far as their construction, operation and maintenance are concerned, energy simulations of buildings are critical for optimizing the energy demands. They can give vital information of the peak loads during the heating and cooling seasons, room temperatures and air velocity distributions for maintaining an adequate indoor environment, and overall energy demands during a year. This information can be used, for example, at the design of the HVAC to reduce energy costs.
Buildings can be considered as thermal systems interacting with the surroundings through heat transfer and fluid flow processes. The prediction of the thermal behaviour of buildings is challenging due to the large and complex geometry involved, transient boundary conditions, natural convection airflows, stack and wind effects, infiltration of ambient air and mechanical ventilation, and the mixture of free and forced convection flows which are often turbulent. A numerical approach to handle the heat transfer and fluid flow in such systems not only helps in saving the full scale

experiment time and cost, but also helps in optimizing the governing parameters for the efficient functioning of the entire system, including HVAC.
The air quality inside buildings is one aspect that is increasingly receiving more attention and is a key aspect in HVAC design of a building. Three main sources are responsible for indoor air pollution in buildings: presence and activities of occupants, construction materials and furniture and the external environment [1–3].
The indoor air quality (IAQ) discipline includes many aspects and it is difficult to define because there are many pollutants that can affect air quality [4–6]. The most important are the volatile organic components (VOCs), microorganisms, CO and NO. Given the difficulty and the cost of measuring these components (chromatographs should be used to make accurate analyses) and especially due to the low concentrations of such substances in buildings, CO_2 is used as an indirect indicator of air quality [7]. The amount of CO_2 present in the buildings is not dangerous, but since CO_2 is emitted by humans when they breathe, it gives an idea of how clean is the air in a building and the degree of ventilation. To maintain pollutants at acceptable levels, the American Society of Heating, Refrigerating and Air-Conditioning Engineers (ASHRAE) has established minimum quantities of fresh outdoor air that is to be supplied to buildings in order to dilute and flush out the pollutants. Therefore, it is common practice to measure CO_2 levels to determine if these recommended quantities of fresh air are being provided to the space being measured.
Different studies [8, 9] have shown that some energy efficient buildings reduce their energy consumption by means of reducing the operation of HVAC systems and they focus on minimizing energy use and cost, however they usually have a low indoor comfort and a poor IAQ. Therefore in order to find the compromise between energy consumption and IAQ it is important to find an appropriate control strategy. An efficient control strategy should attempt to keep the HVAC systems operating at the low possible levels while maintain the IAQ. The development and testing of the appropriate control strategy requires the use of buildings simulation tool to provide a dynamic simulation of a virtual building environment where to test the functionalities and efficiency of the controller.
In this context, the building simulation program NEST is employed in the reproduction and simulation of a real semi-detached residential dwelling located in Lemmer (Netherlands). The tool is aimed to simulate, in a fast and reliable way, the airflow, heat and pollutant (CO_2) transfer in the house in order to optimize energy consumption and indoor environment quality.
The potential of the code is illustrated through the simulation of three different modes of operation. First, the free-float mode where the house is simulated without heating and ventilation system, the need of the heating system will be highlighted and the minimum mechanical ventilation required to maintain the minimum ventilation is determined. Second, the ideal mode where the heating is operating all the time to

maintain comfort level, the energy consumption is evaluated and optimized function of the ventilation regimes and function of different scenarios of the interior doors status (open/closed). Finally, the real conditioned mode where the occupants, their activities and a controlled heating and ventilation systems are considered and simulated. The energy and IAQ performance are evaluated and by using the controlled heating and ventilation systems, a compromise between energy consumption and IAQ will be sought. Later, the semi-detached dwelling simulation program in NEST will be used as a test bench for an external control system. The controller software is embedded into NEST and its functionalities and routines will be tested on the simulated house.
A part of the results of this work has been done within the framework of the research project DCCS [10].

4.2 House description and modelling

The studied building is a real intermittently-occupied 3 bedroom semi-detached house located in Lemmer (Netherlands). The house has a floor area of 126 m^2 and consists of two floors and 12 rooms. The house has three façades: The main one is oriented south-west (azimuth $+20^o$) and the rest oriented norh-east and east-south. There are not big shading on these façades. The west-north external wall of the house is adjoined to a neightbouring house of the same type. The architectural plans of the house are shown in Figure 4.1.

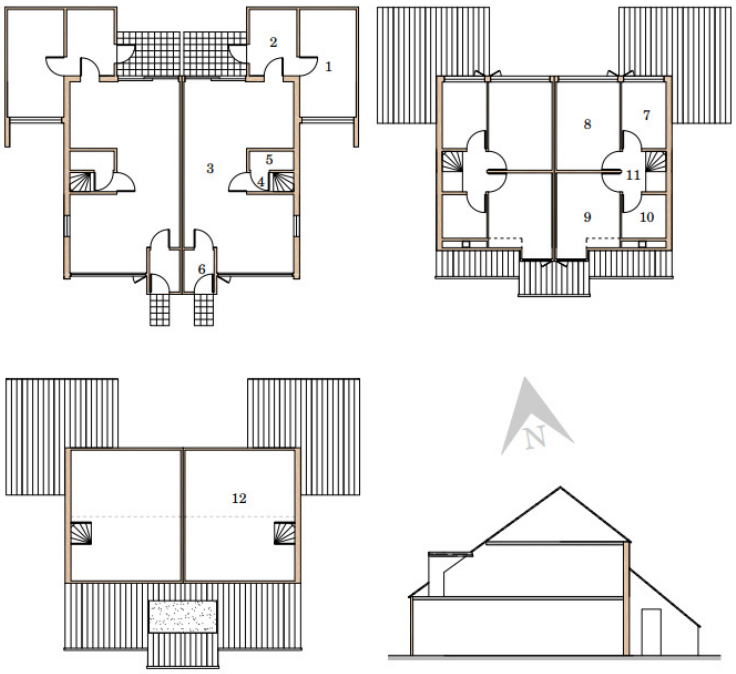

Figure 4.1: architectural plans. From top to bottom and left to right: ground, first and attic front views and building lateral view. The drawing scale is 1:42.

Figure 4.2: At the left side is shown a front view of the house (S-SW). Ground floor: livingroom window (room3), first floor: bedroom window (room9) and bath room small roof window (room10). At the right side is shown a back view of the house (N-NE). Ground floor: garage and scullery (brick wall), livingroom sliding doors, first floor: bedrooms (room7 and room8), attic: roof window (room12).

Table 4.1 describes the functions of the rooms depicted in the architectural plans (Figure 4.1) and the characteristics of its windows, radiators and ventilation.

SW and NE façades of the house are made of wood with no brick at the inside (SW wall and a small part of north wall of room 3, a small part of east wall of room 6, north wall room 8 and a small part north wall room 7). The remain façades of the house are made of brick (NE wall of room 1 and room 2 and ES façades). All floors are made of concrete and the finishing layers are wood and tails on the ground floor, tails on the first floor and carpet on the attic. The materials of some other parts of the house are unknown and have been assumed: inner walls and the roof have been assumed as brick walls, garage and the scullery floors are assumed as concrete, finishing wall material have not been considered in the simulation only the paints in terms of thermal radiation. The thermophysical properties of the materials used to simulate the house are presented in Table 4.2. Since the focus is in simulating heat, airflow and CO_2 in the house, the hygric properties of the materials are not considered in this work.

Table 4.1: Description of the rooms of the house and the characteristics of its windows, radiators and ventilation.

Room	Function	Window description		Radiator description		Ventilation
		Type	Width x Height	Type	Width x Height	
1	Garage	-	-	-		Openings around garage door
2	Scullery	-	-	ES façade - 1 plate radiator	0.30 x 2.00	
3	Living room with open kitchen	NW façade - double pane sliding doors ES façade - double pane window SW façade - double pane window	2.40 x 2.40 0.75 x 1.05 2.60 x 1.85	SW façade window - 3 plate radiator WN façade 2 plate radiator (close to sliding doors)	2.75 x 0.40 1.25 x 0.60	Openings above sliding doors Central exhaust
4	Hallway with stairs	-	-	-	-	
5	Hallway with front door			-	-	Central exhaust
6	Hallway with front door	SW façade - single pane window	0.82 x 2.03	ES façade - 2 plate radiator	0.75 x 0.40	
7	Bedroom / office	NE façade - single pane window	1.90 x 1.04	NE façade - 1 plate radiator	0.95 x 0.70	
8	Master bedroom	NE façade - single pane window	2.80 x 1.24	NE façade - 1 plate radiator	1.12 x 0.70	
9	Bedroom / office	SW façade - single pane window	1.31 x 1.04	SW façade - 2 plate radiator	0.95 x 0.70	
10	Bathroom	SW façade - double pane window	0.37 x 0.45	WN façade - Towel dryer	0.70 x 1.55	Central exhaust
11	Hallway with stairs	-	-	-	-	
12	Attic	NE façade - double pane window	0.98 x 1.01	-	-	

Table 4.2: Thermal and optical properties of the different building materials used in the house [11] [12].

Material	$\lambda[W/mK]$	$\rho[kg/m^3]$	$c_p[J/kgK]$	$\epsilon_{thermal}$	α_{solar}	τ_{solar}
White plastic paint	-	-	-	0.90	-	-
Carpet	-	-	-	0.90	-	-
Air brick	0.450	1786	840	-	-	-
Concrete	1.105	2106	880	-	-	-
Glass	0.917	2700	800	0.96	0.08	0.86

4.2.1 House modeling

The semi-detached house is modelled using the collection of NEST elements described in chapter 2. The house windows and exterior doors are simulated using the one-way opening model as seen in section 2.3.5. When they are closed the cross section of the opening is reduced to the area of an air gap in order to consider infiltrations. The interior doors, when they are open, are simulated using double-way opening model described in section 2.3.5 and when they are closed the infiltration is taken into account in the same manner as for the one-way opening model. The discharge coefficient Cd is fixed to 0.6.
The exhaust system element presented in section 2.3.7 is used to simulate the mechanical ventilation system of the house. An exhaust fan having three velocities is used to suck air from the kitchen in (room 3) and from the toilet (room 5) and bathroom (room 10). The performance curves for the three velocities of the fan are taken from a manufacturer Zehnder [13] as representative fan of a dutch house and is presented in Figure 4.3.

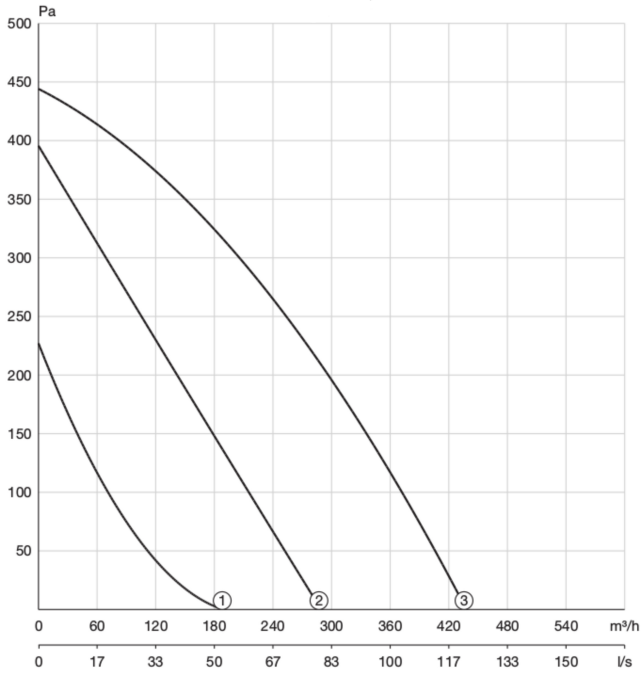

Figure 4.3: Zehnder exhaust fan performance curve for the velocities 1, 2 and 3.

A central heating system composed of boiler and radiators elements is used in the house simulation. The boiler is connected with the temperature in room 3. The radiators locations are presented in Table 4.1.

4.2.2 Initial and boundary conditions

The house is set initially to a constant temperature field. However, in order to ensure that the obtained results are no longer depending on the setted initial values, the simulation starts 3 weeks before the wished period. Typical weather is taken from Eelde which is the closest location provided by Meteonorm.

4.2.3 Standards and requirements

Standards and regulations are considered in order to fix the reference lines of temperature, CO_2 concentrations and ventilation required to maintain a good indoor

environment quality in the house, they allow also a better evaluation and analysis of the simulation results.
ASHRAE standards are used for this work. They describe the required necessary ranges to provide minimal acceptable indoor air quality and comfort level for typical situations inside buildings. They define temperature, pollutants concentrations, infiltrations, mechanical ventilation and air distribution rates.
The ASHRAE standard 55-2013 [14] presents different detailed and specific ways to determine the required indoor thermal comfort in buildings. To simplify the problem the standard ranges the ideal indoor temperature approximately between 19^oC and 28^oC.
Based on ASHRAE standard 62.2-2010 [15], a residential building like the simulated house with a volume of 318 m^3, a floor area of $126m^2$, 4 master rooms and using a continues exhaust ventilation, should have a minimum ventilation rate of 100 m^3/h and a maximum of 954 m^3/h. The standard specifies also the airflow distribution in the house when using continuous exhaust ventilation system: it is 50 m^3/h for the kitchen (room 3), 33 m^3/h for the bathroom (room 10) and 17 m^3/h for the toilet (room 5).
ASHRAE standard 62.1-2016 [16] recommends an indoor CO_2 levels not exceeding 700 ppm above outdoor levels. In Lemmer, Netherlands the outdoor CO_2 is at around 500 ppm, then the indoor air quality in the simulated house is considered poor when the CO_2 concentration exceed 1200 ppm.

4.3 Operation modes

The objective of the numerical simulation of the house is to study the thermal and ventilation performance in order to optimise and find a compromise between indoor air quality and energy consumption. To this end, the whole house has been simulated in three different modes of operation.

- Mode 1: free-floating mode, the house is simulated with no occupants nor heating system. All doors and windows are assumed to be closed and air infiltration through them is considered. First, the house is simulated only under the variation of outdoor conditions and the natural ventilation inside it has been discussed. Then, in order to achieve the minimum ventilation required by the standards explained in section 4.2.3, the convenient mechanical ventilation speed is determined.
- Mode 2: ideal mode, the house is simulated without occupants and the heating system is used to keep a minimum temperature in the main rooms. The ideal mode is tested under different scenarios of interior doors status (open/closed) and under 4 different regimes of ventilation: first considering only the natural ventilation, then 3 situations using the mechanical ventilation with a fan fixed velocity going from 1

to 3. The energy consumption to achieve the ideal comfort level for each case has been evaluated.
- Mode 3: real conditioned mode, the house is simulated under real conditions, the occupants presence and activities have been introduced into the simulation, a controlled heating system depending on the occupants schedule is used and both fixed and controlled mechanical ventilation are tested. The IEQ and energy consumption have been evaluated and discussed.

For all the modes, two periods of two months in winter (January and February) and two months in summer (June and July) have been simulated using a time step of 60 seconds. For the seek of clarity in the analysis only one week in February and in July are shown in the figures.

4.3.1 Free floating mode

The house is simulated in free floating mode and the incoming and the outgoing airflow rates from/to the outdoor through the different openings are shown in Figures 4.4 and 4.5 for both February and July. The figures legends represent the room numbers of the openings and their orientations north, south or when they are connected with duct of the ventilation system. The total incoming air (positive airflow rates) through the different openings are equal in absolute value to the total outdoing air (negative airflow rates) since mass conservation of air in the house is satisfied.
The ventilation inside the house is natural due to wind and stack effects. All doors are assumed to be closed and the air circulates through the openings by infiltration. It can bee seen in Figures 4.4 and 4.5 how the total incoming airflow rate is following a pattern similar to the wind velocity that hits the north façade. The entering ventilation rate through the north opening of the room 3 ($r3_S$) is the highest which is due to the existing of a high infiltration area in the sliding door in the north side of room 3. The days when the wind velocity is low as in July, the total incoming airflow rate is below the minimum required by the standard for the house ventilation (section 4.2.3) as presented by dashed red line in Figures 4.4 and 4.5. Thus, the use of a mechanical ventilation system is required to maintain the minimum ventilation rate.

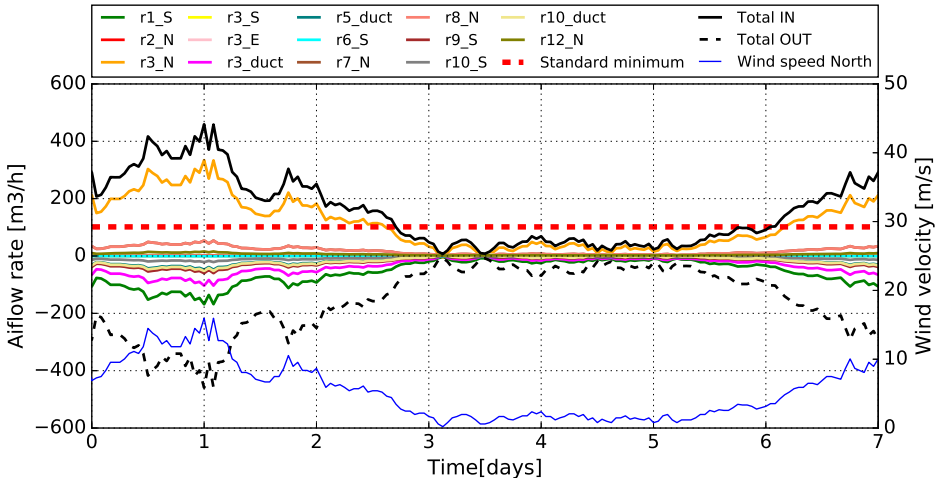

Figure 4.4: Airflow rates in the house in free floating mode during one week in February.

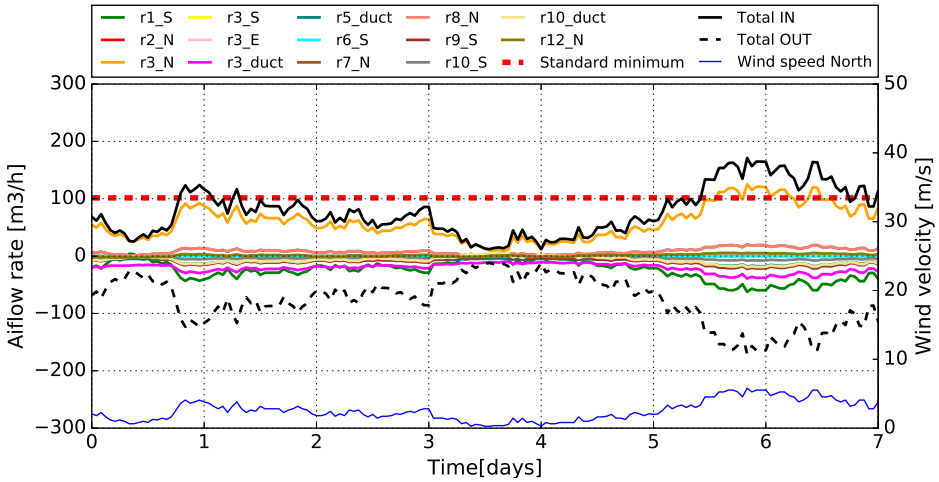

Figure 4.5: Airflow rates in the house in free floating mode during one week in July.

Figures 4.6 and 4.7 show the airflow rates in the house using the exhaust fan with speed 1. Using fan speed 1 the total ventilation rate fits well the minimum required by the standard described in section 4.2.3. The exhaust fan creates a depression in the house so the air is forced to flow from the outdoor through infiltrations. The exhaust fan is connected to the room 3, room 5 and room 10. As shown in Figures 4.6 and 4.7 the exhausted airflow rate using mechanical ventilation with fan speed 1 is always above $57m^3/h$ in the kitchen, above $32m^3/h$ in the toilet and above $40m^3/h$ in the bathroom. Therefore, the distribution of airflow rates using fan speed 1 in these rooms are higher than the minimum rates fixed by the standard in section 4.2.3.

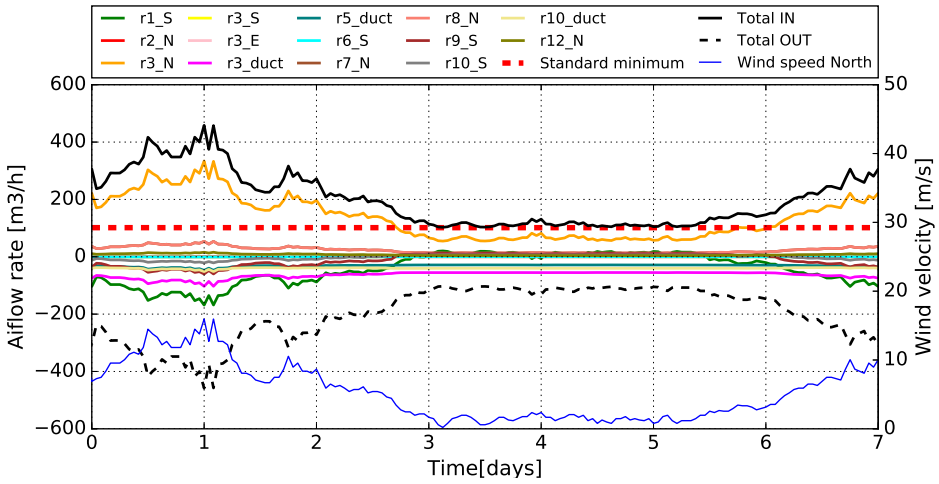

Figure 4.6: Airflow rates in the house with forced ventilation using fan speed 1 during one week in February.

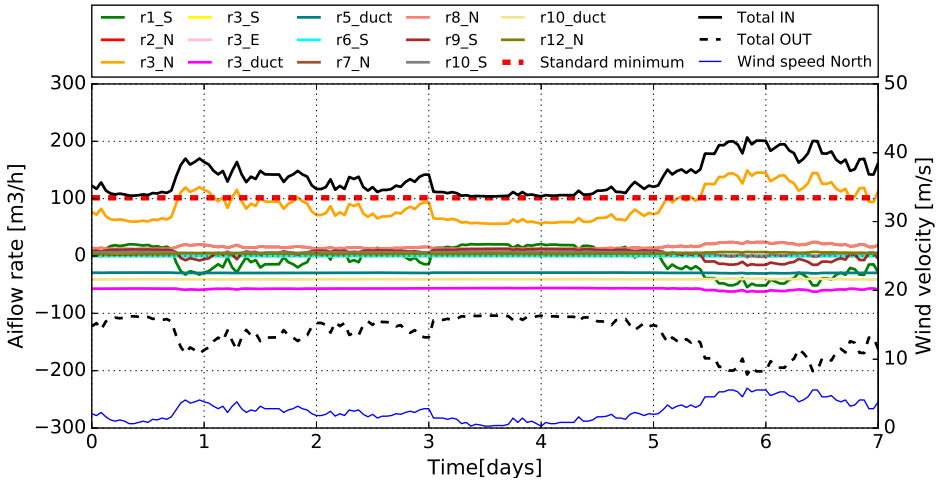

Figure 4.7: Airflow rates in the house with forced ventilation using fan speed 1 during one week in July.

Since the family house has been simulated without heating system, the temperature variations are mainly due to the weather conditions. In that manner, the heating need of the house is highlighted. Moreover, the thermal response of every room to the ambient changes can be identified too. Figures 4.8 and 4.9 present the temperature evolution in the house room in free floating mode during one week in February and July. The room 3 is warmer than the rest of the rooms. This is due to the fact that this room is located downstairs so that it has two more floors on it that provide insulation. The southern rooms (room 9 and room 10) are often warmer than the northern ones (room 7 and room 8). In contrast to room 3 , southern rooms are only warmer than others on sunny days, which emphasizes the benefit of glass windows into these rooms.

The temperatures in all rooms follow the trend of the ambient temperature. However, the oscillations are attenuated due to the inertia of the building. The simulation shows that the rooms with big windows are more sensible to solar radiation. For instance, in the living-room (room 3), which has a big window in the front side and a glassed sliding door in the back side, it can be observed several temperature peaks that match with the irradiation peaks on sunny days. The same is observed for room 9 and room 10, which are both south oriented. Instead, the northern rooms (room 7 and room 8) and the attic (room 12) show smother temperature tendency. On the other side, the hallway stairs (room 11) is the room that shows the lower solar irradiation influence since it has no windows and it has few contact with the ambient.

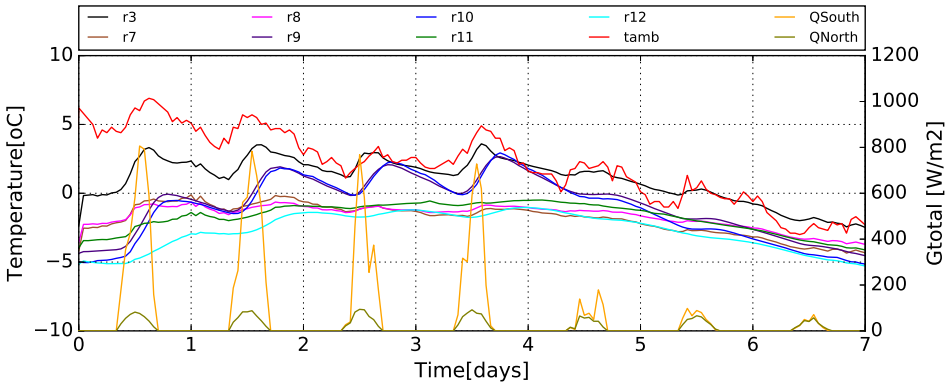

Figure 4.8: Temperature evolution in different rooms of the house in free floating mode during one week in February.

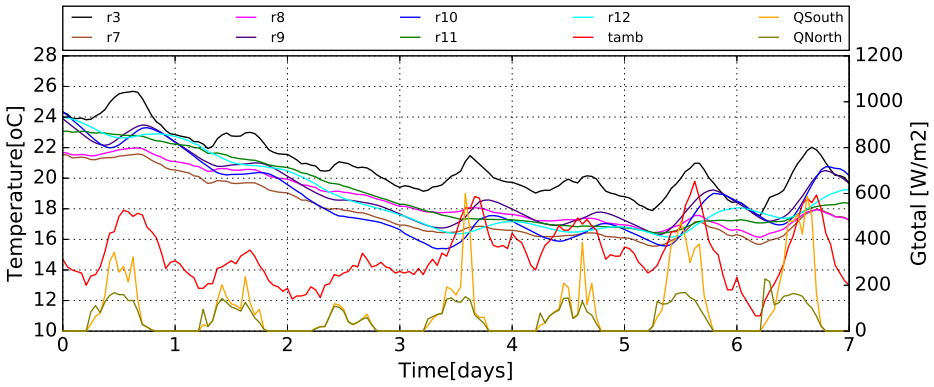

Figure 4.9: Temperature evolution in different rooms of the house in free floating mode during one week in July.

4.3.2 Ideal mode

The numerical simulation, in this mode, is performed without occupancy and by considering the influence of a heating system with radiators that supply heat to the house. The heating system is used to keep a minimum set point temperature of 20^oC in all rooms where the radiators are installed during all the time of simulation. For that reason, it is an ideal case where the minimum thermal comfort is always maintained.

The house has been simulated in ideal mode under 4 different regimes of ventilation: first considering only the natural ventilation, then using the mechanical ventilation with a fan velocity going from 1 to 3. Three different scenarios have been also simulated for the interior doors status. First, scenario 1, where all the doors are closed, second, scenario 2, where all interior doors are open and third, scenario 3, where all doors are closed except the (door 3-4) that connects the ground with the first floor.
In order to compare the energy consumption of the different simulated cases the energy consumption performance indicator (ECPI) has been defined as the sum of the heat output from all radiators of the house during the simulation period. ECPI is in $kW \cdot h$.
Regardless the status of the doors (open or closed) and the season, the higher is the exhaust fan speed, the higher are the infiltrations and the incoming airflow rates from the outside but also the higher is the energy consumption. Table 4.4 presents the EPCI in the house for the different ventilation regimes and scenarios. It can be seen how the EPCI increases by more than $50 kW \cdot h$ in winter and more than 7 $kW \cdot h$ in summer every time the fan speed is increased. On the one hand, this is a disadvantage of using an exhaust system for ventilation, as it exhausts the heated air from the house and sucks fresh air that can be colder than indoor conditions which leads to a loss of energy and so more heating requirement. On the other hand, as shown in the free-floating mode, the mechanical ventilation system is necessary to maintain a minimum ventilation rate in the house, therefore it is recommended to use the exhaust mechanical ventilation system with fan speed 1 in order to achieve the minimum ventilation rate with the lowest possible energy consumption.
The consideration of indoor air circulation between interior rooms is interesting in order to optimize the energy consumption. From the three different simulated scenarios and for fan speed 1, as shown in the Table 4.4, the scenario 1 with all doors closed corresponds to the lowest energy consumption in February, while the scenario 3, where all the doors closed except the door3-4, corresponds to the lowest energy consumption in July. In fact the sucked air from the outdoor by the exhaust fan is colder in winter than in summer. Therefore closing all the doors in winter reduces air circulation, increases the thermal insulation and reduces heating consumption, while opening the door3-4 in summer allows the sucked warmer air to circulate more between the ground and the first floor which leads also to less heating consumption. Therefore, in addition of using the fan speed 1 to maintain the minimum ventilation, it is recommended to follow the scenario 1 for doors status in winter season and scenario 3 in summer season.

Table 4.3: Total ECPI of the house during February for the ideal mode simulation.

Scenario	Natural ventilation	MV: fan speed 1	MV: fan speed 2	MV: fan speed 3
Scenario 1	683.6	719.4	779.2	843.9
Scenario 2	694.6	721.2	787.6	848.3
Scenario 3	688.5	721.0	787.2	842.6

Table 4.4: Total ECPI of the house during July for the ideal mode simulation

Scenario	Natural ventilation	MV: fan speed 1	MV: fan speed 2	MV: fan speed 3
Scenario 1	27.8	39.7	47.9	57.5
Scenario 2	28.5	39.2	46.3	58.4
Scenario 3	29.4	38.5	45.6	55.1

Figure 4.11 shows the heat generated by the radiators using fan speed 1 and scenario 1 for doors in February and scenario 3 for doors in July. It can be seen that in winter all radiators are working continuously unlike in summer season when they are operating only during some periods of time. It can be seen that the living-room (room 3) requires a great amount of heat especially in winter to maintain a comfortable temperature comparing to the other rooms, which is mainly due to its big volume.

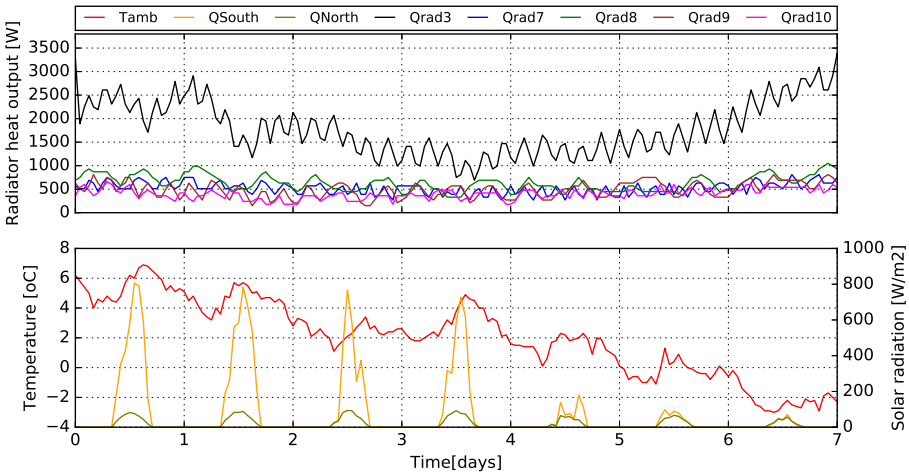

Figure 4.10: Heat generated by the radiators in different rooms of the house during February.

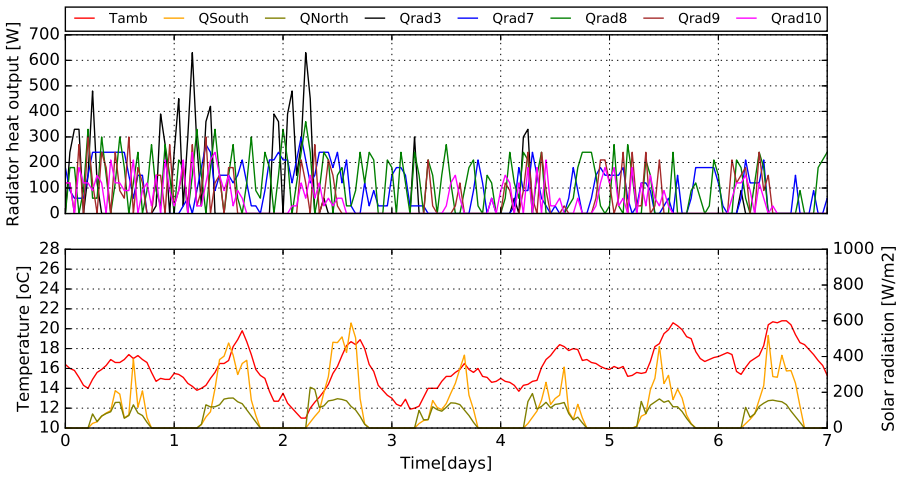

Figure 4.11: Heat generated by the radiators in different rooms of the house during July.

4.3.3 Real conditioned mode

In order to reproduce the house under more real conditions and find a compromise between energy performance, thermal comfort and indoor air quality, the house is simulated under real conditions. To do so, the typical activities and presence of two adult occupants (a couple) in each room have been scheduled and introduced into the simulation. The weekly typical schedule of the occupants is presented in Figure 4.12.

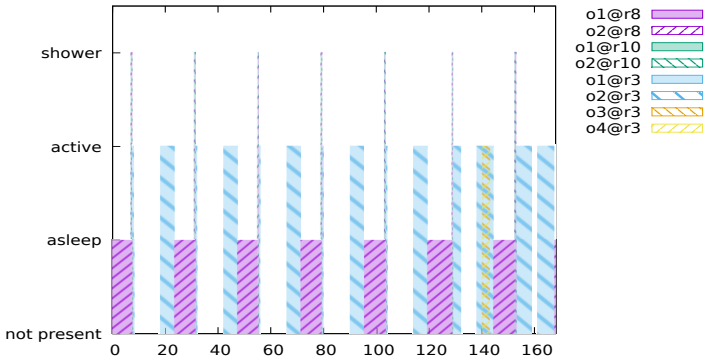

Figure 4.12: weekly occupancy schedule.

During the week, the occupants wake up at 07:00. Each one spend 15 minutes in the bedroom (room 8) while the other is in the bathroom (room 3) having a shower. They move later to the livingroom-kitchen (room 3) to have the breakfast before leaving the house at 08:00. At 19:00 they come back to the house and stay active in the livingroom-kitchen (room 3) before finally they go to sleep at 23:00. During the weekend, unlike the remain days the occupants spend more time in the house. In Saturday at 20:00, two more people enter into the house and stay until 23:00 as shown in yellow in Figure 4.12.
A controlled heating system according to the occupants schedule is considered. The used control is no interactive and is based only a schedule. Since the occupants are located in room 3, 4 and 10, only the radiators of theses rooms are open. The boiler system that supplies heat to the house radiators is controlled by the room 3. As recommended in the previous sections, the mechanical ventilation with exhaust fan is maintained continuously at speed 1 and the doors are assumed to be all closed during February (scenario 1) and all closed except the door3-4 in July (scenario 3).

Figures 4.13 and 4.14 show the temperature evolution in the house rooms during one week in February and July. In contrast to the previous mode, the use of controlled heating system allows the boiler to operate at a set point temperature of 21^oC when the occupants are in the house and active and to operate at a lower set point temperature of 16^oC when the occupants are sleeping or outside the house. The set point temperature is shown in grey colour in Figures 4.13 and 4.14. By applying this control, the energy consumption has been reduced significantly from 719.4 $kW \cdot h$ to 480.4 $kW \cdot h$ in February and from 38.5 $kW \cdot h$ to 5.6 $kW \cdot h$ in July, as shown in Table 4.5.

Table 4.5: Energy consumption performance indicator in ideal mode and by using controlled heating.

Indicator	**Ideal mode**	**Real mode: controlled heating**
ECPI: February	719.4	480.4
ECPI: July	38.5	5.6

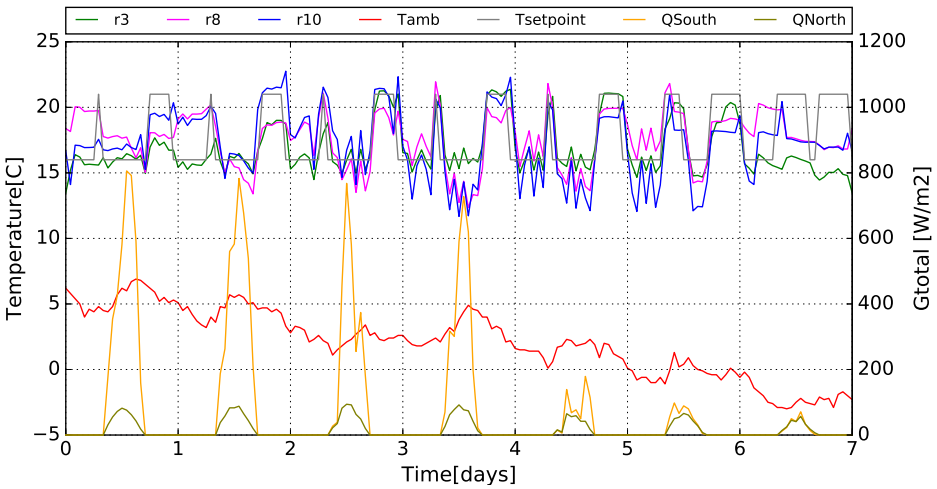

Figure 4.13: Temperatures evolution in the rooms by using a controlled heating system during February.

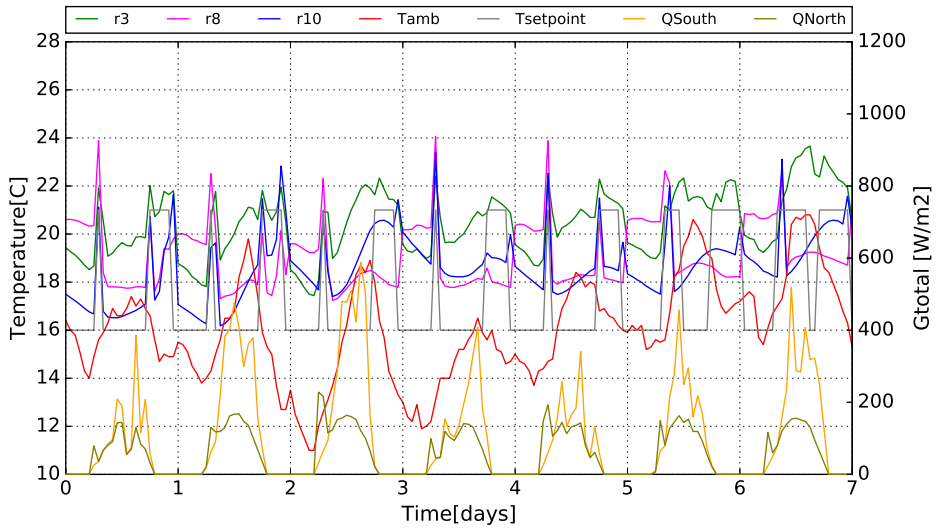

Figure 4.14: Temperatures evolution in the rooms by using a controlled heating system during July.

In order to study and analyse the indoor air quality, the CO_2 concentrations and

transfer in the house have been simulated. The air quality performance indicator (AQPI) defined as the duration that a room when occupied (one or more people present) has a CO_2 level above the threshold of $1200ppm$ (which is given as air quality limit according to ASHRAE standard 4.2.3) has been evaluated. AQPI is in $ppm \cdot min$, thus it gives an indication of the duration and magnitude that the threshold CO_2 level has been exceeded.
Figures 4.15 and 4.16 show the CO_2 concentration in different rooms of the house by using a controlled heating system and a fixed mechanical ventilation during one week in February and July. The occupants activities are reflected in the CO_2 profiles, as shown in the Figures: During night the CO_2 concentration increases above $1200ppm$ in the bedroom (room 8) and reaches a maximum of $2700ppm$ in July. The highest picks of concentration in room 8 correspond to the days with the lowest ventilation rates at the house which is mainly due to the low outdoor wind velocity. The air quality in this room would be regarded as poor.
On Saturday, when there are two guests in the living room (room 3), CO_2 concentration in the living room increases noticeably. On Sunday, the occupants spend almost all day in the house, except for a couple of hours at lunchtime, CO_2 profile shows two peaks according to these occupancy periods. When occupants leave a room, an exponential decay of CO_2 is observed.
The total air quality performance indicator for the simulated house in this case is $1.310^5\ ppm \cdot min$ in February and $4.110^5 ppm \cdot min$ in July, as shown in Table 4.6. The air is poorer during summer than winter season as the CO_2 and AQPI levels are higher, This is mainly explained by the lower wind velocity and ventilation rates during the hot season.

Table 4.6: Air quality performance indicators by using controlled heating system.

Indicator	**Real mode: controlled heating**
AQPI: February	$1.3\ 10^5$
AQPI: July	$4.1\ 10^5$

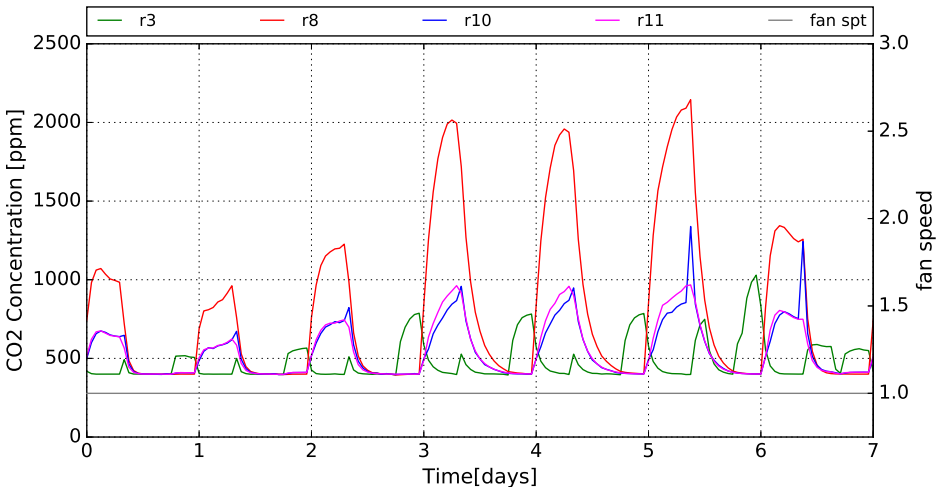

Figure 4.15: CO_2 concentration in different rooms of the house by using a controlled heating during February.

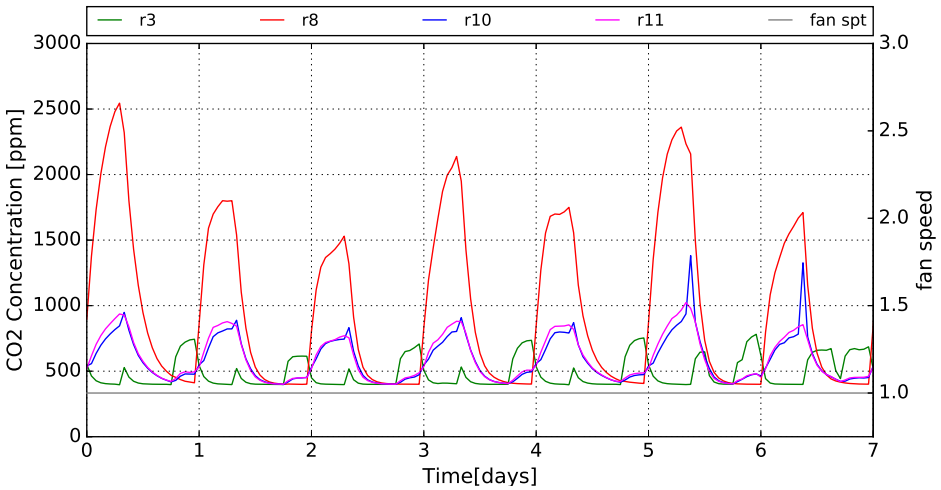

Figure 4.16: CO_2 concentration in different rooms of the house by using a controlled heating during July.

To improve the air quality in the house, a controlled ventilation system is recommended in order to increase the ventilation rate while maintaining low energy consumption. Non interactive control system in NEST is used, the exhaust fan speed is

scheduled and set to speed 2 during one hour in the morning at 07:00 and two hours in the evening at 19:00. Figures 4.17 and 4.18 show the CO_2 concentration in different rooms by using both controlled heating and ventilation during one week in February and July.
The fan speed is shown in the grey line colour of Figures 4.17 and 4.18. It can be seen in the same figure that the CO_2 levels are lower using the controlled ventilation except for the bedroom (room 8) since during night period (for noise reasons) fan speed has been set to the minimum (speed 1).
Table 4.7 summarizes the energy and the air quality performance indicators without any control (ideal mode), with only heating control and with both heating and ventilation control. The occupants and CO_2 transfer are not considered in the ideal mode, hence the AQPIs are not available for this mode. The air quality has been improved when comparing to the case without controlled ventilation, the air quality performance indicator AQPI becomes $1.110^5 ppm \cdot min$ in February and $3.710^5 ppm \cdot min$ in July. However the energy consumption performance indicator has increased to 495.5 $kW \cdot h$ in February and 5.8 $kW \cdot h$ in January. The energy consumption is a little bit higher than the case without controlled ventilation as more ventilation is used.

Table 4.7: Energy and air quality indicators for the different modes and using the optimal conditions of mechanical ventilation speed and interior doors status.

Indicator	**Ideal mode**	**Real mode: controlled heating**	**Real mode: controlled heating and ventilation**
ECPI: February	719.4	480.4	495.5
ECPI: July	38.5	5.6	5.8
AQPI: February	-	$1.3\ 10^5$	$1.1\ 10^5$
AQPI: July	-	$4.1\ 10^5$	$3.7\ 10^5$

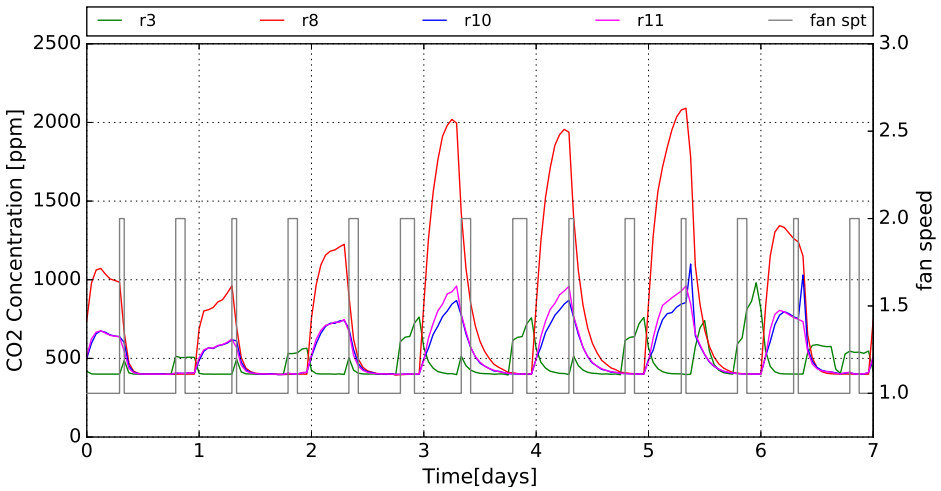

Figure 4.17: CO_2 concentration in different rooms of the house by using both controlled heating and ventilation systems during February.

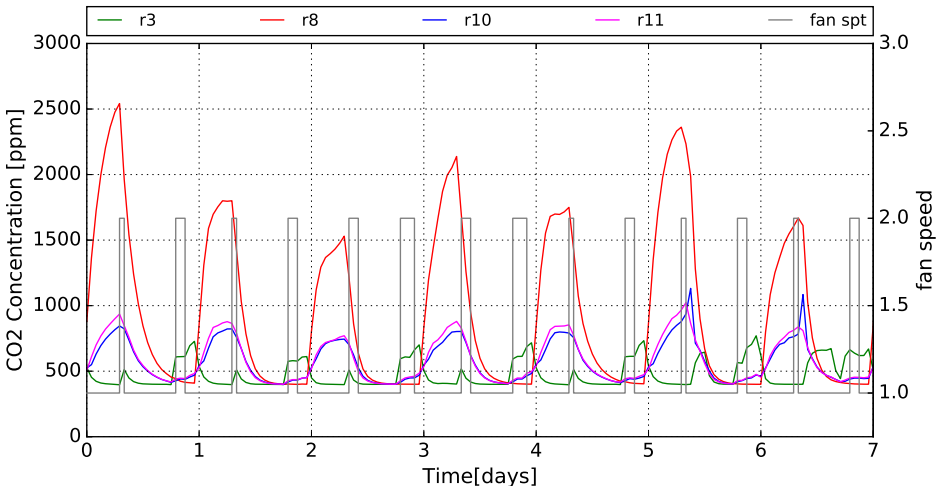

Figure 4.18: CO_2 concentration in different rooms of the house by using both controlled heating and ventilation systems during July.

It has been shown how a compromise between air quality and thermal load has been sought and found in order to reduce the energy consumption in the house while maintaining acceptable levels of thermal comfort and air quality. The NEST software

has provided the necessary tools to simulate the house in real conditions, to predict the best scenario of doors status (open/closed) and to use and control HVAC systems.

4.4 Test environment for controller

In this section, the simulated house model in NEST is coupled with an external advanced control system software developed by Netherlands organisation for applied scientific research (TNO) [17]. Coupling the building simulation tool with an interactive controller system is aimed to optimize the heating and ventilation systems based on smart routines and algorithms and reduce the energy consumption while maintaining a good indoor environment quality.
In this manner, the NEST platform has been used as a test bench (a virtual environment) to test the performance, response and the effect of the external interactive controller software on the energy consumption and air quality of the simulated house. To do so, an interface has been created to integrate the controller software into NEST software. Through this interface, the building environmental parameters in certain areas of the house, that would be sensed by the controller hardware sensors, such as CO_2 and temperature, are delivered as input variables to the controller software which determines the appropriate control outputs based on its routines and algorithms. The controller outputs are fed back again into the house, simulated by NEST, where the HVAC systems updates their operation mode based on the received data. In this manner the dynamic performance simulation of the house while using the interactive controller can be predicted.

Figure 4.19 depicts the variables exchanged between the NEST dwelling model and the controller. The model sends to the controller:

1 Timestamp: the time passed in minutes from the beginning of the simulation. At the beginning of the simulation the model sends to the controller the date and time of the simulation.
2 Livingroom CO_2: CO_2 concentration in the livingroom.
3 Ventilation CO_2: CO_2 concentration in the exhaust duct of the ventilation box, between the extract fan box and the outdoor.
4 Livingroom T: temperature in the living room.
5 Outdoor T: ambient temperature (at the outdoor).
6 Ventilation speed set point: actual fan speed (0 (off), 1, 2, 3 (highest)).

The controller receive these inputs and re-evaluates its outputs variables every minute for the heating system and every 5 minutes for the ventilation system. Simultaneously the controller sends to the model:

1 Boiler water T set point: boiler water set point temperature, acts as the on/off mechanism for the heating system. When the boiler is off, the boiler water set point is set to 10^oC. The model assumes a warming up period of 15 minutes from the off value (10^oC) to the given boiler water temperature set point value.
2 Ventilation speed set point: fan speed (0 (off), 1, 2, 3 (highest)) given to the ventilation box element.
3 Livingroom T set point: set point temperature at the livingroom. It is just used for information and post processing purposes.
4 Occupancy living room: occupancy status in the livingroom evaluated by the controller based on CO_2 concentrations. It is just used for post processing purposes.
5 Occupancy whole house: occupancy status in the whole house evaluated by the controller based on CO_2 concentrations. It is just used for post processing purposes.

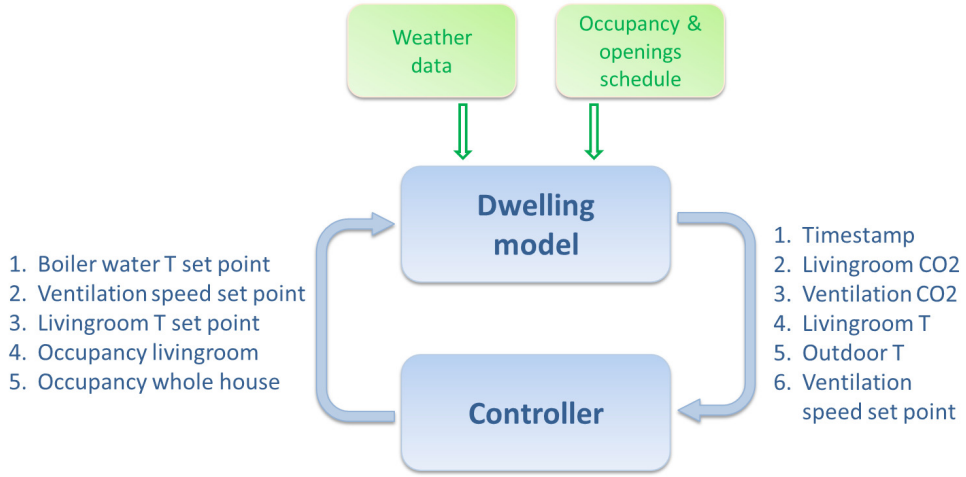

Figure 4.19: Interaction between the dwelling model in NEST and the external controller software.

The external controller is written in Python whereas the NEST platform is written in the C++ programming language. Hence, both applications are not directly compatible. However, NEST is provided with an extendible C++ wrapper for embedding Python code. In order to enable both codes to exchange information, a new element wrapper

has been created to perform the necessary actions for communicating both applications (send dwelling parameters, execute the controller and receive new controller orders).
The controller software carries out many functions and routines to optimize the control of the HVAC systems based on the weather conditions, time, occupants presence and activities, etc. These functions and algorithms are a black box for NEST software and all the focus in this work has been put in linking the two applications, exchanging data during house simulation and post process the results.
The house has been simulated in NEST in the same conditions of the real conditioned mode in section 4.3.3 except for the control system where the external interactive controller is linked now to the simulated house. The heat, airflow and CO_2 transfer are simulated in all the house and the controller algorithm response and functionality have been checked, such as the occupancy detection based on the CO_2, demand controlled ventilation, etc. The impact of the control system on the energy and the air quality has been checked and evaluated.
The simulation results are post processed by NEST software. Figures 4.20 and 4.21 illustrate some of the control routine effects on the CO_2 concentrations and temperatures in the house.

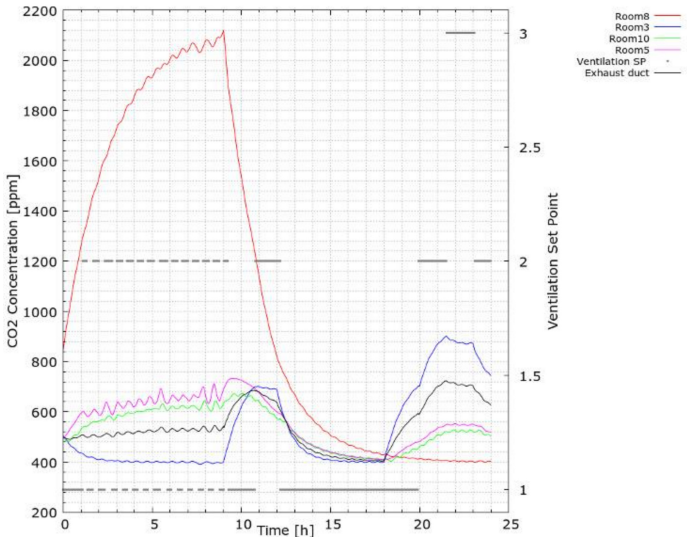

Figure 4.20: The effect of the controller algorithm on the CO_2 concentration in the house.

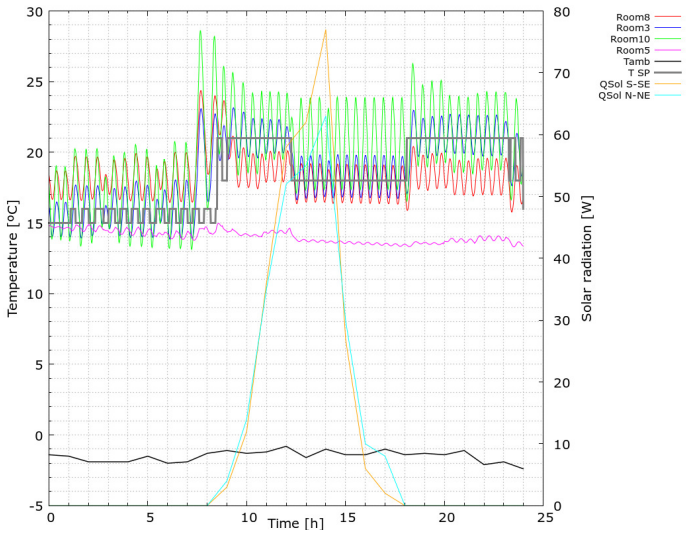

Figure 4.21: The effect of the controller algorithm on the temperature in the house.

4.5 Conclusions

Throughout this chapter it has been shown how the NEST software platform is successfully employed for producing a real building simulation of a residential semi-detached dwelling located in Lemmer (Netherlands).
The house has been simulated over one year under real weather conditions for different modes of operation. First, it was simulated in free-float mode where the importance of heating system to maintain thermal comfort has been highlighted. the natural ventilation has been evaluated and it was not satisfying the minimum ventilation recommended by standards for this type of building. It was checked that a minimum mechanical ventilation with fan speed 1 is sufficient to maintain the minimum ventilation rate required for the house for IAQ. Second, the ideal mode was simulated where the heating system is operating all the time to maintain thermal comfort in all the rooms. The energy performance has been evaluated for different ventilation regimes and for different scenarios of interior door status (open/closed). In order to reduce the energy consumption in the house, the optimum regime of ventilation and door scenarios for interior air circulation has been determined. The scenario of fan speed 1 and all doors are closed leads to the lowest energy consumption in winter, while the scenario of fan speed 1 and the door3-4 between the ground and the first floor is open leads to the lowest energy consumption in summer. Third, the real conditioned mode was simulated, the heating and the ventilation systems were

controlled, occupants presence and CO_2 transfer are simulated. Using NEST basic and non interactive control system, the energy consumption has been reduced significantly, the indoor air quality based on CO_2 concentrations has been evaluated and optimized too using a controlled ventilation system, which led to find a compromise between low energy consumption and high indoor air quality.
The same simulated house has been used to test an external interactive controller software. The controller is developed in Python and embedded with NEST software (C++ software). An interface of communication between the controller and the building simulation software has been developed and described.
The NEST building simulation tool has been used as a test bench for checking functionalities, identifying problems and optimizing the controller algorithm for better energy consumption, indoor air quality and advanced control.
The NEST buildings simulation tool has shown different capabilities to reproduce and simulate the reality, to analyse and predict the behaviour of buildings performance, optimize and find the best operation mode, to adapt to diverse situations and scenarios inside buildings and to link and interact with other codes and software.

References

[1] P. Xue, C.M. Mak, and Z.T. Ai. A structured approach to overall environmental satisfaction in high-rise residential buildings. *Energy and Buildings*, 116:181–189, 2016.

[2] J. Kim, T. Hong, J. Jeong, C. Koo, and K. Jeong. An optimization model for selecting the optimal green systems by considering the thermal comfort and energy consumption. *Applied Energy*, 169:682–695, 2016.

[3] V. Fabi, R.V. Andersen, S.P. Corgnati, B.W. Olesen, and M. Filippi. Description of occupant behaviour in building energy simulation: State-of-art and concepts for improvements. pages 2882–2889, 2011.

[4] J. Varjo, V. Hongisto, A. Haapakangas, H. Maula, H. Koskela, and J. Hyönä. Simultaneous effects of irrelevant speech, temperature and ventilation rate on performance and satisfaction in open-plan offices. *Journal of Environmental Psychology*, 44:16–33, 2015.

[5] H.A. Aglan. Predictive model for CO2 generation and decay in building envelopes. *Journal of Applied Physics*, 93(2):1287–1290, 2003.

[6] M. Hamilton, A. Rackes, P.L. Gurian, and M.S. Waring. Perceptions in the U.S. building industry of the benefits and costs of improving indoor air quality. *Indoor Air*, 26(2):318–330, 2016.

[7] G. Zucker, A. Sporr, A. Garrido-Marijuan, T. Ferhatbegovic, and R. Hofmann. A ventilation system controller based on pressure-drop and CO2 models. *Energy and Buildings*, 155:378–389, 2017.

[8] S.T. Taylor. Increasing efficiency with VAV system static pressure setpoint reset. *ASHRAE Journal*, 49(6):24–32, 2007.

[9] C.S. Koulani, C.A. Hviid, and S. Terkildsen. Optimized damper control of pressure and airflow in ventilation systems. 2014. Proceedings of the 10th Nordic Symposium on Building Physics.

[10] Dwelling Climate Control System (DCCS). `http://www.kic-innoenergy.com/innovationproject/our-innovation-projects/dwelling-climate-control-system-dccs`, 2013-2016. EIT-KIC InnoEnergy.

[11] Y. A. Cengel. *Heat transfer. A practical approach*. McGrawHill, 1998.

[12] *Handbook Fundamentals, SI Edition*. ASHRAE, 2009. Chapter 15.

[13] *Zehnder Group Ibérica Indoor Climate, S.A.* `http://www.zehnder.es/`.

[14] *Thermal Environmental Conditions for Human Occupancy*. ASHRAE, 2013. ANSI/ASHRAE Standard 55-2013.

[15] *Ventilation and Acceptable Indoor Air Quality in Low-Rise Residential Buildings*. ASHRAE, 2012. ANSI/ASHRAE Standard 62.2-2010.

[16] *Ventilation for Acceptable Indoor Air Quality*. ASHRAE, 2016. ANSI/ASHRAE Standard 62.1-2016.

[17] Netherlands Organisation for Applied Scientific Research-TNO. `https://www.tno.nl/en/`.

5

General Conclusions

5.1 Concluding remarks

This PhD thesis has been focused on the development of a modular object-oriented software called NEST for the numerical simulation of buildings systems involving several physical phenomena simultaneously. The software is aimed to solve in a dynamic, fast and reliable way, all the possible multi-physics in buildings, in order to contribute in achieving low energy consumption, high indoor environment quality and high performance in the field of buildings simulation.
The NEST platform is developed on the basis of object oriented programming, in this manner, it provides a library of basic elements for users to assemble a building and simulates the multi-physics of heat, moisture, airflow and pollutants transfer inside it. The implemented elements (or objects) represent an abstraction of the models of rooms, walls, composite walls, multi-glass, openings, HVAC systems, control systems, outdoor, solar and thermal radiations and occupants. They are implemented in general way so they can be reused by the CTTC researchers and adapted to any other applications like solar systems, compressors, etc.
Furthermore, the software is in continuous improvement to update and add new elements and models, it is aimed to be a complete tool since no building simulation software including altogether the models of heat, moisture, airflow and pollutants in the whole building parts has been found. The reliability and accuracy of the implemented, previous mentioned models, have been checked by the validation and verification with a list of significant test cases from the literature. There is a lack of references in the literature including altogether different validation cases for the whole buildings simulation. So, the list of test cases (test suite) used to validate NEST, cover all the aforementioned models in buildings and it can be used as a reference for the validation of other simulation tools.
Finally, the potential of the developed code has been illustrated in real application cases. It has been used as to analyse the hygrothermal behaviour in several public

buildings located in different countries in Europe (Spain, Sweden and UK) before their retrofitting. The hygrothermal behaviour in different representative rooms in these buildings has been predicted and analysed. Different weak points in the rooms envelope have been identified and discussed. Then the annual thermal and moisture loads before and after the proposed solutions for retrofitting are calculated in order to evaluate the efficiency of these solutions. The moisture impact on material durability and indoor environment quality has been highlighted since it is usually neglected and not very considered in buildings simulation.
The platform has been used also to simulate and analyse heat, airflow and pollutant transfer in a residential house in Netherlands. The numerical tool has been used to simulate different operation modes of the house in order to find a compromise between energy consumption and indoor environment quality. The software has been used as a test environment to evaluate the performance of an external control algorithm inside the virtual residential house simulated by NEST.
The NEST buildings simulation tool has shown different capabilities to reproduce and simulate buildings performance, and to predict heat, moisture, airflow and pollutants transfer in order to optimize the operation mode, increase materials durability and decrease energy consumption while maintaining a good indoor environment quality.

5.2 Future work

The objectives that were initially fixed at the beginning of this thesis have been successfully fulfilled. However, in order to improve the software and develop a very complete and advance building simulation tool, it will be interesting to take into account the following aspects:

- Improving the moisture transfer model by predicting the mould growth in the materials and by introducing rain from weather data base as boundary condition for the wall element.
- Accounting for the simulation of heat, moisture and pollutants transfer of furnitures inside buildings.
- Introducing two and three dimensional simulation for wall element.
- Evaluating more the thermal comfort in buildings based on detailed models.
- Incorporating new models for visual comfort, lighting and solar shading since they form part of the indoor environment quality in buildings.

- Extending the use of sub-system concepts to the whole building, e.g., reduce an entire floor into a sub-system element in a system of a building tower having several floors.

- Extending the buildings simulation to district level.

Regarding the core the software (high level code), it will be worthwhile to investigate these issues:

- Implementing and testing the zonal and CFD methods for the simulation of indoor space.

- Investigating the use of distinct and dynamic time step for each element. As different multi-physics are simulated in the same time, using the same fixed time step for all the system is practical but not necessary efficient.

- Optimizing and giving more attention in the parallel approach in NEST, since using to many parallel processors can lead to important data communication bottle-necks.

In summary, there is much work and investigation to be done in NEST. Some of the work is focused on the development of the platform itself. Other work relies on the improvement and extension of the buildings physics modelling. The NEST software is designed to grow and simulate all the multi-physics inside buildings, so that even the physical phenomena that is not planned today can be integrated tomorrow.